Stian Ingebrigtsen

The Influence of Chemical Composition on Streamer Initiation and Propagation in Dielectric Liquids

NTNU
Norwegian University of
Science and Technology

Stian Ingebrigtsen

The Influence of Chemical Composition on Streamer Initiation and Propagation in Dielectric Liquids

NTNU

Norwegian University of
Science and Technology

NTNU
Norwegian University of
Science and Technology

Thesis for the degree of philosophiae doctor

Fakultet for Naturvitenskap og Tenknologi
Institutt for Kjemi

List of Papers

1. S. Ingebrigtsen, L. E. Lundgaard, and P.-O. Åstrand, "Effects of additives on prebreakdown phenomena in liquid cyclohexane: I. Streamer initiation," Journal of Physics D: Applied Physics, vol. 40, pp. 5161-5169, 2007.

2. S. Ingebrigtsen, L. E. Lundgaard, and P.-O. Åstrand, "Effects of additives on prebreakdown phenomena in liquid cyclohexane: II. Streamer propagation," Journal of Physics D: Applied Physics, vol. 40, pp. 5624-5634, 2007.

3. S. Ingebrigtsen, H. S. Smalø, P.-O. Åstrand, and L. E. Lundgaard, "Effects of Electron-Attaching and Electron-Releasing Additives on Streamers in liquid Cyclohexane," IEEE Transactions on Dielectrics and Electrical Insulation, submitted, 2008.

4. S. Ingebrigtsen, N. Bonifaci, A. Denat, and O. Lesaint, "Spectral analysis of the light emitted from streamers in chlorinated alkane and alkene liquids," accepted for publication in Journal of Physics D: Applied Physics, 2008.

Abstract

Effects of electron-attaching and electron-releasing additives in cyclohexane on the initiation and propagation of positive and negative non-breakdown streamers have been studied qualitatively and quantitatively. Fast impulses (<20 ns, <40 kV) were applied to the plane electrode of a 10 mm point-to-plane gap and studied by shadowgraphic imaging and a 0.1 pC sensitive differential charge measurement technique. The additives studied are 1,1-difluorocyclopentane, perylene, perfluoromethylcyclohexane, perfluoro-1-heptene, trichloroethene, perfluoro-*n*-hexane, 1,4-benzoquinone, 1,2-dichloroethane, 1-methylnaphthalene, di-*n*-propylether, toluene, 2,3-dimethyl-2-butene, indole, *N,N*-dimethylaniline, tetramethyl-*p*-phenylenediamine and tetrakis-dimethylamino-ethylene. The characteristics of both positive and negative streamers depend on the specific electronic characteristic of the additives. Electron-attaching additives facilitate the propagation of negative streamers, whereas the most effective electron-releasing additives reduce initiation voltages and facilitate the propagation of positive streamers. Depending on the reactivity and concentration of the additives, streamer filaments become thinner and fewer while propagating faster and further. 1,1-difluorocyclopentane is the only additive without a measurable effect in either point polarity. The results follow expectations, considering point cathode streamers to be governed mainly by injection of epithermal electrons from a gaseous phase, and point anode streamers to be governed mainly by more energetic (hot) electrons, extracted from the liquid at higher electric fields. The Townsend–Meek theory for streamer inception in gases has been adapted to a solution and applied to analyze the voltage dependence of the positive streamer propagation. Results show a quantitative dependency on the ionization potential and additive concentration in agreement with experimental trends. This implies that electron avalanches in the liquid phase are responsible for a particularly fast propagation mode. The fast mode extends from initiation until terminated by a slower mode which is not affected by the additives. Transient conduction currents of measurable magnitudes in the nano- to microampere range are observed for voltages around initiation for both point polarities, and may be induced by ions left behind by the avalanches that are not sufficiently developed to initiate streamers.

In another part of this thesis work, the time-averaged optical emission from fast, filamentary, and luminous positive and negative streamers in chlorocarbons liquids under pulsed divergent field conditions have been studied. The liquids were dichloromethane, 1,2-dichloroethane, tetrachloromethane, trichloroethene, and tetrachloroethene. Light emitted from the first 10–15 μm trail of a few thousand streamers were accumulated. Atomic lines of hydrogen, chlorine and carbon as well as excited states of C_2 radicals (Swan bands) have been observed, and with sufficient resolution for evaluating line and band-shapes. The characteristic broadening, shift and asymmetry of atomic lines varied significantly between the liquids. Differences between the two streamer polarities were comparatively small. Densities of electrons and neutrals in the illuminated phase have been deduced from broadening of atomic lines, atomic excitation temperatures from absolute line intensities, and rotational and vibrational temperatures from the Swan bands. The gas densities of the propagating streamers were generally very high (~10% of critical) and with a high degree of ionization (~1‰). Dichloromethane and 1,2-dichloroethane produced re-illuminating streamers with densities close to atmospheric conditions, in agreement with a rapid pressure relaxation. Rotational temperatures were high and in the range $2 \times 10^3 - 6 \times 10^3$ K for the different liquids. Results can be interpreted to suggest a partial local thermodynamic equilibrium in the streamer plasmas. It is believed that the high pressure and the high electron density help equilibrate the temperatures of the various particles. The energy-consumption and qualitative chemical composition of the illuminated phase are similar to that of an equivalent system in complete thermodynamic equilibrium.

Acknowledgements

Trondheim, October 2008

Stian Ingebrigtsen

1. LIQUID INSULATION IN RESEARCH AND APPLICATION

1.1. Electrical Insulation

The main purpose of electrical insulation is to provide a dielectric barrier between two conductors or between one conductor and ground, thereby "isolating" energized components of an electric system. The ability of a material to act as an electric insulator has traditionally been given by its "dielectric strength", often also called the "breakdown voltage". The dielectric strength of a material is the critical electric field magnitude at which the insulating property of the material fails. It is expressed as volts per unit material thickness, and can be found tabulated for several gases, liquids and solids, e.g. in [1]. A higher dielectric strength means that a higher voltage can be applied before the material suffers a "dielectric breakdown". In liquids and gases, a breakdown is completed through the initiation and propagation of a so-called "streamer". The streamer is a conductive plasma channel that initiates in a region with high electric fields and propagates through the material until it bridges and short-circuits the voltage gap. At this point, the conductive channel is commonly referred to as an arc. As implied by the name, dielectric breakdown can lead to severe and irreversible damages to the electrical system under operation. This included damages to the insulation material itself, resulting from a sudden release of electric energy during the discharge process. High-voltage equipment forms an important part of any national infrastructure, which demands for a high degree of reliability during operation. In such, research to understand and control the mechanism leading to electrical failure of insulating materials is important.

1.2. Insulating Liquids in Electrotechnical Applications

The insulation technologies used in power systems can be divided into three categories; solid insulation, liquid insulation and gaseous insulation. Liquid insulation has been used since the beginning of the manufacturing of high-voltage electrical equipment, and is often preferred to solids and gases. The high density of a liquid compared to that of a gas results in higher breakdown voltages and a more efficient dissipation of thermal losses. Compared to a solid, a liquid has a superior ability to conform to complex geometries, while maintaining the self-healing/recovery capabilities typical for gas-insulated systems. Consequently, liquids are often used in combination with solid

insulation, replacing gas cavities therein to improve the partial discharge characteristics of the insulation system. In addition to having a high dielectric strength, a good insulating liquid can be characterized by a low dielectric dissipation factor, a high chemical stability, a low volatility, a high oxidation resistance, a high flashpoint, a high rate of dielectric recovery following an arc, and a good compatibility with other insulating materials. Materials with good insulating properties are necessary to achieve high efficiencies in AC and DC power generation and transmission [2], and for larger energies in pulsed power applications [3]. In these cases it is preferable to operate at the highest voltage levels with minimum volume. Traditionally, insulating liquids have found the widest use for power -and distribution transformers. The liquid acts here both as an electrical insulator and a heat transfer fluid, which means that the liquid should also have a suitable density, kinetic viscosity, thermal expansion coefficient, and heat conductivity [4]. Recently, there has been a growing interest in insulating liquids in connection with a rapid development of high-voltage pulsed power for various applications [5]. Due to the widespread use of insulating liquids, these should also be non-flammable, non-toxic, and inexpensive.

Vegetable oils were among the earliest insulating liquids used in the manufacture of electrical apparatus. Due to their poor dissipation factor and gassing properties, vegetable oils are used mainly for the impregnation of DC capacitors [6]. However, some attempts have been made to use vegetable oils in combination with aromatic hydrocarbon liquids in AC capacitors. There is also an ongoing research to test vegetable oils (e.g. rape seed oils) for possible uses in high-voltage transformers [7-9].

The liquid most commonly used in high-voltage transformers, cables, capacitors, switches, and circuit breakers are mineral oils; by-products in the refining of crude oils to produce gasoline. These liquids are complex mixtures of paraffinic ($C_{2n}H_{2n+2}$), naphthenic ($C_{2n}H_{2n}$) and aromatic (C_nH_n) hydrocarbons, depending on source and refining procedure [4]. Small amounts of sulphur compounds, nitrogen compounds, and oxygen compounds also occur [4]. The paraffinic and naphthenic content give the liquids their desired physical properties like density, viscosity, and pour point, whereas the aromatic compounds controls the oxidation resistance, the gassing properties and the electric strength for impulse voltages [6]. The synergy between aromatic

hydrocarbons and sulphur compounds is effective for oxidation stability [4]. Refining is normally performed so to obtain a balanced concentration of these compounds; 10-20 w% and > 0.5 w%, respectively [4]. In addition, some mineral oils have small amounts of antioxidants added.

The dielectric strength of mineral oils is typically around 12 kV/mm, and the resistivity greater than 10^{10} Ωm. The mineral oils are highly flammable, being mainly a concern for applications in electric power transmission and distribution. Polychlorinated biphenyls (PCBs) were commonly added to increase the fire resistance of the liquids until they were banned from regular use during the 60's and 70's. The ban resulted in a search for new natural or synthetic oils that were biologically and environmentally safe, yet still had superior insulating properties [6]. Several halogenated aliphatic hydrocarbons (e.g. tetrachloroethene) were first used as replacement for PCBs, but are now rarely considered due to an increasing awareness of their environmental and toxicological impact [4,6]. PCBs were thus mainly replaced by synthetic aromatic hydrocarbons, e.g. alkylnaphthalenes and alkyldiphenylethanes.

Today, non-toxic synthetic insulating liquids are used instead of mineral oil when special properties such as fire resistance or thermal stability are required [6]. Synthetic liquids are manufactured from petrochemical products, and have a simple and well defined molecular composition, e.g. silicone-based liquids (polydimethylsiloxanes), high-molecular weight ester liquids (polyolesters), polybutenes, poly-α-olefins and alkyl-substituted aromatics [10]. These liquids have found a broad use in high-voltage cables, impregnated capacitors, distribution transformers and instrument transformers [6]. The silicone-based oils have been regularly used in the transformer industry owing to their good oxidation resistance and thermal stability compared to mineral oil [11]. They also come in a large range of viscosities and flash points. However, the silicone-based liquids are not readily biodegradable and more expensive than mineral oils. The ester-based liquids, on the other hand, are promoted as biodegradable, but have again poor oxidation resistance. An antioxidant additive is therefore required to impart an acceptable level of stability. Despite limited knowledge concerning the stability and ageing performance in long term perspectives, an increased tendency is emerging amongst utilities and other users of liquid filled transformers to use synthetic biodegradable liquids [12]. This is motivated by more restrictive environmental regulations.

High dielectric strengths and low dielectric losses are the two most important properties of high-voltage capacitors. Since to the banning of PCBs, new liquids had to be developed for high-voltage capacitors as well [6,10]. During this work, a great improvement was simultaneously obtained of the dielectric strength of the new liquids, which again led to a large reduction of the capacitor dimensions. Both aliphatic and aromatic liquids are now used in high-voltage capacitors. Most commonly used are isopropylbiphenyl, propylbiphenyl, methylated diphenylethane, phenylxylylethane, benzylneocaprate, camylphenylethane, ditolyether, dioctylphthalate, phosphate esters, and mono/dibenzyltoluene [4,10]. Since these liquids are more flammable than the original PCBs, dry capacitors have been developed for uses where fire-resistant materials are strictly required.

1.3. *Trends in Liquid Dielectric Research*

The technique of high-voltage insulation includes disciplines within physics, chemistry and electrical engineering, and research to improve the insulating capability of a liquid is often generic. The interdisciplinary research originates from the various demands placed on a good insulating liquid, see section 1.2. The dielectric strength of a material is nevertheless the most important property, and research on the mechanism leading to voltage breakdown is vital to our understanding of the dielectric performance of candidate materials. The events preceding the actual breakdown are termed 'prebreakdown processes' and have been studied experimentally during the last four decades, accompanied by steadily improved measuring techniques. In the following, a historical review is presented on the evolution of these techniques.

In the 1950's and early 60's, most researchers worked with simple hydrocarbon liquids such as n-hexane or benzene. With small electrode gaps and available power supplies (ramping DC and AC) they produced sufficiently high (uniform) electrical fields to cause breakdown. The main interest in that period was the conduction mechanism and the effect of molecular structure on the overall breakdown mechanism [13-19], including effects of additives [20]. The researchers had typically not sufficient time resolution to observe details of the breakdown mechanism, and had to be satisfied with recording only the nominal voltage of the voltage supplier when breakdown occurred. Results were typically reported in terms of the "dielectric strength" (see section 1.1), and

electric breakdown were recognized to be a statistical process depending on several factors over which the experimenter had little if any control [21,22].

At the start of the 60's, optical techniques became of interest and were applied to the study of the prebreakdown process [23,24]. The photographic techniques available made it possible to obtain from one to three exposures of the phenomena at pre-selected times. In order to obtain exposures with short intermittent delays, the optical beam was typically split into several beams that were delayed relative each other by using different optical lengths. The light emitted from the streamer was studied with photomultiplier tubes, whereas the geometry of the streamer was studied with shadowgraphic and schlieren techniques. Several pictures had to be taken for each interesting image obtained, and it was generally difficult to obtain more than one interesting image at a time. The plane electrode geometry used also made it necessary to observe a large volume in order to detect local prebreakdown events.

From the mid 60's, it was reasoned that the optical observations would be facilitated if one could confine the prebreakdown phenomena to one a single region, such as a needle point. At the same time, asymmetric electrode arrangements allowed locally higher electric field stresses at the cost of lower voltages. Geometries, such as needle-to-plane, sphere-to-plane, and similar arrangements were used [25-28]. It had previously been found that the polarity of the streamer-initiating electrode was not immaterial, and now these polarity effects could be studied in more detail. At the same time, the type of voltages to be used became of importance. It was argued that slowly rising voltages (0.5–3 kV/s) provided sufficient time to permit formation of space charges, affecting the field distribution in the high-field regions prior to the initial events of the prebreakdown.

The entry of fast electro-optical techniques during the 70's, involving image converter cameras and pulsed laser or flash lamp illumination, made it possible to obtain series of images during one streamer, with intervals ranging from several microseconds down to 50 ns. These technologies made it possible to carry out more reliable and more detailed studies of the structure and development of prebreakdown processes [29-32]. During the 80's, measuring techniques were complemented by non-contacting registrations of the electric

field re-distributions and (or) changes in the liquid density, based on the electro-optic Kerr effect [e.g. 33].

Until today, point-to-plane electrode arrangements with impulse voltages and fast electro-optical techniques have remained the most widely used techniques for studying breakdown and prebreakdown phenomena, and a wide variety of investigations have been carried out worldwide (France, Russia, USA, Great Britain, Norway, Sweden, Japan, Poland, India, China, and more). A recent review on the international trends in dielectric research in general, from 1980 to 2004, can be found in reference [34]. A little-used, but promising technique for the future is streamer emission spectrometry [35-38]. The technique was first utilized to investigate the gaseous nature of both prebreakdown and breakdown plasmas in hydrocarbon liquids [32].

1.4. Characterisation Methods for Liquid Dielectric Performance

The dielectric strength of a liquid or solid is not an intrinsic parameter of the material, but rather that of the insulating system. The dielectric strength depends on the sample thickness, the electrode geometry, the type of applied voltage, and the interface towards other materials. This situation has been recognized by most national and international standardizing organizations, and has led them to develop test procedures for some intended applications. For mineral oils for example, two IEC standards have been issued, one for transformers and switchgear (IEC 296), and one for oil-filled cables (IEC 465).

The first test used for mineral oil were breakdown tests for AC voltages, existing in a multitude of variants using different electrode shapes and separations, and with different rate of rise and frequency of applied voltage [39]. These tests have mainly been used for acceptance testing of oil supplies and as a decision aid for maintenance actions. However, the main dimensioning criterion in many cases will be the ability of the insulating system to withstand impulse voltages. As a consequence of the focus on impulse testing for high-voltage power transformers, the American Society for Testing and Materials (ASTM) issued in 1974 an impulse test that was adapted to the International Electrotechnical Commission (IEC) in 1987 [40,41]. The standards specify a point-to-sphere electrode geometry and 1.2/50 µs impulse voltages. The point is made from a gramophone needle, and the electrode separation is 25, 15 or 10

mm, depending on the breakdown characteristics of the oil. The test procedure is either five sequences of stepwise increases of pulse levels until breakdown occurs, or a sequential test where pulses of fixed amplitudes are applied. Under these conditions, breakdown voltages correlate to the aromatic content of the oil using a point cathode, whereas a correlation has not been found with a point anode [42-45].

In order to gain more insight into the physical processes responsible for the prebreakdown phenomena, an alternative characterization method has been used in some research departments and research companies [46-48]. Common for these studies are impulse voltages where the rise-time is fast enough to avoid an influence of space-charge during the initial events leading to streamers (< 50 ns), and where the voltage level is stable during the progression of the phenomena. So far, these procedures are combined with diagnostic methods such as measurements of currents induced by the phenomena on the terminals, recordings of emitted light, and high-speed shadowgraphic imaging. The majority of liquids used for electric insulation are more or less transparent to visible light and may therefore be subjected to this kind of tests. The characterization methods reveal the evolution of the prebreakdown phenomena, which in many respects determines the dielectric strengths of the liquid. Their experimental techniques are founded on the past decades' experimental advances (section 1.3), and moreover lay the experimental basis for the present research, see section 3 of this introduction.

1. Liquid Insulation in Research and Application

2.   STREAMERS: A MULTIPHYSICS, MULTISCALE TOPIC

2.1.   *Mechanisms and Qualitative Streamer Models*

There is no satisfactory theory for the mechanisms leading to electric breakdown in liquids. Moreover, a general theory describing excess electrons in liquids does not exist. Mainly phenomenological treatments have been used in both cases, and often originate from models developed for gases or ordered solids. In gases, the term "streamer" is used for prebreakdown processes with defined physical properties. In liquids, the same term is loosely assigned to all observable liquid prebreakdown and breakdown phenomena reported in the literature. Streamers therefore exhibit a variety of propagation characteristics depending on the experimental conditions, and one expects a variety of mechanisms to be involved. Individual mechanisms are often described in detail, dealing with either the generation (and recombination) of free charge carriers at the electrode interface or in the bulk of the liquid, the electrohydrodynamic convection of ions in the inter-electrode region, or the gaseous dynamics of a charged "bubble" subjected to electric fields. Many of these mechanisms are well-known from linked areas of research where experimental conditions (e.g. field-distribution) are better defined. Only a few of the proposed mechanisms can be linked to the governing processes behind streamer propagation, whereas none are capable of fully describing the dynamics of streamer propagation. A propagating streamer eventually leading to breakdown is an intricate interplay between processes occurring on a wide range of timescales [49], from picoseconds electronic processes to microsecond hydro-mechanical processes. The unique level of complexity of a prebreakdown phenomena in a liquid is well reflected in the literature, and several review articles treat the different aspects involved [50-62]. A few simplified streamer models have also been suggested, and will be mentioned in brief below.

In a point-to-plane electrode arrangement, a positive streamer most typically refers to a point anode, whereas a negative streamer refers to a point cathode. Experimentally, their behaviour of initiation and propagation differ. Four different propagation modes for positive streamers have been indicated from the appearances of streamer shadowgraphic photographs, from the first mode occurring just after initiation up to the fourth mode (fast events [63]) occurring well above breakdown levels [64,65]. Similarly, for negative point polarity,

three propagation modes have been distinguished. Mainly the first two streamer modes have been discussed in the literature for both cases. The first, slow mode (< 200 m/s) is characterized by a bubbly or bushy shape, basically consisting of vaporized liquid with low conductivity, while the second mode (>1 km/s) is characterized by a filamentary structure containing more ionized gas.

In 1988, Felici suggested that the first mode negative streamer is a bubble-like, low conductivity vapor cavity with repetitive internal voltage collapses (partial discharges) [66]. Accordingly, propagation involves bombarding the liquid phase in front of the cavity with electrons produced in the discharges, thereby inducing local vaporization by inelastic collisions in the liquid, see Figure 1. For a second and faster type of negative streamers, mechanisms of liquid ionization have been proposed [67,68]. Devins *et al*. proposed already in 1981 a recursive "two-step" process for negative streamers [67]. According to this model, electrons entering the liquid are first trapped, forming negative ions. This space charge sets up an electric field which ionizes the liquid when being above a critical value. The process repeats itself as electrons are readily supplied by the trailing plasma channel, driving the streamer with a velocity determined by the characteristic times for each step. A review of Devins' model can be found in reference [69]. Later, in 1991, the importance of electrostatic and hydrodynamic forces for the negative streamer propagation was experimentally and theoretically demonstrated [70].

Qualitative models for positive streamers are rarely approached in literature. Instead, one has generally referred to a streamer mechanism similar to the mechanism for streamers in gases [71,72], as outlined in Figure 2. Experimental investigations have taught us that processes responsible for the continuous formation of the gas / liquid interface occur both within the gaseous void and in the liquid [73]. A slow propagation mode has been associated with a mechanism in the gas as it is readily quenched by elevated hydrostatic pressures [73]. During a faster propagation mode, processes in the liquid are considered primary and the dynamics of the gas channel secondary, but there is no model compatible to this duality. Electronic processes are considered important, but there is a discrepancy in the literature concerning the origin of excess electrons in the liquid. Both field ionization [67] and impact ionization [49] have been invoked as main contributors.

$$AX + e^- \underset{\longleftarrow}{\overset{k_a}{\longrightarrow}} AX*^- \rightarrow X*^- + A*$$
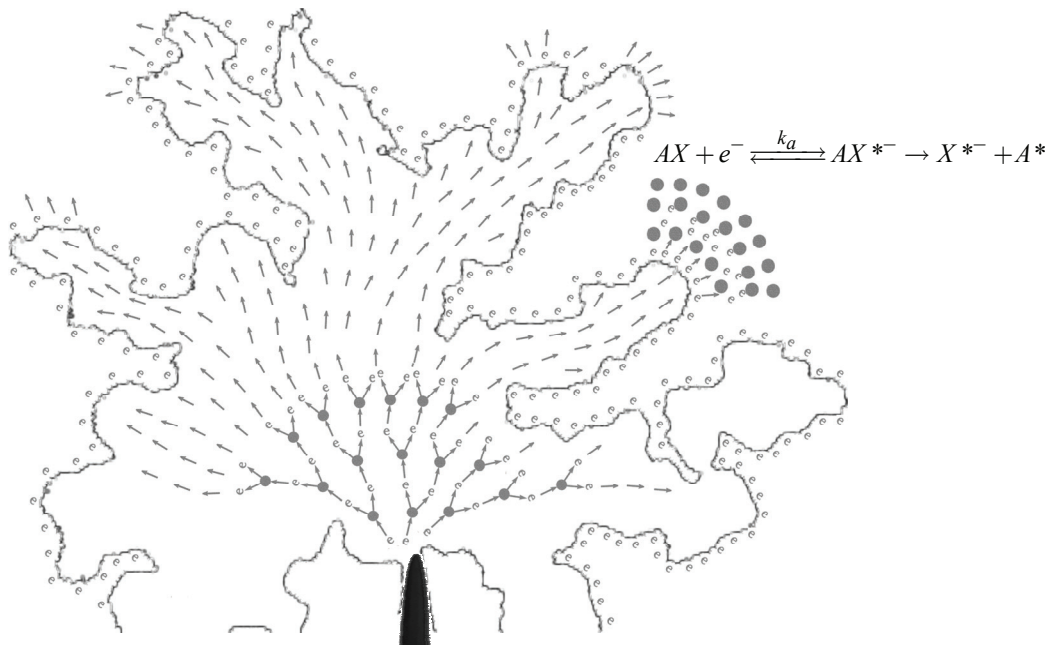
Figure 1. The propagation of slow negative streamers occurs via repetitive partial discharges in a gaseous void (contour-line). Electrons produced by the electron-avalanches in the gas bombard the liquid in front of the cavity, thereby inducing local vaporization by inelastic collisions, as well as electrohydrodynamic instabilities. The accumulation of charge at the gas-liquid interface also influences the field distribution in the void.

$$AX + e^- \rightarrow AX^+ + 2e^-$$
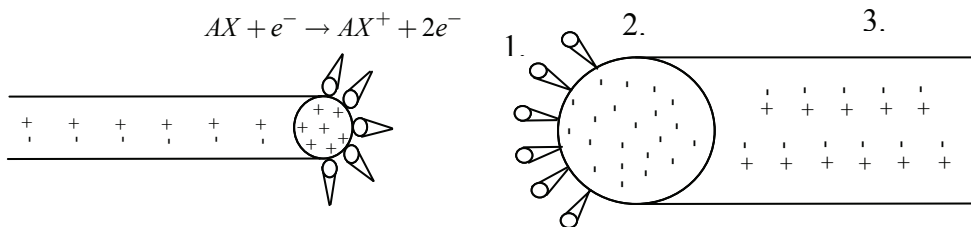
Figure 2. Outline of simplified propagation mechanism for a fast positive streamer (left), and a fast negative streamer (right). Electron-avalanches (1) define the ionization region in the liquid phase, leaving behind a preheated, ionized trail for the streamer to follow. A moving ionization region is called a 'streamer head' (2), and the trailing plasma filament a 'streamer channel' (3). The streamer head has the same net polarity as the electrode from which it extends. It partly negates the electric field at this electrode and enhances it outwards, pushing the ionization region towards the opposite electrode. In order for the streamer to propagate, the positive or negative ions left behind in the streamer head must cause sufficient space-charge distortion of the electric field, and is promoted by an extended electron multiplication.

2.2. *Descriptors for Streamer Propagation*

In order to build empirical knowledge, streamer studies have been performed in a number of liquids [74]. Results have been analysed with respect to molecular parameters such as molecular weight and chain length [75], molecular branching and structure, molecular double and triple bonds [76,77], special atoms or functional groups within the molecule [76,78] and bulk parameters such as viscosity [79-81], boiling point [79,82], conductivity [83] and permittivity [75,83]. There is generally no correlation between the streamer propagation characteristics and the bulk properties of the liquid, including specific heat, heat of vaporization, surface tension, compressibility, vapor pressure, charge mobilities and lifetimes [62]. On the other hand, characteristics of streamer propagation have sporadically been traced to the type of molecules in the liquid. In particular, studies have shown that adding small amounts of molecules with specific electrochemical properties drastically changes the propagation behaviour of streamers [67,69,84-86]. Starting with the pioneering work of Devins *et al*. [67], it has generally been demonstrated that molecules with electron-attaching capabilities such as perfluoro-*n*-hexane and tetrachloro-methane encourage faster propagation velocities and thinner structures for negative streamers, whereas the same effects have not been observed for positive streamers [67]. Conversely, additives with low ionization potentials, such as *N,N*-dimethylaniline and pyrene speed up positive streamers [67,85].

3.   SETUP FOR STUDY OF ADDITIVES IN CYCLOHEXANE

3.1.   Experimental Outline

High-voltage rectangular pulses were applied to the plane electrode of a 10 mm point-to-plane gap, and the streamers initiated at the point electrode were studied with a shadowgraphic depiction technique and by measuring the charge induced in an external circuit. The general experimental outline will be described below. A test-cell with a point-to-plane electrode arrangement was placed in a 4 m long optical bench made of two Newport X95 rails and several carriers with three-axis micrometer positioning systems. As shown in Figure 3, the imaging system consists of a high-intensity white light-emitting diode or a xenon flash-lamp, an auto-collimator, a lens system and a single-shot intensified CCD camera.

The test cell and electrode arrangement is described in section 3.3 and 3.4. High-voltage pulses with steep fronts were supplied from an impulse generator as described in section 3.6. The high-voltage pulses were measured by integrating the current from a capacitive probe, using a passive integrator as described in section 3.7. The charge induced to the point electrode was measured with a 0.1 pC sensitive differential charge measurement technique, and is described in section 3.5. All experiments were carried out at room temperature under atmospheric pressure, using purified cyclohexane with different additives. Additives and procedures for sample preparation are described in section 3.8. Section 3.9 gives a brief description of the data analysis.

After manually adjusting the high-voltage level, the experiment in Figure 3 is fully automated and controlled via a customized LabView program. This program communicates with the digital delay/pulse generator (4) and the oscilloscope via a National Instruments GPIB-USB-B controller. The program thus effectively operates the trigging of the two Thyratron pulsers (7) used to ignite the main high-voltage impulse generator (9), the trigging of the light source (6), and the trigging of the camera via its control unit (2). In order to reduce the number of ground loops, these connections are made with fiber optics. After a streamer has been recorded, the same program in sequence reads and stores each channel from the oscilloscope holding the electrical measurements, and the corresponding shadowgraphic image from the camera control unit via a frame grabber card. Electrical measurements are stored in format ASCII-text,

TIF and HPGL, and each measurement will have a unique filename. Manually set parameters are the duration of -and time in-between each impulse, and the timing of the light pulse and camera exposure. Typically, at least 30 streamers were recorded at each voltage level with 3 minutes intermittent delays.
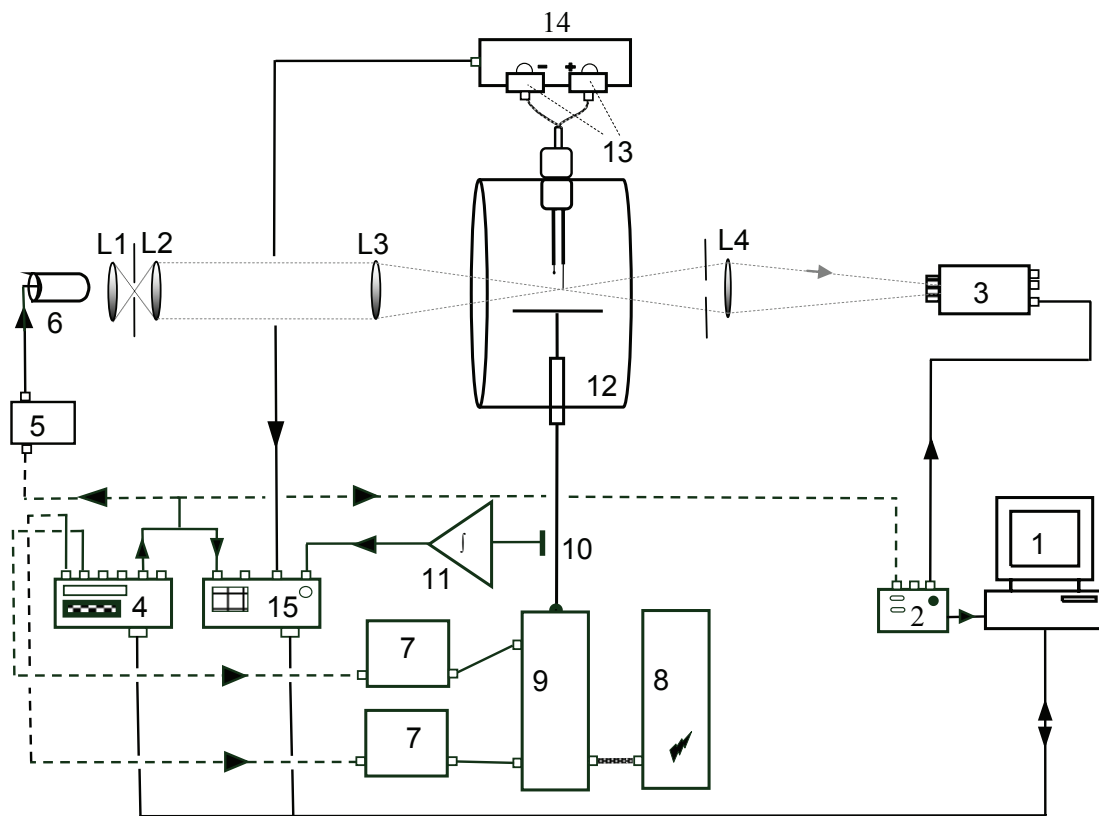
Figure 3. General outline of the experimental setup, (1) computer, (2) Proxitronic control unit, (3) Proxitronic Nanocam® NCA fast shutter camera, (4) SRS-DG535 four channel digital delay/pulse generator, (5) pulse circuit for light-emitting diode, (6) light-emitting diode (Marl Optosource, 5600 mcd) /Xenon flash-lamp, (7) -6 kV Thyratron pulsers, (8) Spellman SL150 DC high-voltage (0–±100 kV) supplier, (9) high-voltage impulse generator, (10) BNC capacitive probe, (11) 60 ms passive integrator, (12) test cell, (13) capacitive voltage divider circuits, (14) Lecroy DA1850 100 MHz differential amplifier, (15) Tektronix TDS 540A digitizing oscilloscope (record length 15000). Dashed connections are made fiber-optically with Agilent HFBR-1412/2412 miniature fiber optic components. Electric devices are galvanically separated from the mains voltage, and grounded in the metal case of the impulse generator (9).

3.2. *Shadowgraphic Imaging*

Since a streamer has a lower refractive index than that of the liquid, it deflects any light passing through the streamer region. Thus, by using a background light-source, the streamer can be visualized as a shadow on images taken with a gated light-sensitive camera. This is shadowgraphic imaging. Single-shot images synchronized to the streamer events were recorded with a Proxitronic intensified gated video camera capable of preset exposure durations as short as 5 ns (internally set exposure). The shutter is opto-electronicly controlled and operates with a trigger delay of 53 ns. The shutter could alternatively be externally gated with TTL pulses with minimum pulse widths of 100 ns. The duration of the exposures were chosen so to give the best image contrast possible. Exposures were typically in the range 0.5–1.0 µs using a synchronously pulsed white light-emitting diode, whereas with the xenon flash lamp, having a much higher luminous intensity, exposures were either 5 or 10 ns. The image magnification could be varied by changing the position of the camera and lens relative the test-cell and camera. The highest image resolution obtained was about 1 µm. Digitized shadowgraphic images were normally taken when the streamer reached maximum extension into the gap. After each capture, an analogue image was stored in the camera control unit, and then digitized to a computer with a National Instrument NI-1409 frame grabber card. The streamers always stopped propagating mid-gap before the high voltage pulse was quenched. Ideally, each digitized shadowgraphic image should be taken when the streamer reached maximum extension (length) into the gap. Due to the randomness in the phenomena, some experience was required in order to determine the "best" timing relative the typical streamer lifetime. Images were occasionally also deliberately taken during streamer propagation.

3.3. *Test Cell*

The point-to-plane electrode gap is located inside a 1.5 litre cylindrical PTFE test cell, see Figure 4. The cell has two optically aligned 130 mm diameter windows made of borosilicate glass. A micrometre screw adjusts the height of a 90 mm diameter plane electrode until the correct gap distance is obtained. The high-voltage is applied to the plane electrode via the same micrometre screw. Next to the point electrode is a rounded probe for displacement current

compensation during the charging of the plane electrode. The probe and the point electrode are both guarded and effectively grounded. A grounded metal shield is placed on the inner wall of the test-cell in order to obtain more defined and symmetric stray capacitances. The test cell can be cleaned by removing both electrodes and both glass windows. It is filled with liquid samples by first removing one of the PTFE screw caps, see Figure 4.
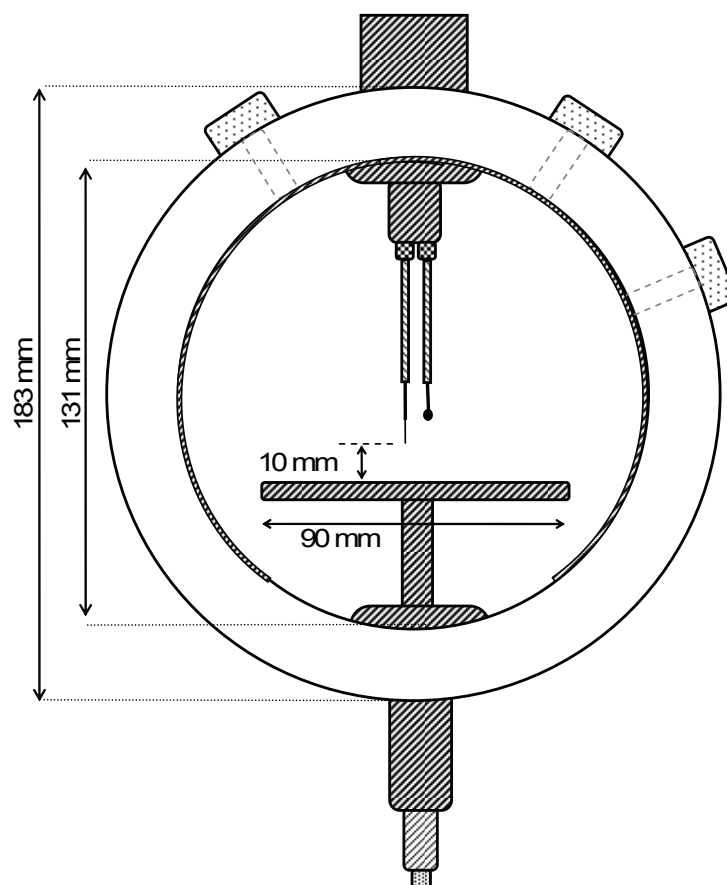
Figure 4. The cylindrical PTFE-test cell (120 mm deep) with a 10 mm point-to-plane electrode geometry, and cylindrical metal shield at the interior wall. Three PTFE screw caps are located on the top.

3.4. Point and Probe Electrode Arrangement

The electrode design is based on the Brüel & Kjær JP0012 miniature connector. It involves a manually threaded steel tube and a PTFE tube that must be properly stretched to fit both into the steel tube and onto a chromatograph needle, see Figure 5. For the point electrode, a 100 μm diameter wolfram wire is carefully pulled through the chromatography needle. It is then etched into a near-hyperbolically shaped point with point radii in the range 1.3–1.5 μm. A careful

clamping on the needle ensures that the wolfram wire will be fixed with a good electrical contact. The probe electrode is simply made from soldering a metal knob directly onto the end of a chromatograph needle.
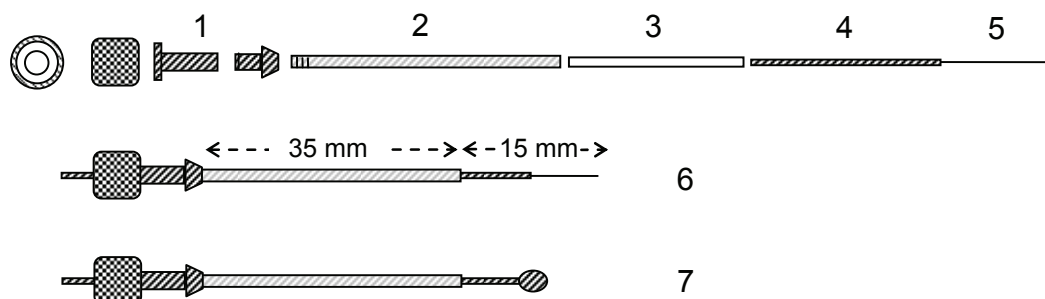
Figure 5. Point and probe electrodes: (1) Brüel & Kjær JP0012 miniature connector, (2) manually threaded steel tube: 2 mm outer diameter, 1 mm inner diameter, (3) VICI Precision Sampling PTFE tube (TTF130): 1.6 mm outer diameter, 0.76 mm inner diameter , (4) VICI Precision Sampling chromatography needle (PS-555550): 0.71 mm outer diameter, 150 μm inner diameter, (5) 100 μm diameter wolfram wire, (6) assembled point electrode, (7) assembled probe electrode with solder knob.

Both the point and the probe electrode are mounted on the low-voltage bushing as shown in Figure 6. The part of the cables extending from the bushing are coated with ferromagnetic ring cores in order to suppress common mode high-frequency noise, and additional shielded with a copper braid to prevent picking up interfering noise (not shown).
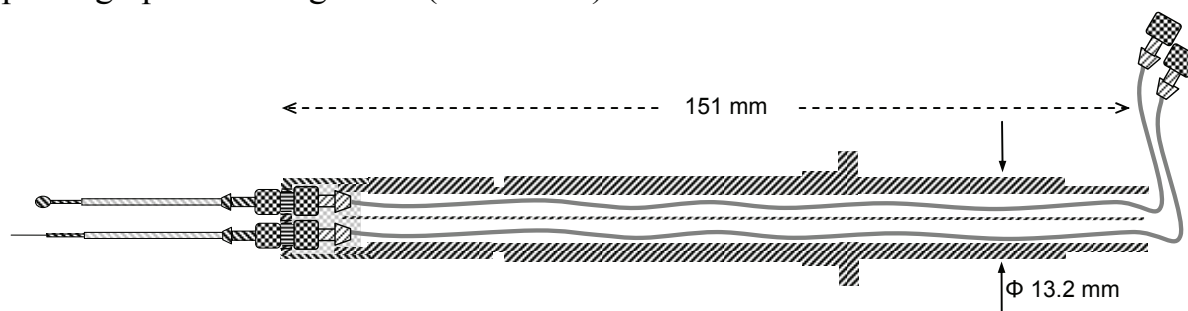
Figure 6. Electrode bushing cross-section with two PTFE insulated low-noise coaxial cables (Brüel & Kjær AC 0005) connecting the point and probe electrodes to the differential amplifier. Cables are of equal lengths (20 cm) and terminated with Brüel & Kjær JP0012 miniature connectors at both ends. Connectors (incl. join connectors) inside the bushing are sealed with epoxy. The bushing is made of brass, whereas an additional shielding between the cables is made of copper.

The etching of the wolfram wire was done electrochemically [87], using a 2 M potassium hydroxide solution and a DC power supply. Typically, 12–14 V was applied, and a steel ring served as the cathode inside the solute. The process is as much a craft as a science. Etching was performed by repeated dipping of the anode (wolfram wire) into the solvent inside the cathode ring. Each dip lasted 3–5 seconds. Point radii were measured with about 0.3 μm accuracy using a microscope. In our case, the approximation to a hyperboloid is typically valid only the first 40–50 μm of the point lengths, see Figure 7. A hyperbolical shape is advantageous since Laplace's equation is separable in prolate-spheroidal coordinates, making it possible to analytically approximate the electric field distribution in the point-to-plane gap prior to a prebreakdown event.
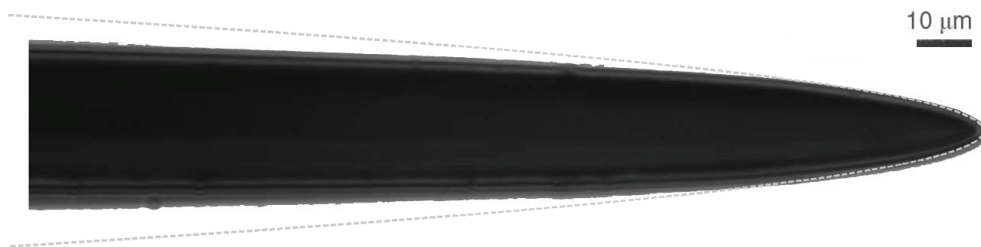
Figure 7. Wolfram wire (100 μm diameter) electrochemically etched to a point with a point radius of about 1.5 μm. The point shape can be approximated to a hyperboloid surface (grey dashed line).

3.5. Differential Charge Measurement

The differential charge measurement makes a capacitive current compensation during the charging of the plane electrode. The technique employs the differential electrode arrangement described in section 3.4, where the signals induced on the probe and point electrodes is subtracted in a differential amplifier ((14) in Figure 3). Since streamers are generated at the point electrode and not at the probe, the technique effectively separates capacitive displacements currents from currents induced by the prebreakdown event.

For the differential electrode arrangement, it is very difficult to position the probe and point electrode in such a way that they are equally coupled to the plane electrode. Their capacitive currents will therefore not be equal, and the measuring circuit must accommodate the difference. In the balancing setup, this

is done by implementing the electrode gap capacitances in a capacitive voltage divider circuit, as shown in Figure 8.
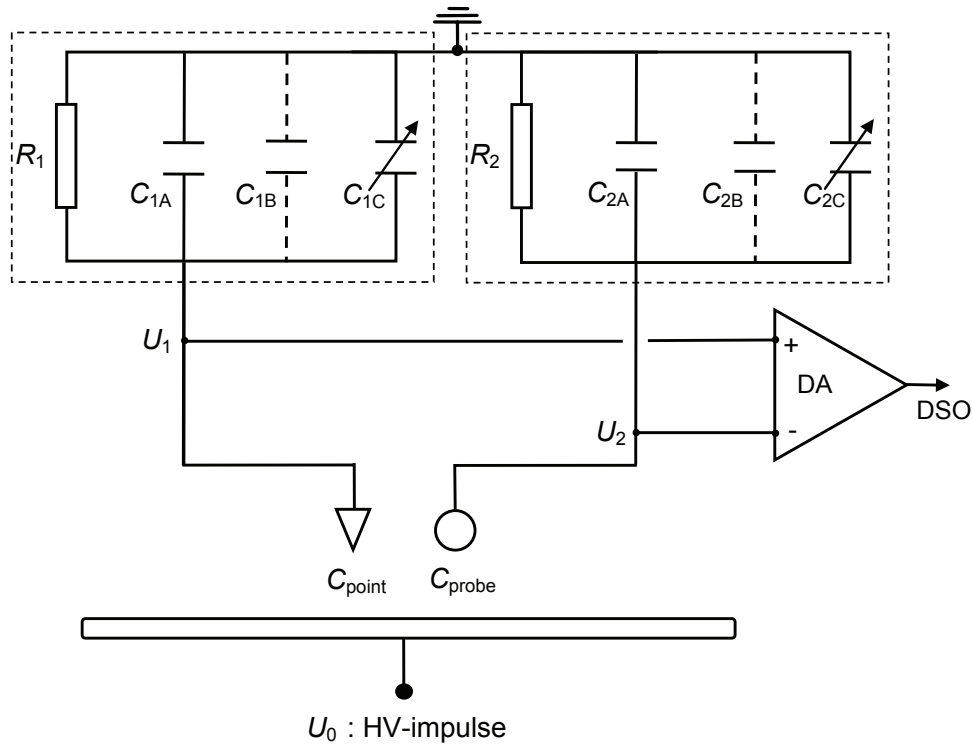
Figure 8. Diagram of the electrode gap and the differential charge measurement circuit: C_{1A} / C_{2A} = 470 ± 0.25 pF - class 1 - 100 V miniature ceramic plate capacitors (BCcomponents), C_{1B} / C_{2B} = differential amplifier input capacitance (20 pF) + coaxial cable capacitance (30.2 pF) = 50.2 pF. C_{1C} / C_{2C} = 5 – 40 pF adjustable air-gap capacitors made of concentric metallic cylinders. R_1 / R_2 = differential amplifier input resistance (selectable 100 or 1 MΩ). DA = 100 MHz differential amplifier of type Lecroy model DA1850 with state-of-the-art overdrive recovery, very low noise, and a common mode rejection ratio (CMRR) of 779 : 1 at 10 MHz, 58824 : 1 at 100 kHz, and 117647 : 1 at 70 Hz. DSO = Tektronix TDS 540A digital sampling oscilloscope, 20 MHz bandwidth limited. The two measuring circuits are built in separate metal boxes (dashed lines) with low-inductive ground connections (and connected directly to the inputs of the differential amplifier with BNC T-connectors).

In practise, the greater part of the calibration is done by manipulating the gap distance between the probe and the plane, thus attempting to match the value of C_{probe} with that of C_{point}. A subsequent fine calibration is performed by adjusting C_{1C} and C_{2C} until the voltage U_2 equals the voltage U_1, when impulse voltages below streamer initiation levels are applied to the plane. The balancing equations are simply,

$$U_1 \;=\; U_2 \tag{3.5.1}$$

$$\frac{C_{\text{point}}U_0}{C_1} \;=\; \frac{C_{\text{probe}}U_0}{C_2} \tag{3.5.2}$$

$$C_{\text{point}}C_2 \;=\; C_{\text{probe}}C_1 \tag{3.5.3}$$

where $C_1 = C_{1A} + C_{1B} + C_{1C}$ and $C_2 = C_{2A} + C_{2B} + C_{2C.}$ The effective capacitors C_1 and C_2 are placed parallel to the input resistors of the differential amplifier and will integrate the current running in the respective electrodes. C_1 is the measuring capacitor for the charge induced by the prebreakdown phenomena. After each calibration, C_1 and C_2 are measured with a Fluke PM6306 automatic RCL meter. The time constant in each bridge is about 50 ms, sufficient to maintain the balance during the time of measurement. Differences in the time constants due to unequal values of C_1 and C_2 have insignificant influence on the balance on this time-scale.

There are four crucial factors affecting the ability to have well-balanced differentiated signal in the millivolt range:

1. The layout of both sides of the "bridge", including the point and the probe electrode, must be made with perfect symmetry in order to obtain equal parasitic capacitances.

2. The shielding of the balancing circuit, differential amplifier, and connecting cables must be very good, and the cables of low-noise, high-quality types. This is to avoid capturing interferences (mainly originating from the impulse generator) that will increase the noise level and reduce the performance of the differential amplifier. Moreover, low-inductive ground connections must be placed directly at the inputs of the amplifier in order to bypass high-frequency ground noise currents.

3. The lengths of the cables connecting the point and the probe to the differential amplifier (Figure 6) should be identical to within a few millimetres. This is to avoid an unbalance at high signal frequencies caused by a physical time delay between both sides.

4.   Measuring capacitors must be carefully selected. Several capacitors produced a "hump" on the signals in the millivolt range with some microsecond durations, frequently observed as a residual signal after differentiation. The reason may be polarization processes with long time constants within the dielectric capacitor material. For C_{1A} and C_{2A}, we, and ended up selecting empirically the best pairs among some class 1 ceramic plate capacitors (as advised by O. Lesaint in *G2E-lab*). We did not find good ceramic trimmer capacitors for C_{1C} and C_{2C}. The ones tested gave a residual signal, significantly influenced by the humidity in the atmosphere around the components. A pair of old air-gap capacitors made of concentric metallic cylinders was used instead. These were of the type originally designed for radio frequency tuning.

The size of the actual measuring capacitor, C_1, was chosen to be approximately 550 pF, where a 0.55 pC charge is measured as a 1 mV voltage step on the oscilloscope. This is just above the noise level and therefore representative of the charge sensitivity for the selected capacitance. Average streamer currents can be derived from the slope of streamer charge versus time, with sensitivities determined by the duration of the measurement. Currents were typically averaged over 20 μs, giving a sensitivity of 25 nA. The total record length for each measurement was 15 000 samples, with a sampling time of 4 nanoseconds. The signal was bandwidth limited to below 20 MHz, using the internal signal filter of the oscilloscope. For streamers above a certain size / length, capacitors can be replaced with larger ones (and the system re-calibrated) to avoid saturation of the differentiated signal (here at 0.5 V). We used the built-in attenuator of the amplifier as a more convenient alternative, but with the disadvantage of reduced input impedance, leading to faster charge drainage from the measuring capacitor. Consequently, charges induced in the range 0.3–3 nC were underestimated by 1–2%. The scatter in measurements due to the randomness of the phenomena is several times larger. At each high-voltage level, the internal amplification of the oscilloscope had to be carefully set in order to obtain the best resolution for the corresponding charge, yet without saturating the largest signals.

3.6. *High-Voltage Impulse Generator*

The high-voltage impulse generator in Figure 9 can be controlled to supply high-voltage pulses with variable pulse widths and with rise and fall times of 15–20 ns. It basically consists of two separately triggered spark-gaps: high-voltage from a Spellman high-voltage DC supplier is switched on by the first, and chopped by the second. The impulse generator has a low-inductance design necessary to generate voltage waveforms with fast rise -and fall-times, and without ringing or oscillations.
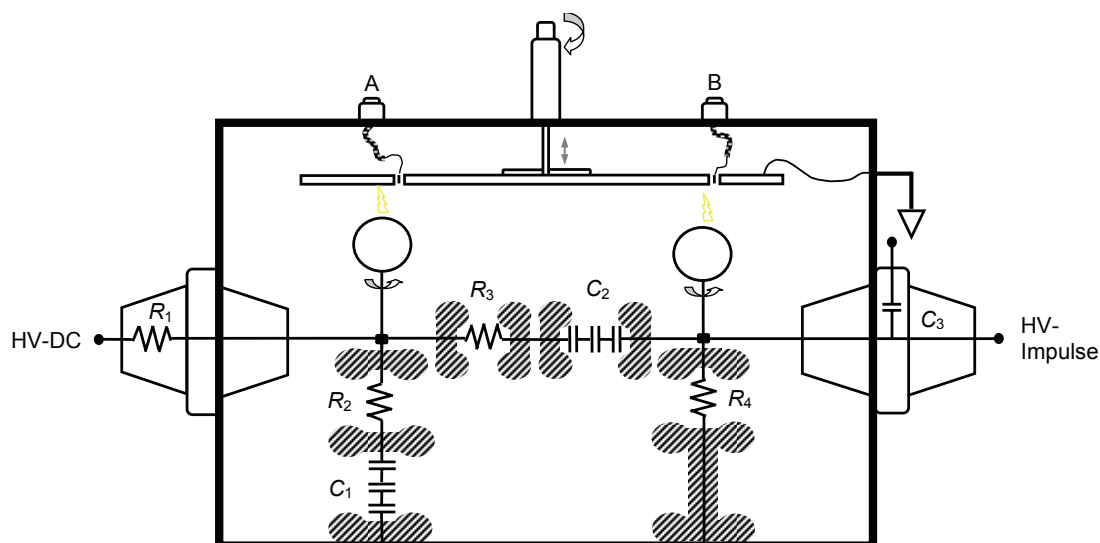
Figure 9. Illustration of the high-voltage impulse generator (~80 cm x 55 cm x 35 cm) with spark gaps located between the respective sphere electrodes and a grounded plane electrode: $R_1 = 50$ MΩ, $R_2 = 200$ Ω, $R_3 = 86$ Ω, $R_4 = 50$ MΩ. R_2 and R_3 are bi-wired to cancel component inductance, C_1 / $C_2 = 3$ x 3.3 nF high-voltage capacitors (Vishay Cera-Mite, 40 kV), $C_3 = 0.14$ pF epoxy insulated capacitive probe. During standby, the left-hand side of C_2 is kept at constant high-voltage while the right-hand side is effectively clamped to ground potential. The sphere-plane gaps are ignited with spark-plugs at the ground plane (off-axis relative the sphere-plane gap), using -6 kV impulses via *A* and *B*. The impulse voltage at the right-hand side of C_2 is maintained at a steady level during tens of microseconds by R_4.

The spark gaps in Figure 9 were triggered with high-voltage pulsers designed to work with the Thyratron 5C22 hydrogen-filled triode tube, providing -6 kV pulses with risetimes of 50 ns into a 50 Ω load. A Thyratron is basically a "controlled gas rectifier". The 5C22 variant has particularly short switching times [88], and is rated for voltages from 4 to 16 kV. It has several other

advantages required for this setup; robustness against return-voltages from the impulse generator, low sensitivity to parasitic and electromagnetic noise, and a trigger jitter as low as 2 ns. The working principle of the Thyratron pulser is shown schematically in Figure 10.
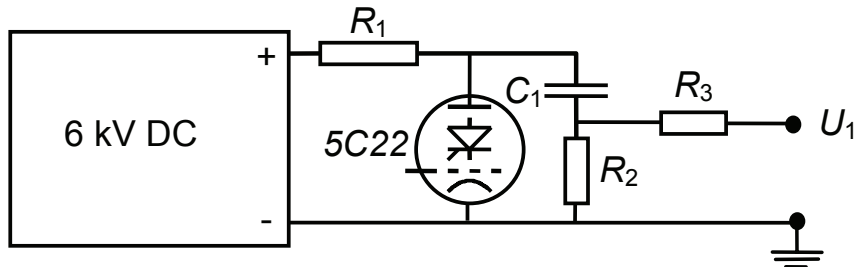
Figure 10. Circuit schematics of a Thyratron pulser: R_1 = 3.9 MΩ (15 W, 30 kV), R_2 = 50 Ω (12 kV), R_3 = 20 kΩ (12 kV), C_1 = 0.1 µF (10 kV ceramic pulse capacitor), 5C22 = Thyratron tube. The capacitor C_1 is charged via R_1 with a 15 V – 6 kV EMCO DC–DC transformer.

Each Thyratron pulser is triggered via a fiber-optic signal, using a fiber-optic receiver from Agilent (HFBR2412) (not shown). The electrical signal from the receiver is transformed into the voltage required to ignite the discharge tube (250 V). When the tube ignites, the anode-side of the pulse capacitor C_1 is pulled toward ground, while the cathode side (U_1) is pulled from ground potential toward -6kV. The length of the impulse generated at U_1 is determined by the size of the pulse capacitor C_1 and the load resistance (R_3 if no external load). The value of 0.1 µF gives for short-circuited terminals a pulse length of 5 µs, optimal for igniting the impulse generator in Figure 9. The output resistance R_2 limits the current running through the tube with short-circuited terminals. It also provides an impedance match to 50 Ω high-voltage coaxial cables connecting the Thyratron pulsers to the impulse generator.

3.7. High-Voltage Probe

The high-voltage pulses from the impulse generator in Figure 9 were measured with a passive integrator connected to the high-voltage capacitive probe (C_3) located in the grounded metal case at the high-voltage outtake, see Figure 11. A circuit diagram of the 60 ms integrator used is also shown in Figure 11, whereas a more detailed description can be found in reference [89].
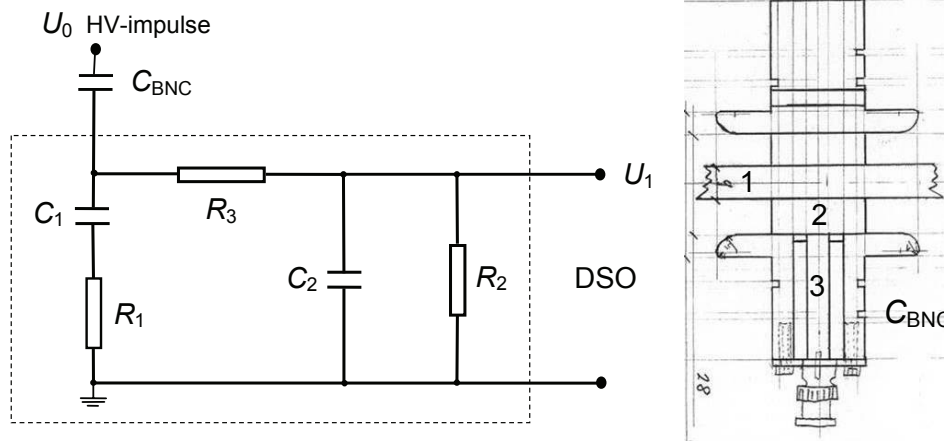
Figure 11. Left: circuit diagram of the passive integrator (in dashed rectangle) used to probe the high-voltage pulses: $C_1 = 0.1\ \mu F$, $C_2 = 74$ pF, $R_1 = 50\ \Omega$, $R_2 = (1\ M\Omega\ \|\ 1\ M\Omega_{DSO.} + 150\ \Omega)$ $\approx 0.5\ M\Omega$, $R_3 = 100$ kΩ. Right: epoxy insulated high-voltage capacitive probe ($C_{BNC} = 0.13$ pF): 1. high-voltage outtake, 2. insulating epoxy, 3. metal cylinder with BNC connector, immersed in transformer oil.

For times longer than the time constant $R_1 \cdot C_{BNC} \approx 6.2$ ps, the current to the integrator is proportional to the time-derivative of the high-voltage pulse U_0,

$$I_0(t) = C_{BNC} \frac{dU_0(t)}{dt} \tag{3.7.1}$$

This current is integrated by the passive integrator, which gives a signal to the oscilloscope (DSO),

$$U_1(t) = \frac{R_1 C_{BNC}}{R_3 C_2} U_0(t) = k U_0(t) \tag{3.7.2}$$

Thus, the signal to the oscilloscope is proportional to the high-voltage impulse by a calibration factor k.

3.8. Chemicals and Procedures for Sample Preparation

Cyclohexane was used as base liquid because it is a simple and well-described alkane and may serve as a model liquid for insulation oils. Cyclohexane is also a good solvent and allows quasi-free electrons to exist long enough to react with

the additives. The cyclohexane liquid used in this study is of type Merck LiChrosolv® with purity better than 99.9%. Cyclohexane was first dried with 3Å Zeochem® Molecularsieve added to the original bottles for a period of no less than two weeks. This reduced the moisture content from ~19 to 1–3 µg/g. After removing the Molecularsieve, cyclohexane was degassed during one week in a closed vacuum reservoir at 70 mbar, using an extraction volume ten times the liquid volume. One additive was mixed with cyclohexane overnight in a closed bottle with argon atmosphere, using a magnetic stirrer. The contents of oxygen gas, carbondioxide gas and nitrogen gas subsequent to degassing and mixing were not measured, but are below their respective saturation levels in cyclohexane; 0.47, 3.90 and 0.25 mg/g [90]. An IRLAB (LDTRP-1) low-voltage, low-frequency conductance-meter was used to measure the low-field conductivities of the liquids. Additives used in this study have been listed in Table 1, whereas their molecular structures are shown in Figure 12.

Figure 12. Molecular structure of additives.
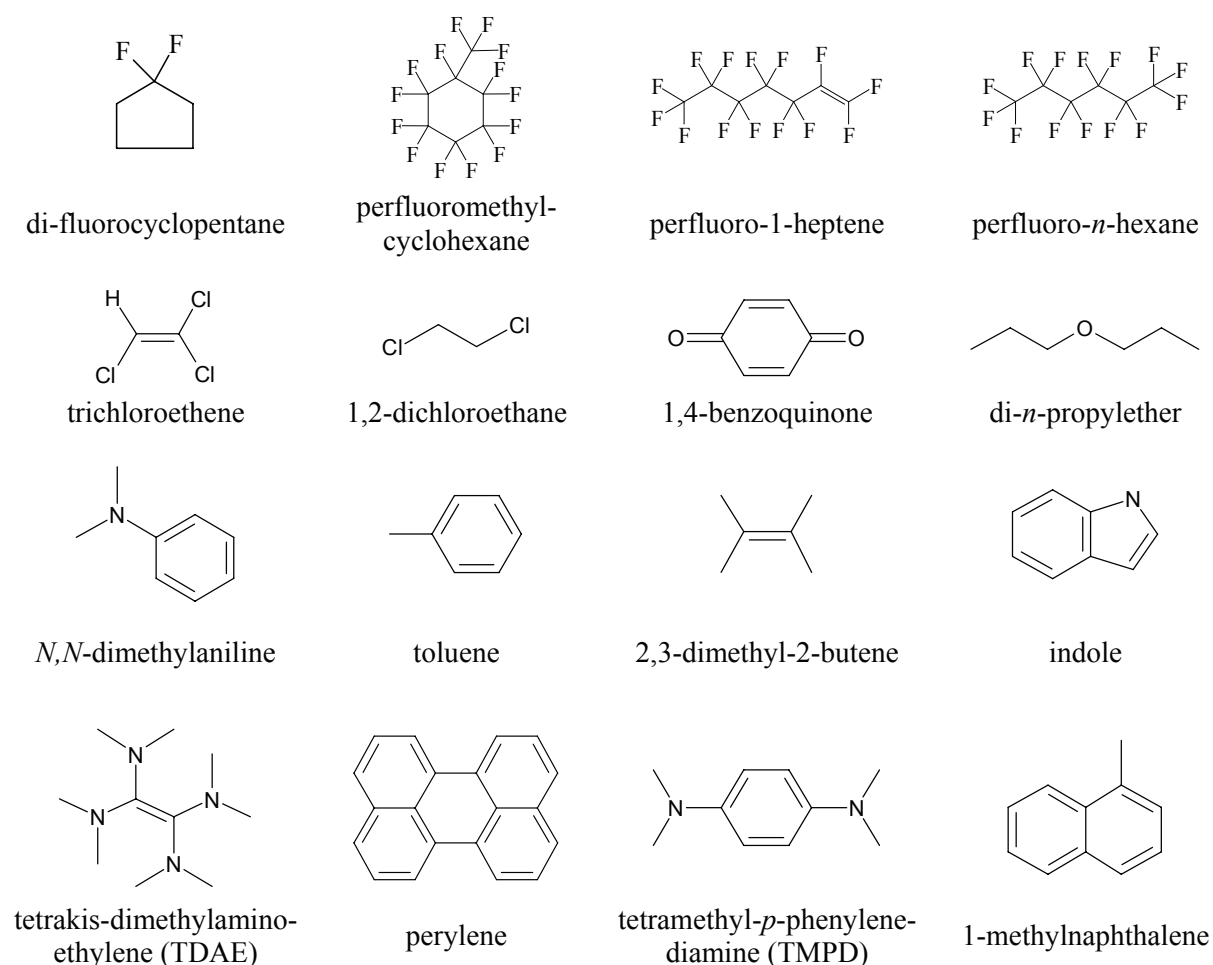
Table 1. Tabulated properties of chemicals; density (ρ), molar mass (M), boiling temperature (T_b), melting temperature (T_m), heat capacitance (C_p), viscosity (η), gas-phase ionization potential (I_1) and relative permittivity (ε_r). Molecules are listed in descending order of ionization potentials.

Liquid	Brand	ρ (g/cm^3)	M (g/mol)	T_b (°C)	T_m (°C)	η (mPas)	I_1 (eV)	C_p (J/gK)	ε_r
perfluoromethylCH	Fluka 77280	1.79[a]	350[a]	76.3[a]	-44.7[a]	1.56[b]	12.1[a]	1.01[a]	1.82[c]
perfluoro-n-hexane	Aldrich 281042	1.70[a]	338[a]	56.6[a]	-88.2[a]	0.67[b]	11.7[j]	0.71[e]	1.76[c]
1,2-dichloroethane	Riedel 34925	1.25[a]	99[a]	83.5[a]	-35.7[a]	0.78[b]	11.0[a]	1.30[a]	10.4[c]
di-fluorocyclopentane	SynQuest	0.93[i]	106[d]	66			10.8[j]		
perfluoro-1-heptene	Apollo PC6040	1.77[i]	350[a]	81.0[a]			10.5[a]		
1,4-benzoquinone	Fluka 12309	1.32[a]	108[a]	sub[a]	115[a]		10.0[a]	1.17[f]	
cyclohexane (CH)	Merck 102827	0.77[a]	84[a]	80.7[a]	6.6[a]	0.90[b]	9.86[a]	1.84[a]	2.02[c]
trichloroethene	Sigma 251402	1.46[a]	131[a]	87.2[a]	-84.7[a]	0.53[b]	9.46[a]	0.95[a]	3.39[c]
di-n-propylether	Fluka 43460	0.75[a]	102[a]	90.1[a]	-115[a]	0.40[b]	9.27[a]	2.17[a]	3.38[c]
toluene	Merck 108327	0.87[a]	92[a]	111[a]	-95.0[a]		8.82[a]		2.38[c]
2,3-dimethyl-2-butene	Aldrich 220159	0.71[a]	84[a]	73.3	-74.1[a]		8.27[a]		
1-methylnaphthalene	Merck 820809	1.02[a]	142[a]	245[a]	-30.4[a]	2.62[b]	7.97[a]	1.58[a]	2.92[c]
indole	Aldrich I3408	1.22[a]	117[a]	254[a]	52.5[a]		7.76[a]		
N,N-dimethylaniline	Merck 803060	0.96[a]	121[a]	194[a]	2.4[a]	1.28[b]	7.12[a]	1.77[a]	5.02[c]
perylene	Merck 820969	1.35[a]	252[a]		278[a]		6.96[a]	1.09[a]	
TMPD	Sigma T7394		164[a]	260[a]	51[a]		6.75[g]		
TDAE	Aldrich 674613	0.87[i]	200[i]	59[i]			6.11[h]		

[a] Ref. [1], [b] Ref. [91] (at 25°C), [c] Ref. [92] (at 25°C), [d] Ref. [93], [e] Ref. [94], [f] Ref. [95], [g] Ref. [96], [h] Ref. [97], [i] data on bottle, [j] Ref. [98]

The majority of the additives were selected to span a wide range of electron-releasing and electron-attaching capabilities, based on documented experimental gas-phase ionization potentials (Table 1), and/or well-studied electron scavenging capabilities (Table 1 in Paper #3). Solubility, low-toxty -and carcinogenicity, availability and price were additional constraints in the selection process. Three of the molecules, perfluoro-n-hexane, 1-methylnaphthalene and *N,N*-dimethylaniline, have previously been used as additives in streamer studies [68,84]. Tetramethyl-*p*-phenylenediamine (TMPD)

was selected because the electron releasing capability of this molecule as an additive in different solvents has been studied extensively [96].

The range of additive concentrations spans from trace impurities (~100 ppm) to higher concentrations (~5 %), except for 1,4-benzoquinone and perylene which we only managed to dissolve in low concentrations (<1 ‰). The additives had purities better than 99%, expect for perfluoro-1-heptene, di-fluorocyclopentane and tetrakis-dimethylamino-ethylene, having purities better than 97%. Additives were not subjected to additional purification.

3.9.   *Data Analysis*

As shown in Figure 13, we obtain from the shadowgraphic images the maximum extension (length) and the streamer shadow area projected to the image plane. This was done using the public domain Java image processing program "ImageJ" [99]. The program can display, edit, analyze and process series of images that share a single window (stacks). The software calculates area and pixel value statistics of user-defined selections, and includes an option for spatial calibration. Data are automatically stored for each image, and the results from a sequence of measurements are exported to a text file.
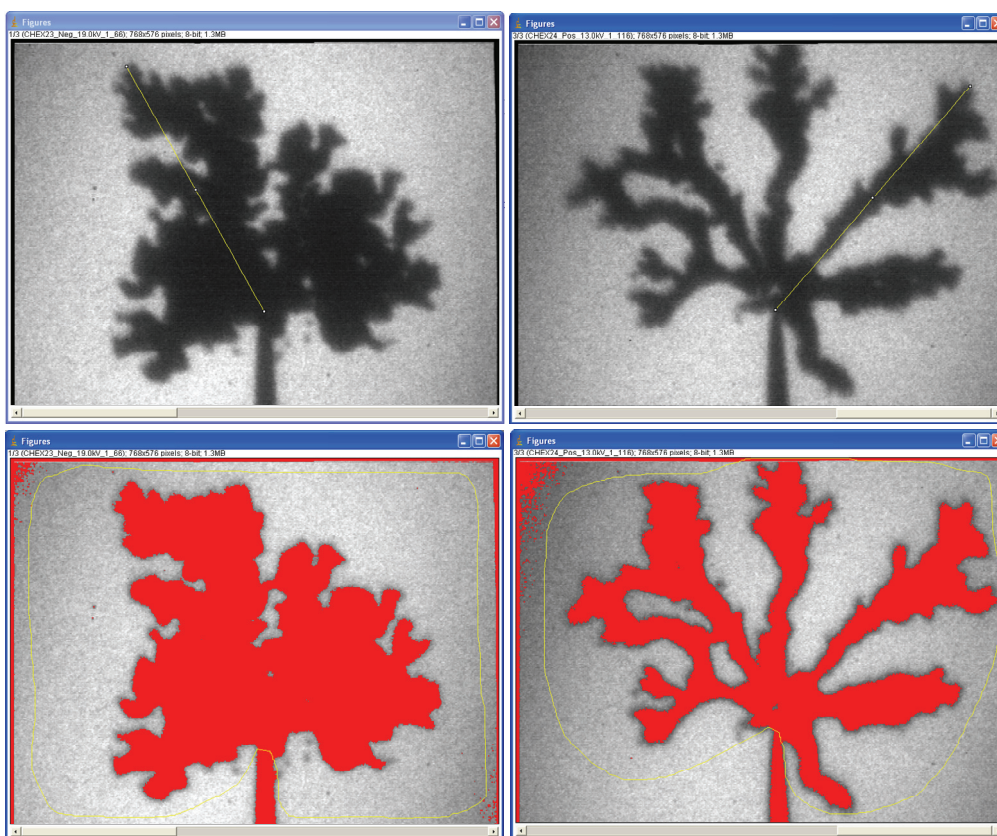
Figure 13. Measurements of radial streamer length (upper), and streamer shadow area (lower) from a negative (left) and a positive (right) streamer, using the software *ImageJ*. Streamer length is measured by placing a line between the apex of the point electrode to the most distant region of the streamer. The area of the shadow is subtracted and measured by making a selection of pixels with pixel levels below a suitable pixel level threshold (red-coloured region). The measurement is made within a user-defined area defined by the yellow contour line.
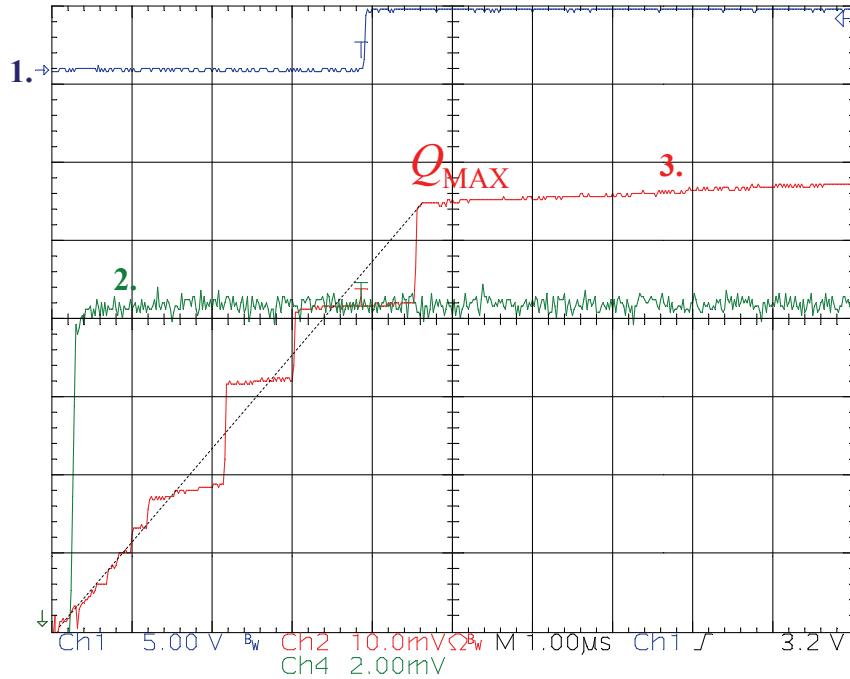
Figure 14. Capture of the oscilloscope display with three active channels: 1. synchronization signal for camera, 2. probed high-voltage signal, 3. charge signal induced by streamer propagation. The average streamer current is the slope of the dashed line.

Files containing numerical signals for streamer charge, applied voltage, and camera-synchronization were automatically imported and analyzed using a Matlab® script. The analysis was based on calibration values provided by the user. Charge signals were first classified into initiations and non-initiations, including various exception-handles to detect abnormal behaviour (e.g. saturated or missing signals, voltage pulses that had been prematurely clipped, etc.). Conduction currents prior to streamer initiation were averaged during the first 20 μs after the voltage pulse was applied. For each streamer, the number of detectable current pulses (charge steps), their sizes and the interval between two consecutive pulses were analyzed. The maximum streamer charge is defined as the charge of the signal after the final charge-step, see Figure 14, and the average streamer current is calculated from the slope of streamer charge versus time up to this point. The raw data, the analysed results and the user-defined parameters for each additive concentration were stored in separate databases. These data could easily be retrieved for graphical presentation or further treatment. Results from the image analysis were imported into the database files. The storage of raw data proved useful in many cases, e.g. one could locate the charge measured at the exact time of the image when plotting the charge of each streamer versus its length or shadow area.

3. Setup for Study of Additives in Cyclohexane

4.   SETUP FOR STREAMER EMISSION SPECTROMETRY

The experiment was designed to study light emitted from luminous positive and negative streamers. It was also designed to make shadowgraphic images, and to measure the current and charge induced to the point electrode during streamer propagation. These experiments were performed in two parts; one for the measurement of individual streamer lengths, illuminations times, streamer charge and current, and one for the spectroscopic investigations, where light emitted from a series of streamers were accumulated. The first part resembles the setup already described in section 3, and will not be described in the same systematic way.

A 5±0.3 mm point-to-plane gap was placed inside a ~10 ml PTFE test cell with two aligned fused silica windows, see Figure 15. Point electrodes were made by electrochemically etching a 100 μm wolfram wire into near-hyperbolical shaped points with radii in the range 1.1–1.3 μm. Alternatively, we used triangular-shaped Ogura™ needles with about the same tip radii. High-voltage 0.1/50 μs impulses with a fixed voltage level of -30 kV were applied either to the point or the plane electrode. In some special cases, +30 kV 0.5/50 μs impulses were applied only to the plane electrode. The high-voltage impulse generator is a vacuum tube rectifier, fed by a Spellman SL150 DC high-voltage supplier. The working principle is similar to that already described in Figure 10.
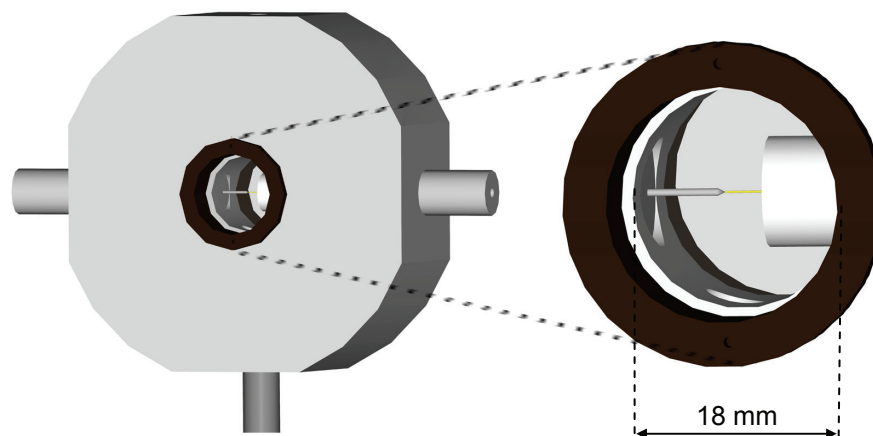
18 mm

Figure 15. Illustration of the PTFE cell with 18 mm diameter fused silica windows, and a 5 mm point-to-plane gap. The gap distance can be regulated by moving the electrodes back and forth (and verified with a long distance microscope mounted on a micrometer positioning system). The distance from the point electrode to each window is about 15 mm.

4.1. Conventional Techniques

The experimental setup involved an image intensifier camera in order to picture the different light-emitting regions of the streamer, a synchronously pulsed high-intensity light-emitting diode for shadowgraphic imaging, alternatively a photomultiplier tube for studying the temporal streamer emission, see Figure 16. Both the time of image and exposure could be varied and were controlled with a TTL gate/delay signal generator, allowing images to be taken during different stages of propagation. Shadowgraphic images were also taken with a conventional analogue CCD camera, for which the effective exposure was determined by the illumination duration of a high-intensity light-emitting diode. The diode performed well with a response time less than 100 ns, and was pulsed with a classical power transistor (MOS) and a 10 Ω resistor in series with the diode to control the current.
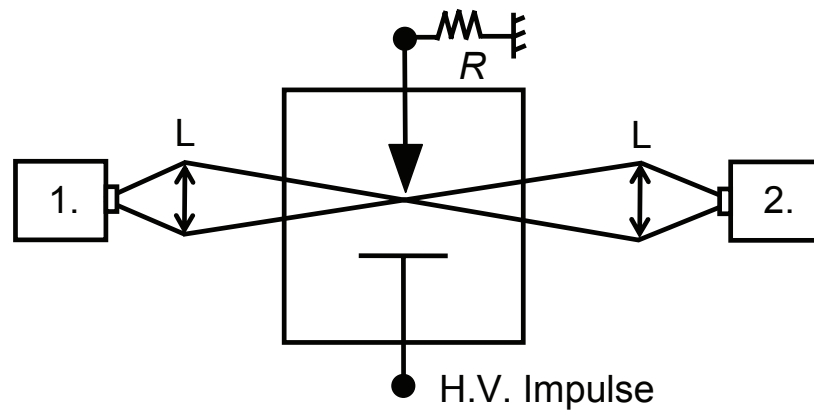
Figure 16. Right; general experimental outline, 1. gated image intensifier camera (Hamamatsu) / analogue CCD camera with sensitivity 0.1 lux (Bosch LTC335) / spectrograph (SpectraPro 300i) , 2. photomultiplier tube / high-intensity light-emitting diode (Philips Luxeon®). The current and charge induced to the external circuit is measured on a resistor / capacitor placed in series with the effectively grounded point electrode. The applied high-voltage is measured with a high-voltage probe (Tektronix P6015).

The streamer current and charge induced to the external circuit were measured respectively on a resistor and a capacitor placed alternately in series with the point electrode on the low-voltage side. As shown in Figure 17-A, the point electrode was insulated from ground, and, in order to reduce capacitance to the plane (and thus the capacitive current), it was shielded up to about one millimeter from the tip. This electrode arrangement was designed for triangular-

shaped Ogura needles only. The measurements of current and charge of negative streamers required the alternative arrangement of a positive high-voltage impulse to the plane electrode. Due to pulse-source limitations, we managed in this case a pulse rise-time of only 500 ns. The electrical measurements for each streamer (current / charge and probed voltage) were stored in separate text files, and later analyzed in detail on a computer. The time in-between each measurement was not strictly controlled, but generally above one minute, being the typical duration of manually storing data from the previous streamer.
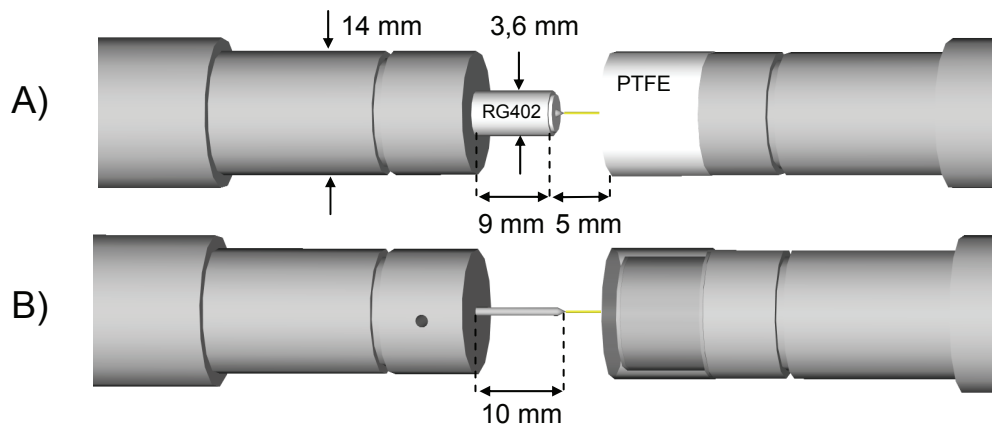
Figure 17. Illustration of the two 5 mm point-to-plane electrode arrangements with and without guarded electrodes (A/B). The guarded arrangement in (A) is made from replacing the center conductor of a semi-rigid 50 Ω microwave cable (RG402) with a 1 mm Ogura™ needle. The cable is positioned axially inside the electrode bushing. The plane electrode is ~12 mm in diameter and insulated with a PTFE cap in order to prevent electric breakdown resulting from streamers traversing the electrode gap. The PTFE cap is made transparent in B.

4.2. Streamer Emission Spectrometry

In the second part of the experiment, a series of high-voltage impulses was applied at 1 Hz repetition rate, controlled by the TTL-signal gate/delay generator. Optical emission from the 10–15 μm region at the apex of the point electrode was collected with a condenser and secondary focusing lens system, see Figure 18. In this setup, the image of the point is focused directly onto the 10 μm wide entrance slit of the spectrograph, located perpendicular to the point-to-plane axis. The small distance (~25 mm) from the point electrode to the condenser lens facilitates the collection of light to the spectrograph. Only (un-guarded) wolfram needles were used for this part, as they were more reliable at producing

streamers for each applied impulse during long series of impulses (Figure 17-B). The total number of impulses applied determined the number of streamers recorded.
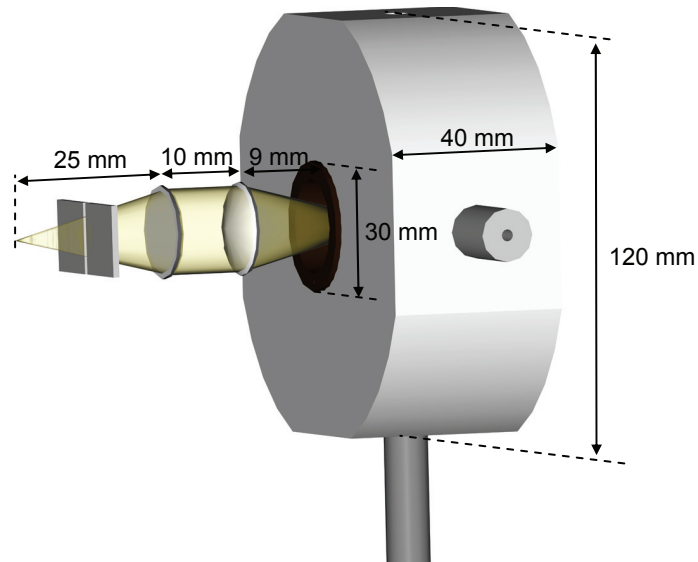
Figure 18. The condenser and secondary focusing lens system for imaging the point electrode onto the 10 μm wide entrance slit of the spectrograph. Both lenses and windows are made of fused silica. There is principally no magnification due to identical plano-convex lenses (18 mm diameter, 25 mm focal length).
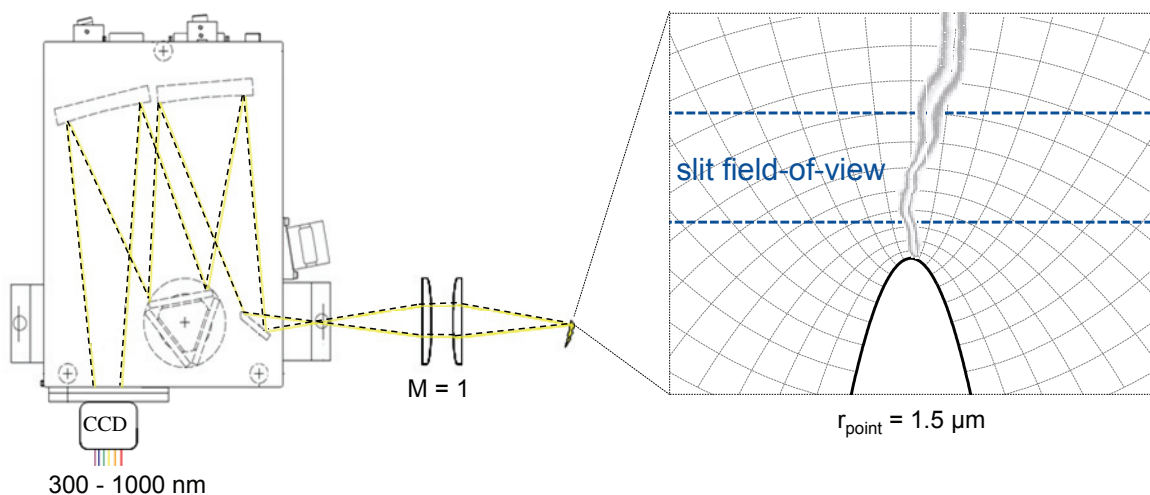
Figure 19. Illustration of the spectrograph, SpectraPro-300i, focal length $f = 300$ mm, $f/4$ aperture, with the triple grating system. The setup accumulates light emitted from the first ~10 μm trail of a streamer, corresponding to the entrance slit of the spectrograph.

A continuously open charge-coupled device (CCD) is located directly on the exit plane of the spectrograph, and cooled to a temperature of 153 K in order to reduce the dark current. Liquid nitrogen was used as cooling medium. Since the detector collects only a small amount of light from each streamer, it was necessary to integrate the light emitted during a series of 1500–2000 streamers in order to obtain useful data. Thus, single acquisitions were performed with exposure durations up to one or two hours.

The spectrograph, is equipped with three blazed (reflection) diffraction gratings with different resolutions, one with 150 grooves per millimetre and two with 1200 grooves per millimetre, blazed at 750 nm and 300 nm. The spectral range of the system in wavelengths is from 300 to 1000 nm, and the instrumental broadening $\Delta\lambda_{ins}$, measured by recording profiles of argon and neon lines from low-pressure discharge lamps, is 0.11 nm for the 1200 grooves per millimetre grating, and 2.8 nm for the 150 grooves per millimetre grating. Radiant energies have been quantified for wavelengths up to 900 nm by measuring the response of the spectrograph arrangement to a broadband light source with known spectral irradiance.

The liquids studied were dichloromethane (Riedel 34908), 1,2-dichloroethane (Prolabo 23341), tetrachloromethane (Merck 102209), trichloroethene (SDS-Chemicals 0740221), and tetrachloroethene (Merck 100964), see Figure 20 and Table 2. The liquids had purities better than 99%, and were not further purified before introduced into the test cell.

| 1,2-dichloroethane | dichloromethane | trichloroethene | tetrachloroethene | tetrachloromethane |
| $\zeta = 0.25$ | $\zeta = 0.40$ | $\zeta = 0.50$ | $\zeta = 0.67$ | $\zeta = 0.80$ |
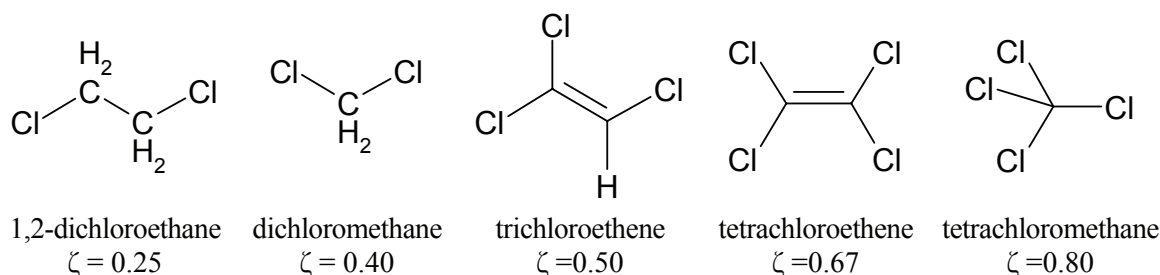
Figure 20. Chemical structure of chlorinated alkanes and alkenes, in ascending order of chlorination degree ζ.

The chlorinated alkane and alkene liquids in Figure 20 were chosen because their chlorination degrees span a relative large range, and the interactions between these molecules and electrons are well-documented in the gaseous phase [100-102]. Streamers in tetrachloromethane have been studied previously [74]. Note that the liquids 1,2-dichloroethane and trichloroethene were used as additives in section 3.

Table 2. Tabulated physical properties of chlorinated liquids: density (ρ), boiling temperature (T_b), melting temperature (T_m), critical temperature (T_c), critical pressure (P_c), critical volume (V_c), specific heat capacitance (C_p), viscosity (η), gas-phase ionization potential (I_1), relative permittivity (ε_r).

Liquid	ρ (g/cm^3)	T_b (^{o}C)	T_m (^{o}C)	T_c (^{o}C)	P_c (MPa)	V_c (cm^3/mol)	C_p (J/mol K)	η (mPas)	I_1 (eV)	ε_r
1,2-dichloroethane	1.25[a]	83.5[a]	-35.7[a]	288[a]	5.40[a]	236[a]	128.4[a]	0.78[b]	11.04[a]	10.4[c]
dichloromethane	1.32[a]	40.0[a]	-97.2[a]	237[a]	6.10[a]		101.2[a]	0.44[b]	11.32[a]	8.93[c]
trichloroethene	1.46[a]	87.2[a]	-84.7[a]	271[a]	5.02[a]		124.4[a]	0.53[b]	9.46[a]	3.39[c]
tetrachloroethene	1.62[a]	121.3[a]	-22.3[a]	347[a]			143.4[a]	0.85[b]	9.33[a]	2.27[c]
tetrachloromethane	1.59[a]	76.8[a]	-22.6[a]	283[a]	4.52[a]	276[a]	130.7[a]	0.93[b]	11.47[a]	2.24[c]

[a] Ref. [1], [b] Ref. [91] (at 25°C), [c] Ref. [92] (at 25°C)

5.   PURPOSE OF EXPERIMENTAL STUDY

5.1.   Working Hypothesis

Despite the large number of experiments already reported for prebreakdown phenomena in dielectric liquids, some clearly indicating the importance of molecular composition, it has not been established a reliable relationship between the dielectric strength and the molecular structure of the liquid to be used as a basis for a theory. The first step in this direction requires the identification of quantitative correlations between molecular descriptors and effects on measurable streamer characteristics. The purpose of the present investigations is to experimentally identify these descriptors and their quantitative correlation with macroscopic properties, such as the current or charge induced in an external circuit, streamer propagation length, velocity or shape (e.g. branching tendency). For this purpose we have generated streamers below the breakdown level in a point-to-plane electrode arrangement, and systematically investigated effects of electrochemically specified molecules dissolved in a simple base liquid. We have chosen cyclohexane as a base liquid because it is a simple and well-described alkane that may serve as a model liquid for insulation oils.

Two of the most interesting questions in the field of prebreakdown phenomena are; 1) how can energy be transferred from the electric field into the liquid, and 2) how can large concentration of net charge be formed in the liquid during some modes of streamer propagation. We believe that these questions are tightly connected to the electronic properties of the molecules comprising the liquid. Electron-molecule interactions, occurring both in the liquid and in the vapour, determine the transfer of energy and to a large extent the propagation behaviour of the streamer. We have focused on the abilities of the additives to either attach or detach electrons. These are traditionally described by the electron affinity and the ionization potential of a molecule, as well as cross-sections for electron-molecule interactions. Such parameters are either obtained empirically or from quantum chemical calculations. Our basis has primarily been existing data describing gas phase molecules and reactions, whose validities for the liquid phase have been evaluated. The study of additives is probably not the same as the study of the same molecules forming a continuous medium. The base liquid determines the electron energy distribution and the

field-dependence of this. Interactions between electrons and added molecules depend on the electron energy as well as the molecular structure of the additive, and it is not obvious that results obtained with cyclohexane are quantitatively transferable to another base liquid. However, the study gives a better foundation for assessing a molecular descriptor on an "equal footing" using different additives.

In a second part of this thesis work, streamers have been studied in five simple chlorinated alkane and alkene liquids (no additives). It is well known, that, for relative low voltages (below the breakdown level), faster, more filamentary and generally more luminous streamers emerge from halogenated liquids such as tetrachloromethane [74]. Similar experience has been made for liquid nitrogen [103] and for water [104]. The mechanisms behind the streamer acceleration particular for these liquids are not fully understood. In the present study, molecules with different degrees of chlorination have been selected, two of which were previously used as additives in cyclohexane solvent. The purpose was to study the streamers with techniques similar to those used in the study of the additives (which may elucidate the role of such molecules as additives and base liquids), including spectroscopic investigation of the emitted light. Streamer emission spectrometry is a promising technique for probing the physical conditions in a streamer, but needs to be experimentally and theoretically developed before it can be systematically employed to assess effects of e.g. additives. The luminous filaments / channels particular for streamers in the chlorinated liquids make it possible to consider high-resolution spectroscopic techniques.

5.2. Papers Presented

In Paper #1 we directed our attention to the initiation of streamers and the influence of additives. Results in pure cyclohexane were generally in line with those already reported under similar experimental conditions, but conclusive effects of the additives on the initiation of streamers were not found. In Paper #2, effects of the same additives were presented for streamer propagation. Qualitative results for positive and negative streamers were consistent with the electron-accepting and electron-releasing capabilities of the additives, and without a correlation to other physical or chemical parameters. These results

basically confirmed our hypothesis, and also what could be anticipated from earlier experimental evidence reported in the literature. Paper #3 focuses deeper on the electron-accepting and electron-releasing molecular properties in order to establish a quantitative relation to the propagation characteristics of streamers. The paper reports effects of a few more additives, selected to span the widest possible range of the electron-accepting and electron-releasing molecular properties. Quantitative correlations were found, and the Townsend–Meek theory for streamer inception in gases were adapted to a solution and applied to analyze the voltage dependence of the transition from a slow to a faster and more filamentary positive streamer mode. We also provided some clarification as to the origin of the two streamer modes for positive streamers, linking propagation to initiation. Paper #3 moreover addresses the problem with reproducibility of initiation voltages concerning electrode replacements, first reported in Paper #1. By using the same point electrode for different solutes, we found a statistically better agreement between each reference measurement. Paper #3 finally presents conclusive effects of additives with (very) low ionization potential on the initiation voltages for positive streamers. Paper 4# presents results of the spectroscopic investigations with the chlorinated liquids. Both positive and negative streamers are accelerated in these liquids, despite that no effects were observed from chlorinated additives on the propagation of positive streamers in cyclohexane [Paper #3].

The results accumulated from our work support the following overall picture concerning the prebreakdown phenomena in liquid cyclohexane: Both positive and negative streamers are initiated by an electron avalanche-like mechanism in the liquid phase at the tip of the point electrode. Differences between the two polarities with respect to initiation probabilities arise from the stochastic event of having a seeding electron available and suitably placed in the high-field volume [Paper #1]. For the electrode geometry used, typical initiation voltages for negative streamers are 7–8 kV, representing a lower bound for streamer initiation voltages (irrespective of point polarity) [Paper #3]. For voltages below this level, the distance from the point within which the electric field is above a critical value reduces very fast. In fact, effects of easily ionizable additives on the impact ionization rate are always inferior to the opposite effect of reducing the applied voltage below 7–8 kV. Initiation voltages for positive streamers are normally higher, 12–13 kV, and may so be reduced by adding molecules with (very) low-ionization potentials.

If we were to strictly apply the terminology from gas discharge physics, only the 2nd mode positive streamer propagation qualifies as a 'streamer'. The 1st mode negative and positive streamers are mainly "slower" consequences of multiple partial discharges within a gaseous void. These phenomena supply charges to the liquid interface, in such taking on a role analogous to coronas in gases. For negative streamers, these charges are electrons whose low-energetic interactions with electron-attaching additives in the liquid favours evaporation and local field-enhancements. However, the most profound effect of additives is observed for the positive streamer propagation. Here, electrons are constantly extracted from the liquid under field conditions capable of generating electron avalanches. For an exponentially decaying electron energy distribution, the net increase in ionization frequency during electron multiplication is exponential with the difference in ionization potential between the base liquid and a more easily ionizable additive. Moreover, a proportionality between this increase and the additive concentration implies, at least for centimetre gaps, an insignificant reduction of the impulse strength from trace concentrations.

The mechanism by which halogenated liquids accelerate positive and negative streamers is not clear. However, it is feasible that the speed of propagation is related to the speed of temperature equilibration during the supercritical state in the propagation front. A partially thermalization occurs on a nanosecond timescale and at very high kinetic energies, probably subsequent to an even faster ionizing stage.

My contribution to this scientific work has involved major responsibilities for the experimental setups, for the running of the experiments, for the theoretical interpretations, and for the writing of the journal papers. Main experimental components existed from start-up, but had to be improved and complemented along the way. The experiment with additives became the most time-consuming part of the work. A large amount of data was needed in order to compare average streamer characteristics, often without knowing until the final analyses if results had supported our hypothesis or not. Despite automated measurement routines, a great deal of manual supervision was required. Experiments with additives have been running almost continuously for a 1⅔ year period during the two years spent in Trondheim as a part of the thesis work. One additive concentration required typically 4–6 days of measurements (for both point polarities), whereas the signal and image analysis required 2–3 days. Typically, new experiments were performed while results from previous measurements

were analyzed. Cleaning and drying of the test cell in-between each measurement required 2 days. In order to "blind-test" candidate molecules, a more efficient experimental routine would be beneficial. For the less than one-year of spectroscopic work in *G2E-lab* in Grenoble, a new experimental setup had to be planned and realized. Measurements were performed during ⅔ of that year. Compared to the study of additives, spectroscopic measurements could be analyzed with a limited amount of pre-processing. Measurements and analyses therefore went more hand in hand. In addition, less time-consuming experimental procedures left more time to attack theoretical aspects, such as the simulation of atomic lines and molecular bands.

5.3. *Future Perspectives*

Further analysis may be performed on the accumulated data from the study of additives in cyclohexane. Advanced Matlab® image-processing routines are being developed in order to obtain a more efficient analysis of the streamer length and area, including the measurement of filament diameters and the number and lengths of streamer branches. Future analyses may for instance provide a better correlation between the charge and the length of one streamer filament.

Results reported from the study of additives at voltages below the breakdown level, e.g. concentration dependencies, may not be representative for voltages above the breakdown level in longer electrode gaps. Different streamer modes may have different feed-forward mechanism, e.g. may photo-ionization be rate determining for streamers with velocities about 10-100 times of those reported in this study (fast events). The transferability of the results in the present work should therefore be tested for longer gaps using higher over-voltages.

As mentioned in section 5.2, the most important mechanisms for streamer propagation would be those responsible for the high propagation velocities observed here for the 2nd mode propagation. However, there is a need of data concerning molecules subjected to electric fields in order to evaluate fast electronic and photonic processes. These may be obtained from ab initio calculations for molecules of interest, and verified with data obtained empirically under well-controlled experimental conditions. Pioneering advances

in theoretical chemistry and physics would possibly be required in order to fully describe interactions with an impacting electron. For experimental validations, it is recommended to pursue the well-documented photo-ionization and electron-attachment studies carried out by Christophorou and co-workers, mostly in gases, but also in liquids (see for example reference [105]). Finally, future theoretical studies should consider the thermodynamics of the supercritical state at the propagating streamer front, and the influence of chemical composition. Time-resolved streamer emission spectrometry should be further developed for the purpose of evaluating the energetic processes and transient physical conditions in prebreakdown phenomena in general.

A final remark is made concerning the imbalance between the number of publications treating experimental results to those treating streamer simulations. There may be different reasons for this. One is that modelling requires better knowledge of the driving mechanisms that cannot directly be assessed in conventional streamer experiments. Despite the theoretical obstacles, it is nevertheless my belief that progress can be made by combining different cultures within experimental and computational chemistry/physics. Advances are made continuously and independently within each field, and collaborations may in a longer run provide a tool for quantitative evaluations of the proposed mechanisms, which may again help to direct the field of experimental research.

6.   CONCLUDING REMARKS

The propagation characteristics of both positive and negative streamers depend qualitatively and quantitatively on the electronic characteristic of an additive in cyclohexane. Electron-attaching additives facilitate the propagation of negative streamers, whereas electron-releasing additives facilitate the propagation of positive streamers. For negative streamers, the propagation efficiency at all voltages has an asymptotic dependence on both the electron scavenging efficiencies and concentrations of additives, observable at even trace concentrations. For positive streamers, the transition from a slow to a faster mode of propagation is shifted towards lower voltages by increasing concentration and decreasing ionization potential of additives. However, this is difficult to observe at trace concentrations. Filamentary positive and negative streamers propagate considerably faster in pure chlorinated liquids than in cyclohexane with chlorinated additives. The fast propagation is associated with dense plasmas at very high temperatures, but the role of the chlorinated molecules is unclear.

6. Concluding Remarks

References

[1]   D. R. Lide, *Handbook of Chemistry and Physics* 84th ed., 2004 (Boca Raton, FL: CRC Press).

[2]   William M. Flanagan, *Handbook of Transformer Design & Applications,* 2nd edition, (New York: McGraw-Hill Book Company), 1986.

[3]   M. Zahn, Y. Ohki, D. B. Fenneman, R. J. Gripshover, and V. H. Gehman, Jr., "Dielectric properties of water and water/ethylene glycol mixtures for use in pulsed power system design," Proceedings of the IEEE, vol. 74, pp. 1182-1221, 1986.

[4]   M. Nishimatsu, T. Miyamoto and T. Suzuki, "Liquid Insulation" in *Wiley Encyclopaedia of Electrical and Electronics Engineering*, ed. J. G. Webster, 1999 (John Wiley & Sons).

[5]   V. Y. Ushakov, V. F. Klimkin, and S. M. Korobeynikov, *Impulse Breakdown of Liquids*, 1 ed. 2007 (Springer).

[6]   N. Berger, M. Randoux, G. Ottmann, and P. Vuarchex, "Rewiev on insulating liquids," Electra, vol. 171, pp. 33-56, 1997.

[7]   C. T. Duy, A. Denat, O. Lesaint, N. Bonifaci, Y. Bertrand, W. Daoud, and M. Hassanzadeh, "Influence of ageing on conduction and breakdown in rape-seed and mineral oils," International Conference on Dielectric Liquids (ICDL), Poitiers, France, 2008.

[8]   C. T. Duy, O. Lesaint, N. Bonifaci, A. Denat, and Y. Bertrand, "High voltage breakdown and pre-breakdown properties in rape-seed insulating oil," Conference on Electrical Insulation and Dielectric Phenomena (CEIDP), Vancouver, Canada, 2007, pp. 623-626.

[9]   R. Badent, M. Hemmer, U. Koenekamp, Y. Julliard, and A. J. Schwab, "Streamer inception field strengths in rape-seed oils," Conference on Electrical Insulation and Dielectric Phenomena (CEIDP), Victoria, Canada, 2000, pp. 272-275.

[10]   R. Bartnikas, "Electrical Insulating Liquids" in *Engineering Dielectrics*, vol. 3, 1994 (Philadelphia: ASTM, Monograph 2).

References

[11]   P. Lonsky, "Some characteristics of silicones developed as lubricants," Journal of Synthetic Lubrication, vol. 1, pp. 302-313, 1985.

[12]   T. V. Oommen and C. C. Claiborne, "Biodegradable insulating fluid from high oleic vegetable oils," International Conference on Large High Voltage Electric Systems (CIGRE), Paris, France, 1998, vol.5.

[13]   I. Adamczewski, "Induced conduction in dielectric liquids," British Journal of Applied Physics, vol. 16, pp. 759-770, 1965.

[14]   R. W. Crowe, A. H. Sharbaugh, and J. K. Bragg, "Electric strength and molecular structure of saturated hydrocarbon liquids," Journal of Applied Physics, vol. 25, pp. 1480-1484, 1954.

[15]   G. M. L. Sommerman, C. J. Bute, and E. L. C. Larson, "Impulse ionization and breakdown in liquid dielectrics," Transactions of the American Institute of Electrical Engineers, Part I (Communications and Electronics), pp. 147-155, 1954.

[16]   A. H. Sharbaugh, R. W. Crowe, and E. B. Cox, "Influence of molecular structure upon the electric strengths of liquid hydrocarbons," Journal of Applied Physics, vol. 27, pp. 806-808, 1956.

[17]   P. K. Watson and A. H. Sharbaugh, "High-field conduction currents in liquid n-Hexane under microsecond pulse conditions," Journal of the Electrochemical Society, vol. 107, pp. 516-521, 1960.

[18]   E. O. Forster, "Electric conductance in liquid hydrocarbons. II. Methyl-substituted benzenes," Journal of Chemical Physics, vol. 40, pp. 86-90, 1964.

[19]   E. O. Forster, "Electric conduction in liquid hydrocarbons. III. Comparison of saturated and unsaturated hydrocarbons," Journal of Chemical Physics, vol. 40, pp. 91-95, 1964.

[20]   L. Angerer, "Effect of organic additives on electrical breakdown in transformer oil and liquid paraffin," Proceedings of the Institution of Electrical Engineers, vol. 112, pp. 1025-1034, 1965.

[21]   T. J. Lewis and B. W. Ward, "A statisical interpretation of the electrical breakdown of liquid dielectrics," Proceedings of the Royal Society of London, Series A (Mathematical and Physical Sciences), vol. 269, pp. 233-248, 1962.

References

[22]   C. E. Evangelou, A. A. Zaky, and I. Y. Megahead, "The effect of organic additives on the breakdown strength of transformer oil," Journal of Physics D (Applied Physics), vol. 6, pp. 60-62, 1973.

[23]   S. S. Hakim, "Phenomena in n-hexane prior to its electric breakdown," Nature, vol 189, p. 996, 1961.

[24]   B. Farazmand, "Study of electric breakdown of liquid dielectrics using schlieren optical techniques," British Journal of Applied Physics, vol. 12, pp. 251-254, 1961.

[25]   W. G. Chadband and G. T. Wright, "A pre-breakdown phenomenon in the liquid dielectric hexane," British Journal of Applied Physics, vol. 16, pp. 305-313, 1965.

[26]   W. G. Chadband, R. Coelho, and J. Debeau, "Electrical discharges in liquid dielectrics," Journal of Physics D (Applied Physics), vol. 4, pp. 539-540, 1971.

[27]   N. Shammas, C. W. Smith, and J. H. Calderwood, "Coronas in insulating liquids," Journal of Physics D (Applied Physics), vol. 7, pp. 2587-2592, 1974.

[28]   B. Singh, "Prebreakdown processes in electrically stressed insulating liquids," Journal of Applied Physics, vol. 5, 1457-1467, 1972.

[29]   E. O. Forster and P. Wong, "High speed laser Schlieren studies of electrical breakdown in liquid hydrocarbons," IEEE Transactions on Electrical Insulation, vol. EI-12, pp. 435-442, 1977.

[30]   P. B. McGrath and J. K. Nelson, "Optical studies of prebreakdown events in liquid dielectrics," Proceedings of the Institution of Electrical Engineers, vol. 124, pp. 183-187, 1977.

[31]   H. Yamashita, H. Amano, and T. Mori, "Optical observation of pre-breakdown and breakdown phenomena in transformer oil," Journal of Physics D (Applied Physics), vol. 10, pp. 1753-1760, 1977.

[32]   P. P. Wong and E. O. Forster, "The dynamics of electrical breakdown in liquid hydrocarbons," IEEE Transactions on Electrical Insulation, vol. EI-17, pp. 203-220, 1982.

References

[33] E. F. Kelley and R. E. Hebner, Jr., "Electric field distribution associated with prebreakdown phenomena in nitrobenzene," Journal of Applied Physics, vol. 52, pp. 191-195, 1981.

[34] I. J. Youngs, G. C. Stevens, and A. S. Vaughan, "Trends in dielectrics research: An international review from 1980 to 2004," Journal of Physics D (Applied Physics), vol. 39, pp. 1267-1276, 2006.

[35] N. Bonifaci and A. Denat, "Spectral analysis of light emitted by prebreakdown phenomena in nonpolar liquids and gases," IEEE Transactions on Electrical Insulation, vol. 26, pp. 610-614, 1991.

[36] P. Barmann, S. Kroll, and A. Sunesson, "Spectroscopic measurements of streamer filaments in electric breakdown in a dielectric liquid," Journal of Physics D (Applied Physics), vol. 29, pp. 1188-1196, 1996.

[37] P. Barmann, S. Kroll, and A. Sunesson, "Spatially and temporally resolved electron density measurements in streamers in dielectric liquids," Journal of Physics D (Applied Physics), vol. 30, pp. 856-863, 1997.

[38] N. Bonifaci, A. Denat, and P. E. Frayssines, "Application of emission spectroscopy in the study of electric discharge in liquids," Journal of Electrostatics, vol. 64, pp. 445-449, 2006.

[39] L. E. Lundgaard, Ø. Hestad, and S. Ingebrigtsen, "Review of test methods for dielectric properties of liquids for high-voltage transformer," Nordic Insulation Symposium (NORD-IS), Trondheim, Norway, 2005.

[40] ASTM D3300-00, "Standard Test Method for Dielectric Breakdown Voltage of Insulating Oils of Petroleum Origin Under Impulse Conditions", American Society for Testing and Materials.

[41] IEC 60897, "Methods for the determination of the lightning impulse voltage of insulating liquids", International Electrotechnical Commission.

[42] K. N. Mathes and T. O. Rouse, "Influence of Aromatic Compounds in Oil on Pirelli Gassing and Impulse Surge Breakdown," Conference on Electrical Insulation and Dielectric Phenomena (CEIDP), Washington, US, 1975, pp. 129-140.

References

[43] C. Hosticka, "Dependence of uniform/nonuniform field transformer oil breakdown on oil composition," IEEE Transactions on Electrical Insulation, vol. EI-14, pp. 43-50, 1978.

[44] J. Perret, "Study of the dielectric breakdown of insulating mineral oils under impulse voltages," IEEE Transactions on Electrical Insulation, vol. EI-16, pp. 339-345, 1981.

[45] L. Johansson and K. Andersson, "Chemical factors affecting dielectric breakdown in insulating liquids," Nordic Insulation Symposium (NORD-IS), Vaasa, Finland, 1994.

[46] P. Gournay and O. Lesaint, "A study of the inception of positive streamers in cyclohexane and pentane," Journal of Physics D (Applied Physics), vol. 26, pp. 1966-74, 1993.

[47] H. Yamashita, K. Yamazawa, and Y. S. Wang, "Effect of tip curvature on the prebreakdown streamer structure in cyclohexane," IEEE Transactions on Dielectrics and Electrical Insulation, vol. 5, pp. 396-401, 1998.

[48] O. L. Hestad, G. Berg, S. Ingebrigtsen, and L. E. Lundgaard, "Streamer injection and growth under impulse voltage: a comparison of cyclohexane, Midel 7131 and Nytro 10X," Conference on Electrical Insulation and Dielectric Phenomena (CEIDP), Boulder, CO, USA, 2004, pp. 542-546.

[49] A. Denat, "High field conduction and prebreakdown phenomena in dielectric liquids," IEEE Transactions on Dielectrics and Electrical Insulation, vol. 13, pp. 518-525, 2006.

[50] W. F. Schmidt, "Elementary processes in the development of the electrical breakdown of liquids," IEEE Transactions on Electrical Insulation, vol. EI-17, pp. 478-483, 1982.

[51] R. Tobazeon, "Electrohydrodynamic instabilities and electroconvection in the transient and a.c. regime of unipolar injection in insulating liquids: A review," Journal of Electrostatics, vol. 15, pp. 359-384, 1983.

[52] W. F. Schmidt, "Electronic conduction processes in dielectric liquids," IEEE Transactions on Electrical Insulation, vol. EI-19, pp. 389-418, 1984.

[53] T. J. Lewis, "Electronic processes in dielectric liquids under incipient breakdown stress," IEEE Transactions on Electrical Insulation, vol. EI-20, pp. 123-132, 1985.

References

[54]   W. F. Schmidt, "Electronic conduction and breakdown in nonpolar liquids," Revue de Physique Appliquee, vol. 22, pp. 113-116, 1987.

[55]   R. A. Holroyd and W. F. Schmidt, "Transport of Electrons in Nonpolar Fluids," Annual Review of Physical Chemistry, vol. 40, pp. 439-468, 1989.

[56]   E. O. Forster, "Progress in the field of electric properties of dielectric liquids," IEEE Transactions on Electrical Insulation, vol. 25, pp. 45-53, 1990.

[57]   W. F. Schmidt, "Electrons in non-polar dielectric liquids," IEEE Transactions on Electrical Insulation, vol. 26, pp. 560-567, 1991.

[58]   T. J. Lewis, "Basic electrical processes in dielectric liquids," IEEE Transactions on Dielectrics and Electrical Insulation, vol. 1, pp. 630-643, 1994.

[59]   R. Tobazeon, "Prebreakdown phenomena in dielectric liquids," IEEE Transactions on Dielectrics and Electrical Insulation, vol. 1, pp. 1132-1147, 1994.

[60]   W. F. Schmidt and E. Illenberger, "Low energy electrons in non-polar liquids," Nukleonika, vol. 48, pp. 75-82, 2003.

[61]   P. Atten, "Electrohydrodynamic instability and motion induced by injected space charge in insulating liquids," IEEE Transactions on Dielectrics and Electrical Insulation, vol. 3, pp. 1-17, 1996.

[62]   M. Zahn, "Conduction and breakdown in dielectric liquids" in *Wiley Encyclopaedia of Electrical and Electronics Engineering*, ed. J. G. Webster, 1999 (John Wiley & Sons).

[63]   L. Lundgaard, D. Linhjell, G. Berg, and S. Sigmond, "Propagation of positive and negative streamers in oil with and without pressboard interfaces," IEEE Transactions on Dielectrics and Electrical Insulation, vol. 5, pp. 388-395, 1998.

[64]   R. E. Hebner, "Measurements of electrical breakdown in liquids" in *The Liquid State and its Electrical Properties*, NATO Advanced Study Institute, Series B: Physics vol. 193, ed. E. E. Kunhardt *et al.*, pp 519–537, 1988 (New York: Plenum).

[65]   O. Lesaint and G. Massala, "Positive streamer propagation in large oil gaps. Experimental characterization of propagation modes," IEEE Transactions on Dielectrics and Electrical Insulation, vol. 5, pp. 360-370, 1998.

References

[66] N. J. Felici, "Blazing a fiery trail with the hounds," IEEE Transactions on Electrical Insulation, vol. 23, pp. 497-503, 1988.

[67] H. M. Jones and E. E. Kunhardt, "Development of pulsed dielectric breakdown in liquids," Journal of Physics D (Applied Physics), vol. 28, pp. 178-188, 1995.

[68] J. C. Devins, S. J. Rzad, and R. J. Schwabe, "Breakdown and prebreakdown phenomena in liquids," Journal of Applied Physics, vol. 52, pp. 4531-4545, 1981.

[69] A. Beroual and R. Tobazeon, "Prebreakdown phenomena in liquid dielectrics," IEEE Transactions on Electrical Insulation, vol. EI-21, pp. 613-627, 1986.

[70] P. K. Watson, W. G. Chadband, and M. Sadeghzadeh-Araghi, "The role of electrostatic and hydrodynamic forces in the negative-point breakdown of liquid dielectrics," IEEE Transactions on Electrical Insulation, vol. 26, pp. 543-559, 1991.

[71] W. G. Chadband, "On variations in the propagation of positive discharges between transformer oil and silicone fluids," Journal of Physics D (Applied Physics), vol. 13, pp. 1299-1307, 1980.

[72] W. G. Chadband, "The ubiquitous positive streamer," IEEE Transactions on Electrical Insulation, vol. 23, pp. 697-706, 1988.

[73] O. Lesaint and P. Gournay, "On the gaseous nature of positive filamentary streamers in hydrocarbon liquids. I: Influence of the hydrostatic pressure on the propagation," Journal of Physics D (Applied Physics), vol. 27, pp. 2111-2116, 1994.

[74] A. Beroual, M. Zahn, A. Badent, K. Kist, A. J. Schwabe, H. Yamashita, K. Yamazawa, M. Danikas, W. G. Chadband, and Y. Torshin, "Propagation and structure of streamers in liquid dielectrics," IEEE Electrical Insulation Magazine, vol. 14, pp. 6-17, 1998.

[75] T. Schutte, "The influence of the molecular packing on electrical breakdown strength of liquids," Nordic Insulation Symposium (NORD-IS), Vaasa, Finland, 1994, pp. 147-160.

[76] Y. Nakao, T. Yamazaki, K. Miyagi, Y. Sakai, and H. Tagashira, "The effect of molecular structure on prebreakdown phenomena in dielectric liquids under a nonuniform field," Electrical Engineering in Japan, vol. 139, pp. 1-8, 2002.

[77]   N. Hamano, Y. Nakao, T. Naito, Y. Nakagami, R. Shimizu, Y. Sakai, and H. Tagashira, "Influence of molecular structure on propagation of streamer discharge in hydrocarbon liquids," International Conference on Dielectric Liquids (ICDL), Graz, Australia, 2002, pp. 119-122.

[78]   Y. Nakao, T. Yamazaki, H. Tagashira, K. Miyagi, and Y. Sakai, "Propagation of streamer discharge in dielectric liquids with various molecular structure by using high-speed schlieren photography," IEEE International Conference on Dielectric Liquids (ICDL), Nara, Japan, 1999, pp. 261-264.

[79]   P. K. Watson, W. G. Chadband, and M. Sadeghzadeh-Araghi, "The role of electrostatic and hydrodynamic forces in the negative-point breakdown of liquid dielectrics," IEEE Transactions on Electrical Insulation, vol. 26, pp. 543-559, 1991.

[80]   W. G. Chadband, "Electrical breakdown-from liquid to amorphous solid," Journal of Physics D (Applied Physics), vol. 24, pp. 56-64, 1991.

[81]   F. Jomni, F. Aitken, and A. Denat, "Investigation of the behavior of microscopic bubbles in insulating liquids: Transition from the inertial regime to the viscous one," International Conference on Dielectric Liquids (ICDL), Graz, Australia, 2002, pp. 194-198.

[82]   F. M. J. McCluskey and A. Denat, "Bubble formation in synthetic insulating liquids in a pulsed divergent electric field," IEEE Transactions on Dielectrics and Electrical Insulation, vol. 1, pp. 672-679, 1994.

[83]   J. Nieto-Salazar, "Breakdown and Pre-breakdown Phenomena in Water under impulse voltage," Int. Symposium on High Voltage Engineering, Delft, Netherlands, 2003.

[84]   Y. Nakao, H. Itoh, S. Hoshino, Y. Sakai, and H. Tagashira, "Effects of additives on prebreakdown phenomena in n-hexane," IEEE Transactions on Dielectrics and Electrical Insulation, vol. 1, pp. 383-389, 1994.

[85]   O. Lesaint and M. Jung, "On the relationship between streamer branching and propagation in liquids: influence of pyrene in cyclohexane," Journal of Physics D (Applied Physics), vol. 33, pp. 1360-1368, 2000.

References

[86]   W. G. Chadband and T. M. Sufian, "Experimental support for a model of positive streamer propagation in liquid insulation," IEEE Transactions on Electrical Insulation, vol. EI-20, pp. 239-246, 1985.

[87]   M. Fotino, "Tip sharpening by normal and reverse electrochemical etching," Review of Scientific Instruments, vol. 64, pp. 159-167, 1993.

[88]   J. Stokes, *70 Years of Radio Tubes and Valves*, 1982 (NY: Vestal Press) pp. 111-115.

[89]   R. S. Sigmond, "Simple passive electrical filter for discharge diagnostics," Symposium on Elementary Processes and Chemical Reactions in Low Temperature Plasma, Bratislava, Slovakia, 1998, p. 256.

[90]   E. Wilhelm and R. Battino, "The solubility of gases in liquids. The solubility of N_2, O_2, CO, and CO_2 in cyclohexane at 283 to 313 K," Journal of Chemical Thermodynamics, vol. 5, pp. 117-120, 1973.

[91]   C. Wohlfarth and B. Wohlfarth, *Viscosity of Pure Organic Liquids and Binary Liquid Mixtures*, vol.18(B) 2002 (Heidelberg: Springer Berlin).

[92]   C. Wohlfarth and M. D. Lechner, *Static Dielectric Constants of Pure Liquids and Binary Liquid Mixtures*, vol. 6, 1991 (Heidelberg: Springer Berlin).

[93]   Data from NIST Standard Reference Database 69, June 2005 Release: NIST Chemistry WebBook.

[94]   M. Campos-Vallette and F. G. Diaz, "Some physical and thermodynamic properties of n-C_nF_{2n+2} compounds with n = 4-8," Semina (Londrian Braz.). vol. 4, pp. 405-409, 1983.

[95]   K. Ueberreiter and H. J. Orthmann, "Spezifische Warme, Spezifisches Volumen, Temperatur Und Warme-Leitfahigkeit Einiger Disubstituierter Benzole Und Polycyclischer Systeme," Zeitschrift Fur Naturforschung Section a-a Journal of Physical Sciences, vol. 5, pp. 101-108, 1950.

[96]   L.G. Christophorou, *Electron-molecule Interactions and Their Applications*, 1984 (U.S.: Academic Press) p.292.

[97]   Y. Nakato, M. Ozaki, A. Egawa, and H. Tsubomura, "Organic amino compounds with very low ionization potentials," Chemical Physics Letters, vol. 9, pp. 615-616, 1971.

[98]   H. S. Smalø, S. Ingebrigtsen and P.-O. Åstrand, "Calculation of ionization potentials and electron affinities for molecules relevant for streamer initiation and propagation," in preparation, 2008.

[99]   M.D. Abramoff, P.J. Magelhaes and S.J. Ram, "Image Processing with ImageJ", Biophotonics International, vol. 11, pp. 36-42, 2004.

[100] K. Aflatooni and P. D. Burrow, "Total cross sections for dissociative electron attachment in dichloroalkanes and selected polychloroalkanes: The correlation with vertical attachment energies," Journal of Chemical Physics, vol. 113, pp. 1455-1464, 2000.

[101] J. R. Johnson, L. G. Christophorou, and J. G. Carter, "Fragmentation of aliphatic chlorocarbons under low-energy (≤10 eV) electron impact," Journal of Chemical Physics, vol. 67, pp. 2196-2215, 1977.

[102] T. Oster, A. Kuhn, and E. Illenberger, "Gas phase negative ion chemistry," International Journal of Mass Spectrometry and Ion Processes, vol. 89, pp. 1-72, 1989.

[103] P. E. Frayssines, N. Bonifaci, A. Denat, and O. Lesaint, "Streamers in liquid nitrogen: Characterization and spectroscopic determination of gaseous filament temperature and electron density," Journal of Physics D (Applied Physics), vol. 35, pp. 369-377, 2002.

[104] J. N. Salazar, N. Bonifaci, A. Denat, and O. Lesaint, "Characterization and spectroscopic study of positive streamers in water," IEEE International Conference on Dielectric Liquids (ICDL), Coimbra, Portugal, 2005, pp. 91-94.

[105] G. A. Kourouklis, *Photoionization of Organic Molecules in Dielectric Liquids*, Doctoral Thesis, University of Tennessee, 1982.

Paper 1

Effects of additives on prebreakdown phenomena in liquid cyclohexane: I. Streamer initiation

Stian Ingebrigtsen, Lars E. Lundgaard and Per-Olof Åstrand

2007

Effects of additives on prebreakdown phenomena in liquid cyclohexane: I. Streamer initiation

S Ingebrigtsen[1], L E Lundgaard[2] and P-O Åstrand[1]

[1] Department of Chemistry, Norwegian University of Science and Technology,
N-7491 Trondheim, Norway
[2] Department of Electric Power Technology, SINTEF Energy Research, N-7465 Trondheim,
Norway

E-mail: stian.ingebrigtsen@sintef.no

Abstract
Conduction currents and streamer initiation in cyclohexane with various
additives have been investigated with fast impulses applied to a
point-to-plane gap. The studied additives are perfluoro-n-hexane,
N,N-dimethylaniline, 1-methylnaphthalene, di-n-propylether,
1,1-difluorocyclopentane and 1,4-benzoquinone, representing molecules
with different electrochemical properties. We have used shadowgraphic
imaging and a differential charge-measurement technique with a sensitivity
of 0.1 pC to integrate currents induced to the point electrode, below and in
the same voltage range where streamers first appeared. Effects on streamer
initiation are found only for point anode streamers with the additive
1-methylnaphthalene, requiring higher voltages for initiation. We have
observed transient conduction currents of measurable magnitudes in the
nano to microampere range for voltages around initiation in all samples with
a point anode and in 10 out of 21 samples with a point cathode. For a point
anode, the more easily ionizable additives N,N-dimethylaniline and
1-methylnaphthalene induced somewhat larger currents. The results may be
considered to support a hypothesis of electron avalanche induced streamer
initiation, in that transient currents are induced by the ions left behind by the
avalanches that are not sufficiently developed to initiate streamers.

(Some figures in this article are in colour only in the electronic version)

1. Introduction

Since air is one of the first insulators used, electrical breakdown
in air has been studied extensively, and the breakdown
processes in gases are relatively well understood [1,2]. Today
both liquids and solids are used as insulating materials for
electrotechnical applications [3, 4], but less is known about
processes leading to breakdown in the condensed phases due
to the more complex material composition, despite a significant
amount of experimental data [5].

The type of liquids used in transformers are mainly
mineral oils which have been processed to certain standards [6].
Usually these oils contain paraffinic, naphthenic, aromatic
and polyaromatic fractions. Different additives like oxidation
inhibitors, pour-point depressants and metal passivators are
added to improve particular characteristics [3]. An increased
tendency is emerging to use liquids with improved properties
in respect of biodegradability, flammability and with lower
polyaromatic content [3]. Presently, insulating properties
of liquids are tested in somewhat rough, standardized tests
(e.g. IEC) with limited interpretations [7].

For liquids, the general picture is that a breakdown
is completed through the initiation and propagation of a
'streamer'. This is a gas/plasma channel which initiates in
a region with high electric fields and propagates through
the liquid until it bridges the electrode gap and results in a

breakdown. The streamer contains molecules of vapourized liquid and liquid decomposition products, both ionized and electronically excited, and quasi-free electrons. One often distinguishes between initiation where phenomena like space charge effects play a role, and propagation where conduction effects may dominate, resembling what in gas discharge terminology is called a 'leader' [8]. The events preceding the actual breakdown are termed 'prebreakdown processes' and have been studied during the last four decades, accompanied by steadily improved measuring techniques [5, 9].

Prebreakdown processes are usually studied in point-to-plane electrode geometries where high electric fields are easily obtained and effects from voltage polarity can be investigated. Normally, the current induced to an external circuit is measured, and the gaseous phase is characterized by shadowgraphic and schlieren techniques, and by measuring the light emitted by the streamer [10]. Significant influences from experimental conditions have been reported, such as electrode arrangement (gap length and point radius of curvature) [11–13] applied voltage (shape, magnitude, and polarity) [14, 15], chemical nature of the liquid [5], and pressure [14,16–18]. From an experimental point of view, the study of breakdown processes in condensed phases is favourable in liquids for three main reasons. The optical transparency of many liquids allows for visual observations. Secondly, a good contact surface between the liquid and the electrode is easily obtained, and finally, as many liquids are easily mixed, experimental studies of chemical additives are simpler in a liquid than in a solid.

By applying models originally developed for discharges in gases, considerable progress in the understanding of liquid prebreakdown processes has been achieved [19,20]. However, the high-field processes taking place at streamer initiation and propagation are still not fully understood and knowledge about basic parameters is lacking for most hydrocarbon liquids (e.g. mean free path of electrons and photons, quantum mechanical cross-sections for the processes impact ionization and excitation). The streamer process is complex and involves mechanisms of electronic, ionic, optical, thermal, mechanical and hydrodynamic nature [8,16,21–27]. Briefly, the electronic high-field process is two-fold: (1) the release of electrons from the electrodes and from the bulk of the material, and (2) the acceleration of electrons by the electric field and the interactions/collisions with liquid atoms or molecules. Depending on their electronic properties, such as ionization potential and electron affinity, atoms and molecules may act as sources of electrons in the first stage and later, during impacts, interact with the energetic electrons, resulting in electron capture or multiplication. Interactions of this type, both in the liquid and in the vapour, determine the transfer of energy and to a large extent the propagation behaviour of the streamer. The ability of a liquid to resist a streamer thus depends on its ability to prevent local formation of electrons, and the molecular composition of the liquid becomes important for its performance as an electrically insulating material.

We have studied the role of electrochemical properties on prebreakdown processes in a pure and non-polar liquid by introducing selected additives. The investigation is carried out with impulse voltages well below breakdown, activating only the first modes of streamer propagation [28]. In this paper, we present measurements on conduction currents and
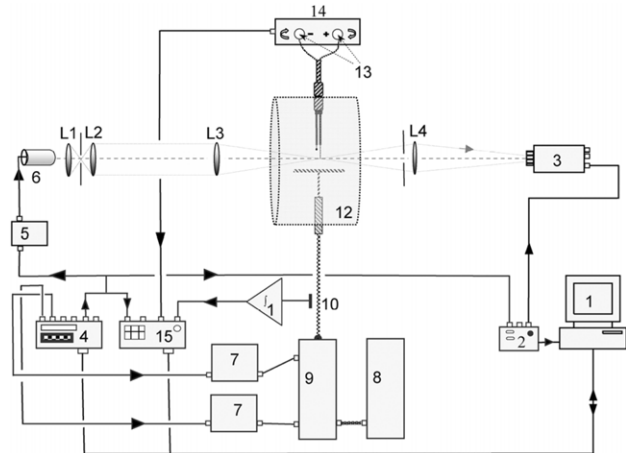
Figure 1. General outline of the experimental setup, (1) computer, (2) Proxitronic control unit, (3) Proxitronic Nanocam NCA, (4) SRS-DG535 four channel digital delay/pulse generator, (5) pulse circuit for LED, (6) white LED/Xenon flash-lamp (7) 6 kV thyratron 5C22 trigger unit, (8) Spellman SL150 dc high-voltage (0–100 kV) supplier, (9) high-voltage pulse battery, (10) BNC capacitive probe, (11) 60 ms passive integrator, (12) test cell, (13) capacitive voltage divider arms, (14) Lecroy DA1850 100 MHz differential amplifier (15) Tektronix TDS 540A digitizing oscilloscope.

initiation voltages for streamers in cyclohexane with additives of different properties and concentrations. In a subsequent paper (part 2), we report effects of the same additives on the phenomena of streamer propagation. Cyclohexane was used as base liquid since it is a simple and well-documented alkane frequently used in prebreakdown and breakdown studies, and it also serves as a simple model liquid for insulating oils. Moreover, cyclohexane is a good solvent for different additives. The additives, perfluoro-n-hexane, N,N-dimethylaniline, 1-methylnaphthalene, di-n-propylether, 1,1-difluorocyclopentane and 1,4-benzoquinone, have been selected on the basis of their abilities to either attach or liberate electrons. Better knowledge about how the electrochemical properties of a liquid may change its dielectric performance may help to design new synthetic liquids and also to avoid possible unwanted consequences from changes of the composition of conventional liquids, e.g. due to environmental regulations.

2. Experiment

2.1. Instrumentation

The experiment is designed to study the streamer by using a shadowgraphic depiction technique, and by measuring the electric charge induced on the point electrode before any streamer initiation occurs. Rectangular high-voltage impulses are applied to the plane electrode of a 10 ± 0.5 mm point-to-plane gap. An in-house made impulse generator supplies the pulses with variable pulse widths, and with rise and fall times of 15–20 ns. The impulse generator basically consists of two triggered spark gaps, where the high voltage is switched on by the first, and chopped by the second. Both gaps are triggered with thyratron pulsers, as shown schematically in figure 1. The impulse generator is designed with a low inductance to give fast rise and fall times without ringing or oscillations. Impulse
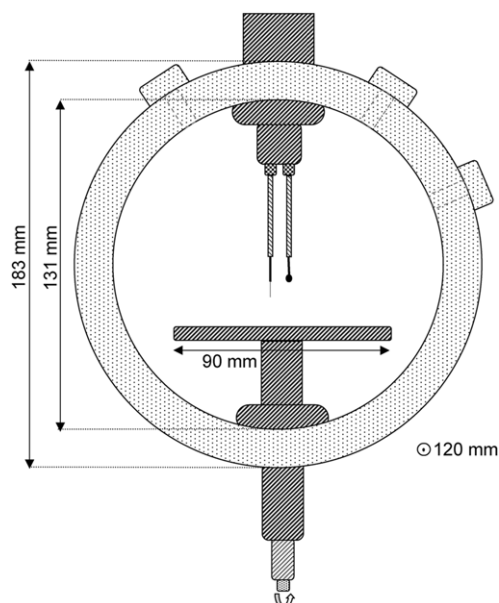
Figure 2. The cylindrical PFTE-test cell showing the point-to-plane geometry with a rounded probe next to the sharp electrode for displacement current compensation during the charging of the plane electrode. Point electrodes are shielded and effectively grounded while high-voltage is applied to the plane electrode via a micrometre screw for gap-size adjustments.

voltages with steep fronts are necessary to avoid influence of space charge on the streamer initiation process. The high-voltage pulses are measured by integrating the current from a capacitive probe, using a passive integrator [29], and injected charge is measured with a 0.1 pC sensitive differential charge-measurement technique [14]. The imaging system consists of a high intensity white LED, an auto-collimator, a lens system and a single-shot intensified CCD camera of type Proxitronic NCA Nanocam® with 5 ns minimum shutter time. A xenon flash-lamp replaced the LED in the later experiments. The best obtainable image resolution is $0.7\,\mu$m. The experiment is automated and controlled via LabView computer software. Point electrodes have been made by electrochemically etching [30] a $100\,\mu$m wolfram wire into near-hyperbolically shaped points with point radii in the range 1.3–$1.5\,\mu$m. We used an IRLAB LDTRP low voltage, low frequency conductance-meter to measure the conductivities of the liquids. A 1.5 litre Teflon® (PTFE) test cell, see figure 2, was filled with argon gas prior to sample-filling and placed in an optical bench as shown in figure 1. The experimental apparatus and conditions used in this study are similar to that used by Dumitrescu *et al* [14], Gournay *et al* [12] and Yamashita *et al* [11].

2.2. Liquids

The cyclohexane used in this study is of type Merck LiChrosolv® with a purity of 99.9%. The additives are perfluoro-n-hexane (>99%), N,N-dimethylaniline (>99%), 1-methylnaphthalene (>97%), di-n-propylether (99%), 1,1-difluorocyclopentane and 1,4-benzoquinone (99.5%). 1,1-difluorocyclopentane is a non-standard chemical and was provided by SynQuest Laboratories, Inc. In our experiments, cyclohexane was first dried with 3 Å Zeochem molecularsieve,

degassed in a vacuum reservoir at 70 mbar using an extraction volume ten times the liquid volume, and then mixed with the additive under argon atmosphere over night. The samples were prepared with additive concentrations of 0, 0.1, 1.0, 10 and $50\,\mathrm{mg\,g^{-1}}$, except for the last three additives where the highest concentrations were excluded. This range was so chosen to span from trace impurities to larger fractions of the samples. In addition to the samples with dried and degassed cyclohexane, also cyclohexane directly from the bottle without additional purification was studied. Drying of cyclohexane reduced the moisture content from 19 to 1–3 μg g^{-1}. The gas content of the samples subsequent to degassing has not been measured, but should be well below the saturation of oxygen gas, carbondioxide and nitrogen gas in cyclohexane, being 0.47, 3.90 and 0.25 mg g^{-1}, respectively [31]. In addition to the above-mentioned additives, distilled water was added at concentrations of 10 and 70 ppm to degassed cyclohexane, 70 ppm being around room temperature saturation [32].

Cyclohexane is a non-polar cyclic alkane with a gas phase ionization potential of $I_{1g} = 9.86$ eV [33]. The six additives have different electrochemical properties as compared with cyclohexane. N,N-dimethylaniline is more easily ionizable, $I_{1g} = 7.12$ eV [33], and perfluoro-n-hexane and 1,4-benzoquinone attaches electrons [34, 35]. Both properties are considered for 1-methylnaphthalene, commonly found in naphthenic oils, $I_{1g} = 7.97$ eV [33, 36, 37]. In order to investigate the effect of a dipole moment and the degree of fluorination for an electron-attaching molecule [38], the additive 1,1-difluorocyclopentane was included, which, in contrast to perfluoro-n-hexane, has a non-zero dipole moment in its equilibrium geometry. Di-n-propylether has electronic properties similar to cyclohexane, thus a significant effect from this additive is perhaps not expected. The choice of di-n-propylether was rather motivated by the frequent use of ether-based structures in synthetic insulating liquids [39]. The molecular properties with highest influence on streamer initiation can be expected to depend on the initiation mechanism and the type of electronic processes involved.

2.3. Measurements

The magnitudes of the high-voltage pulses have been varied in steps of 1 kV, and depending on streamer appearance probability, 30–100 streamers have been recorded at each voltage level with a minimum intermittent delay of 3 min. All experiments were conducted at room temperature and ambient pressure. We used one point electrode per additive, and the tip radius was measured before and verified after each experiment.

The electrical measurements of the prebreakdown events were time-resolved oscillograms of charge stored on a capacitor connected to the point electrode. As shown in figure 2, a rounded electrode is placed beside the point electrode in a differential arrangement in order to compensate for the charging of the electrode system from displacement currents when the high-voltage pulse is applied. The measured charge is then the charge induced by the prebreakdown event, and it represents an underestimate of the charge in the gap [40, 41]. A time-derivation of the charge gives an average current, and we present average currents prior to streamer initiation (preinception currents) with values averaged over
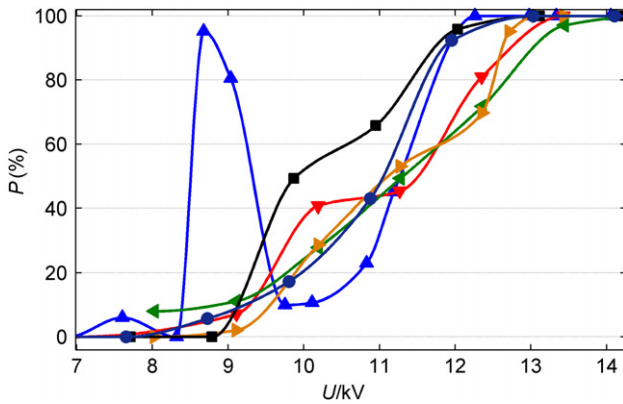
Figure 3. Initiation probability for point anode streamers in cyclohexane with additive perfluoro-n-hexane. Symbols: (▼) dried/degassed, (▲) from bottle, (◄) 0.1 mg g^{-1}, (►) 1.0 mg g^{-1}, (■) 10 mg g^{-1}, (●) 50 mg g^{-1}.
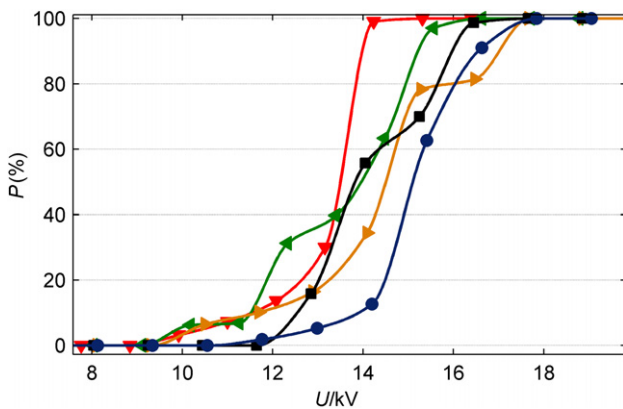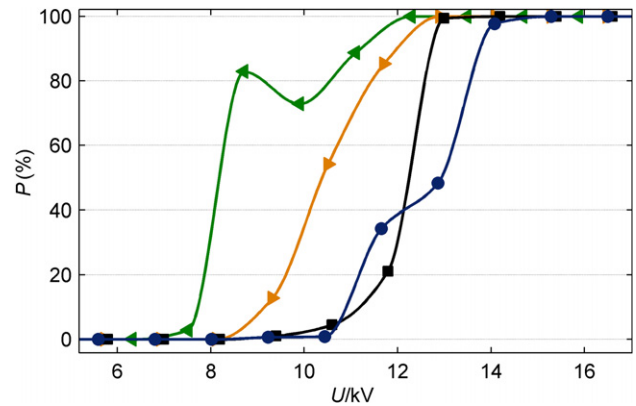

Figure 4. Initiation probability for point anode streamers in cyclohexane with additive N,N-dimethylaniline. Symbols: (▼) 0.01 mg g^{-1}, (◄) 0.1 mg g^{-1}, (►) 1.0 mg g^{-1}, (■) 10 mg g^{-1}, (●) 50 mg g^{-1}.

a time period of 20 μs. The minimum detectable current with this setup is 10 nA. A sudden increase in the charge readings corresponds to the initiation of a streamer. In parallel with optical measurements this allows us to determine the probability distributions for the initiation voltages of streamers. Probabilities are calculated by counting the number of streamer events at each voltage level, where the voltage corresponding to 50% probability is traditionally called the 'initiation voltage' [15].

3. Results

3.1. Streamer initiation probabilities

For positive point polarity, the following initiation voltages were found for the different additives (as compared with 11 kV for pure cyclohexane): 11 kV for the samples with perfluoro-n-hexane (figure 3), 14 kV for N,N-dimethylaniline (figure 4), 8–13 kV for 1-methylnaphthalene (figure 5), 13 kV for di-n-propylether (figure 6) and 10–14 kV for both 1,1-difluorocyclopentane (figure 7) and 1,4-benzoquinone (figure not shown). Streamer initiation probabilities for a point anode generally increase from 0% to 100% initiation over a

Figure 5. Initiation probability for point anode streamers in cyclohexane with additive 1-methylnaphthalene. Symbols: (◄) 0.1 mg g^{-1}, (►) 1.0 mg g^{-1}, (■) 10 mg g^{-1}, (●) 50 mg g^{-1}.
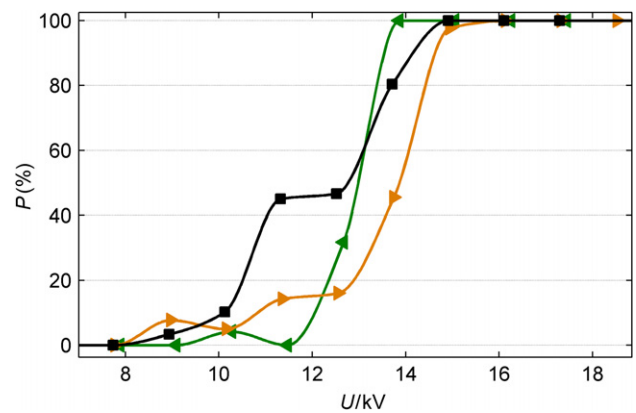
Figure 6. Initiation probability for point anode streamers in cyclohexane with additive di-n-propylether. Symbols: (◄) 0.1 mg g^{-1}, (►) 1.0 mg g^{-1}, (■) 10 mg g^{-1}.

Figure 7. Initiation probability for point anode streamers in cyclohexane with additive 1,1-difluorocyclopentane. Symbols: (◄) 0.1 mg g^{-1}, (►) 1.0 mg g^{-1}, (■) 10 mg g^{-1}.

4 kV voltage interval. Within the range of initiation voltages, there is a systematic increase with increasing concentration for 1-methylnaphthalene. For the other additives, however, the concentration dependence is not conclusive.
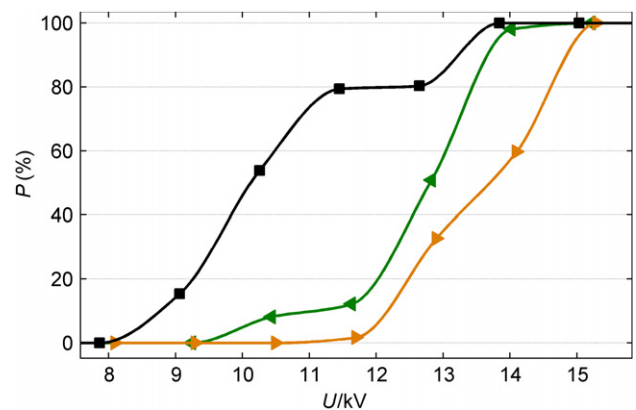
For negative point polarity, the following initiation voltages were found for the different additives (as compared with 10 kV for pure cyclohexane): 8–9 kV for the

Figure 8. Initiation probability for point cathode streamers in cyclohexane with additive perfluoro-n-hexane. Symbols: (▼) dried/degassed, (▲) from bottle, (◄) 0.1 mg g^{-1}, (►) 1.0 mg g^{-1}, (■) 10 mg g^{-1}, (●) 50 mg g^{-1}.
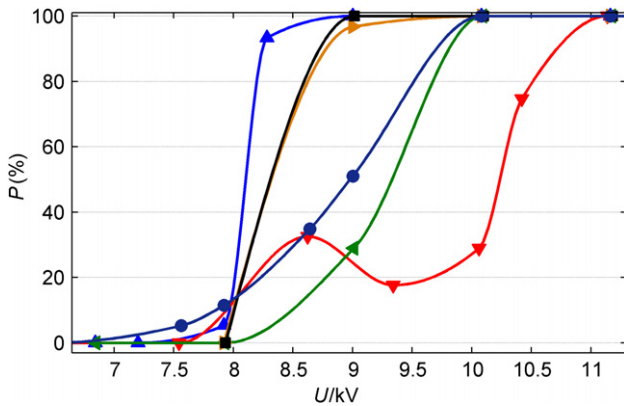

Figure 11. Initiation probability for point cathode streamers in cyclohexane with additive di-n-propylether. Symbols: (◄) 0.1 mg g^{-1}, (►) 1.0 mg g^{-1}, (■) 10 mg g^{-1}.

Figure 9. Initiation probability for point cathode streamers in cyclohexane with additive N,N-dimethylaniline. Symbols: (▼) 0.01 mg g^{-1}, (◄) 0.1 mg g^{-1}, (►) 1.0 mg g^{-1}, (■) 10 mg g^{-1}.
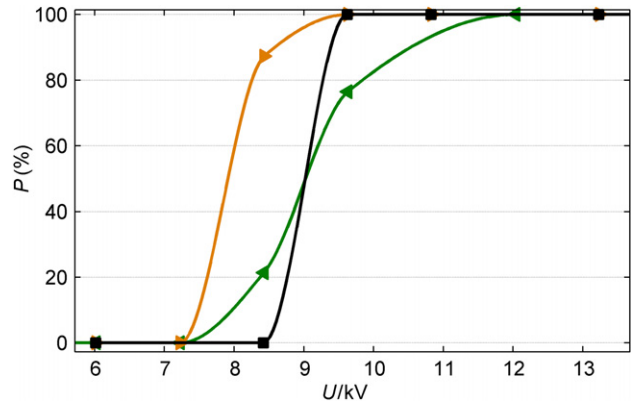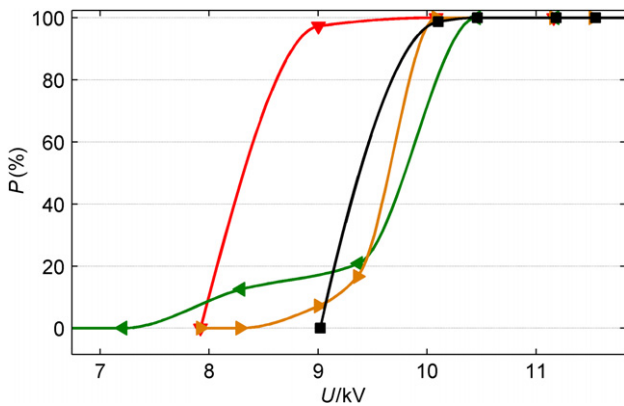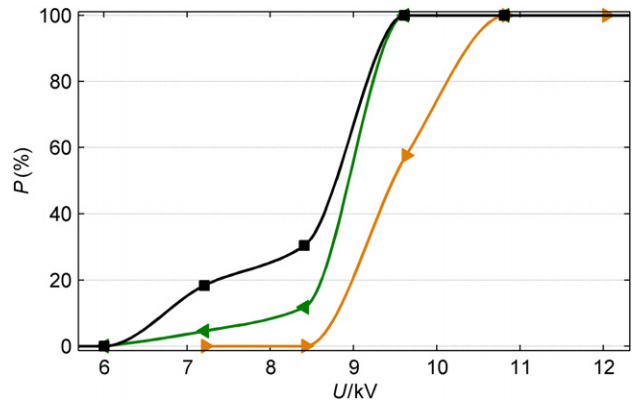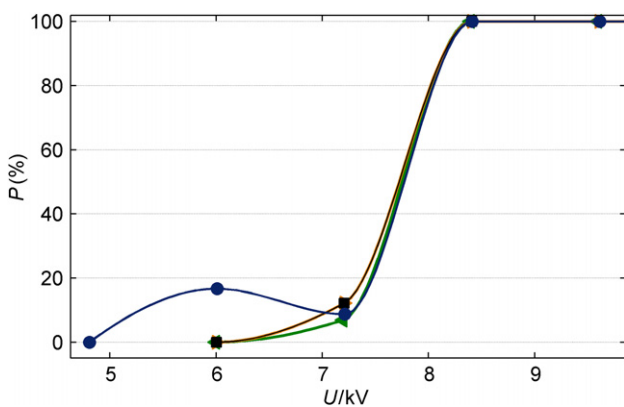

Figure 12. Initiation probability for point cathode streamers in cyclohexane with additive 1,1-difluorocyclopentane. Symbols: (◄) 0.1 mg g^{-1}, (►) 1.0 mg g^{-1}, (■) 10 mg g^{-1}.

Figure 10. Initiation probability for point cathode streamers in cyclohexane with additive 1-methylnaphthalene. Symbols: (◄) 0.1 mg g^{-1}, (►) 1.0 mg g^{-1}, (■) 10 mg g^{-1}, (●) 50 mg g^{-1}.

samples with perfluoro-n-hexane (figure 8), 8.5–10 kV for N,N-dimethylaniline (figure 9), 8 kV for 1-methylnaphthalene (figure 10), 7.5–9.0 kV for di-n-propylether (figure 11), 8.5–9.5 kV for 1,1-difluorocyclopentane (figure 12), and 9–10 kV for 1,4-benzoquinone (figure not shown). Initiation

probabilities generally increase from 0% to 100% initiation over a 1–2 kV voltage interval.

With the large number of experiments around streamer initiation, the number of streamers at each voltage level, which should be binomially distributed, can be approximated by a continuous normal distribution, and gives for the determination of initiation probabilities a standard deviation of about 5%. However, due to an often inhomogeneous distribution of streamer events at each voltage level, variations in voltages for initiation between repeated experiments can be as high as 1.0 and 1.5 kV for negative and positive point polarity, respectively.

Electric field values at the apex of the point electrode corresponding to the initiation voltages can be calculated by using a hyperbolical approximation for sharp points [42]. The estimated error in the calculated electric field value is 11% based on the error of measurement of the tip radius and the gap length. Our results for cyclohexane 'from bottle', 14 MV cm^{-1} and 10 MV cm^{-1} for point anode and cathode streamers respectively, may be compared with values reported in literature. For point anodes with the same tip radius, 13 MV cm^{-1}, has been obtained by Yamashita *et al* [11], whereas a lower value, 8 MV cm^{-1}, has been obtained by
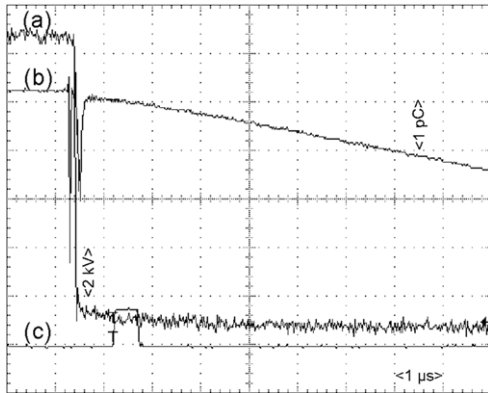
Figure 13. Oscilloscope capture of one current event with readings of: (a) probed high-voltage pulse, (b) charge stored on the measuring capacitor positioned between the point electrode and ground (ref. differential arrangement at #13 in figure 1). (c) camera synchronization pulse showing time of camera exposure. The measured charge is induced by ionic movement in the high-field zone.
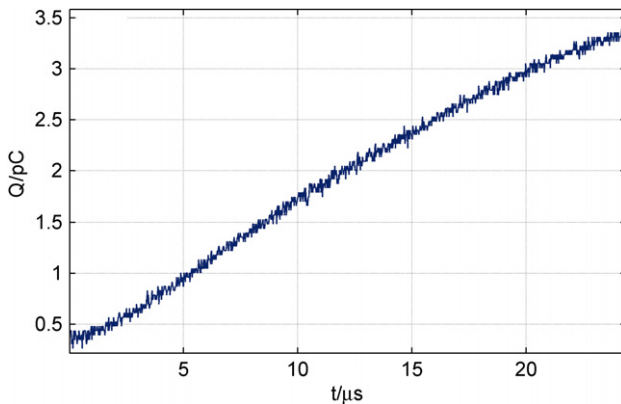
Figure 14. Charge reading of one current event (ref. (b) in figure 13) demonstrating how the current (slope of charge versus time) slowly decreases on a time-scale longer than 10 μs. A constant high voltage is applied from $t = 0$.

Lesaint *et al* [12, 15]. Likewise, initiation fields close to 8 MV cm^{-1} have been reported for point cathode streamers [11, 14]. For our dried/degassed samples, the initiation field remained unchanged for point anode streamers, but increased to 12 MV cm^{-1} for point cathode streamers.

3.2. Conduction currents prior to streamer initiation

For voltages around the onset level for streamers, in the absence of streamers, a seemingly continuous current to the point electrode has been measured for both point polarities, see figure 13. Conduction currents of this kind have previously been observed with a point anode [14]. The currents tend to increase the first few microseconds after applying the voltage, and always decrease slowly on a larger time-scale as shown in figure 14. Depending on the discrete voltage levels, it is often observed that these currents gradually become measurable. The currents are observed in all samples with a point anode, while with a point cathode in 10 out of 21 samples. It is, however, not trivial to deduce any systematic trends for the appearances in negative point polarity.
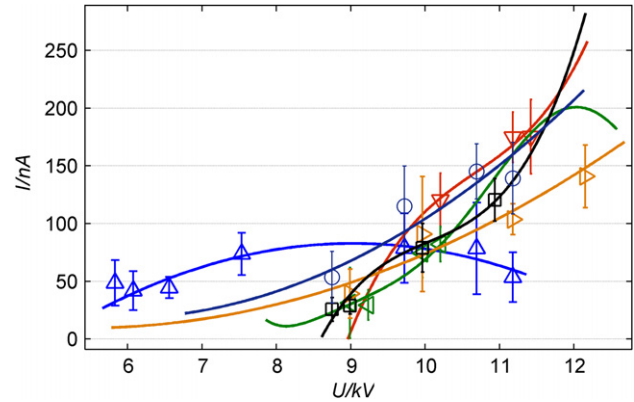
Figure 15. Mean conduction currents to a point anode in cyclohexane with additive perfluoro-n-hexane. Symbols: ($\triangledown$) dried/degassed, ($\triangle$) from bottle, ($\triangleleft$) 0.1 mg g^{-1}, ($\triangleright$) 1.0 mg g^{-1}, ($\square$) 10 mg g^{-1}, ($\bigcirc$) 50 mg g^{-1}.
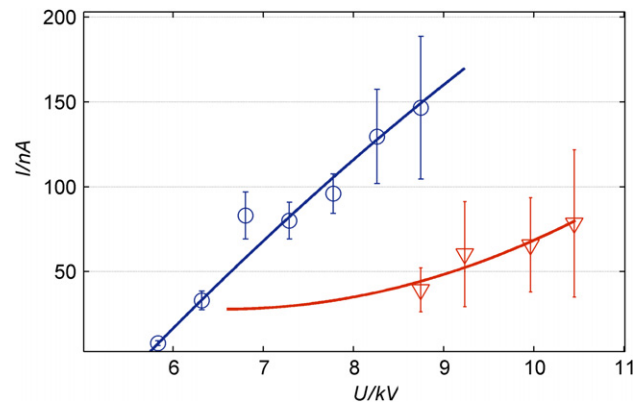
Figure 16. Mean conduction currents to a point cathode in cyclohexane with additive perfluoro-n-hexane. Symbols: ($\triangledown$) dried/degassed, ($\bigcirc$) 50 mg g^{-1}.
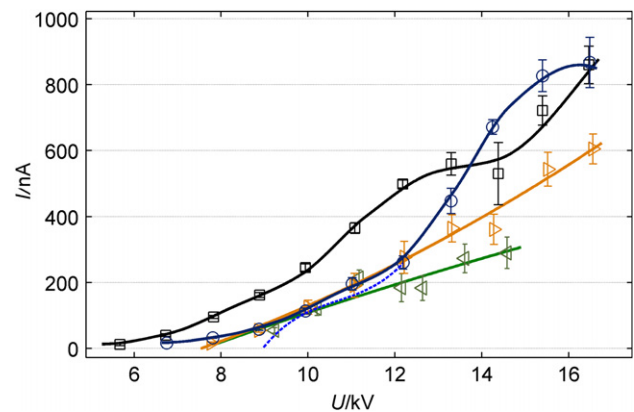
Figure 17. Mean conduction currents to a point anode in cyclohexane with additive N,N-dimethylaniline. Symbols: ($\triangledown$) 0.1 mg g^{-1}, ($\triangleright$) 1.0 mg g^{-1}, ($\square$) 10 mg g^{-1}, ($\bigcirc$) 50 mg g^{-1}.

Average conduction currents are calculated from the slope of charge versus time, and presented in plots with average values and standard deviations in figures 15–21. The continuous lines are either polynomially fitted to all data or interpolated between a number of averaged values, and they serve as trend-lines to improve the readability of the
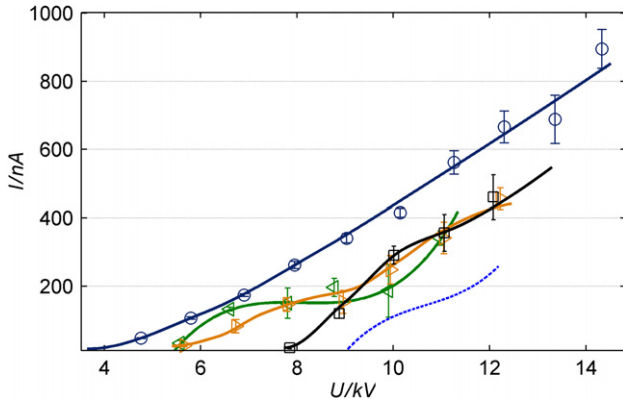
Figure 18. Mean conduction currents to a point anode in cyclohexane with additive 1-methylnaphthalene. Symbols: (◁) 0.1 mg g^{-1}, (▷) 1.0 mg g^{-1}, (□) 10 mg g^{-1}, (○) 50 mg g^{-1}.

Figure 21. Mean conduction currents to a point anode in cyclohexane with additive 1,4-benzoquinone. Symbols: (◁) 0.1 mg g^{-1}, (▷) 1.0 mg g^{-1}.
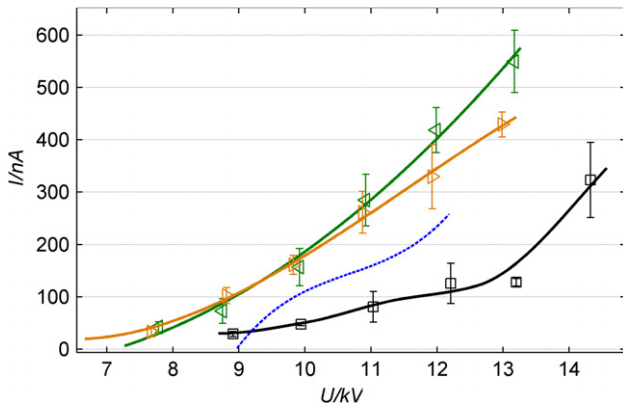
Figure 19. Mean conduction currents to a point anode in cyclohexane with additive di-n-propylether. Symbols: (◁) 0.1 mg g^{-1}, (▷) 1.0 mg g^{-1}, (□) 10 mg g^{-1}.
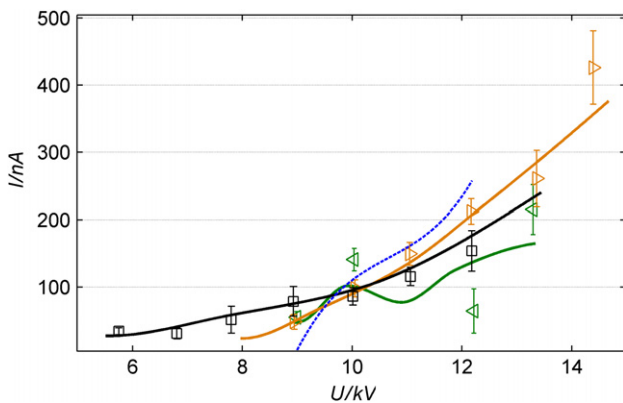
Figure 20. Mean conduction currents to a point anode in cyclohexane with additive 1,1-difluorocyclopentane. Symbols: (◁) 0.1 mg g^{-1}, (▷) 1.0 mg g^{-1}, (□) 10 mg g^{-1}.

plots. A minimum of 15 measurements have been used in the calculation of each averaged value and standard deviation. In some plots, a dashed reference line for the case with no additive has been included.

Effects of additives were only observed for a point anode for the additives N,N-dimethylaniline and 1-methylnaphthalene as shown in figures 17 and 18. Here we measured somewhat larger currents as compared with the other additives, increasing

with increasing concentration up to one micro ampere, but with concentration dependences varying over the voltage range. For negative point polarity, conduction currents are more often observed in pure cyclohexane when great care is taken to remove and avoid dissolved water and atmospheric gases. The current–voltage characteristics vary from liquid to liquid, but there is generally a quasi-linear increase with voltage. The current magnitudes are not correlated with the low-field conductivities of the liquids which were seen to vary due to the additives. Normally, nothing is observed optically during conduction currents. However, in some rare cases just below 100% streamer initiation, we accidentally captured a diffuse shadow of a 15–20 μm diameter bubble at a distance from the point electrode. The rare bubble was observed for all additives (but not for all concentrations) with a point anode, while even more rarely and only with 1,1-difluorocyclopentane with a point cathode.

4. Discussion

For a point cathode in cyclohexane, streamer initiation is experimentally well documented from dc and impulse conditions and attributed to electron avalanches in the liquid phase [43]. Each avalanche current pulse, independently of pressure, induces a shock wave and also a single vapour bubble near the point cathode if the hydrostatic pressure is below the critical pressure of the liquid [44, 45]. The electron avalanche mechanism is well accepted for gases but has generally been difficult to observe in liquids, although evidence has started to emerge when the electric field is very high [22, 46]. The mechanism should be particularly influenced by molecular properties, such as excitation and ionization energies: however, effects of the additives on initiation of point cathode streamers were not observed.

The streamer initiation mechanism for positive point polarity is less clear. According to an experimental study in various non-polar hydrocarbon liquids, where some contained impurities with abilities to produce or retain electrons different from the base liquid, initiation voltages varied mainly with electrode gap parameters [15]. We have observed that initiation voltages fluctuate more in this point polarity, and we find an effect only with 1-methylnaphthalene, giving higher initiation

voltages with increasing concentrations. With an electron avalanche mechanism for streamer initiation, one would on the contrary expect reduced initiation voltages with the additives N,N-dimethylaniline and 1-methylnaphthalene, being more easily ionizable than cyclohexane.

We have shown that electric fields necessary to initiate streamers in cyclohexane are in line with what under similar conditions have been reported elsewhere. Since we can present no conclusive effects of the additives on the initiation of streamers in cyclohexane, the different additives we have chosen may not be substantially different with regard to the processes involved. If mainly electrode effects produce the observed variations in initiation voltages, i.e. when replacing the point electrode between additive series, or from erosion or polymerization, the varying electrochemical properties of the additives may be inferior to fluctuations in local electric field conditions. The microscope verification of point shape and radius of curvature was only suited to detect the more coarse modifications of the electrode surfaces.

Pre inception currents are observed below and in the same voltage range where streamers first appear, suggesting that they are related to the same process. If we assume that an electron avalanche-like mechanism is responsible for these currents and for the initiation of streamers, a starting electron must first become available. It can be produced by mechanisms such as ionization in the liquid (point anode) or field emission at the electrode (point cathode). In an electron avalanche, ionic space charge concentrates by a rapid (nanosecond) process of multiple collisional ionizations between electrons and liquid molecules. The process requires that the electric field is high enough to allow the electrons to acquire sufficient energy over their mean free paths. In divergent field conditions, the volume over which this may occur increases with the applied voltage [47]. During the avalanche, electronic energy is effectively converted into thermal energy in small volumes. If sufficient energy is developed locally to vaporize the liquid, discharges may occur in the vapour cavity and a streamer develops [12]. In the opposite case, the initiation process halts and a conduction current is observed induced by movement of the remaining space charge. The magnitude of this current reflects the degree of charge separation in the avalanche. Likewise, if a bubble initially formed by the avalanche mechanism does not collapse or initiate a streamer, it moves into the gap via the electrohydrodynamic convection, in line with our observations. Theoretical progress concerning electron avalanches in liquids is required to validate the proposed chain of events leading to the formation of bubbles and streamers. A semi-empirical estimate for an avalanche ionization coefficient in liquid cyclohexane has been provided for electric fields above $2\,MV\,cm^{-1}$ [48], while specific cross-sectional data for interaction processes such as impact ionization and excitation are needed in order to clarify the high-field energy distribution for electrons in cyclohexane.

Some observed variations for streamer initiation voltages and conduction currents can provide insight into the initiation mechanism. The lower and more defined initiation voltages for streamers from a point cathode suggest that the electron avalanche process responsible for streamer initiation is most effective for this polarity. One element could be that electrons become more abundant due to field enhanced ejection from

a point cathode [23, 49], than for field ionization in the liquid outside a point anode [50]. At the tip of the point electrode one usually defines a critical volume where the electric field strength will be adequately high over a distance large enough to develop an avalanche above a critical size [47]. An electron from a point cathode will here be supplied at the location most favourable to start an avalanche, while a suitably placed seeding electron near a point anode is a stochastic event with comparatively low probability. We therefore expect a distribution of avalanches a distance from the point anode with varying abilities to evapourate the liquid, leaving initiation for this polarity more affected by parameters influencing the evapouration process, e.g. hydrostatic pressure [14]. Possibly, the observed conduction currents reflect the low-efficiency tail of this distribution. The low number of current observations for negative point polarity then either indicates non-measurable currents at the lower voltages, or a more efficient evapouration process. When initiation voltages for point cathode streamers become higher and less defined, conduction currents are observed more frequently and roughly follow the same current-voltage characteristics as for a point anode. Moreover, conduction currents to a point anode increase with the low ionization potential additives 1-methylnaphthalene and N,N-dimethylaniline despite the stochastic nature of these currents, and serves to strengthen the theory of a liquid electron avalanche-like mechanism. However, it is not straightforward to interpret the presented graphs. If an avalanche mechanism is the main mechanism behind initiation of streamers in cyclohexane, electronic energies should be close to the ionization potential of the molecules. Thus, since low-energetic ($<3\,eV$) electrons are required to stimulate the electron-attaching properties of perfluoro-n-hexane, 1-methylnaphthalene and 1,4-benzoquinone [34–37] the electron attaching abilities of these liquids should impose no significant effect on streamer initiation, in agreement with our findings.

Considering a stationary liquid, it is possible to evaluate the transient current induced by a concentration of ions by using an analytical representation of the electric field between a point and a plane electrode in prolate-spheroid geometry [42]. In our case, ions will drift only some micrometres into the gap during the duration of the applied pulse, and space charge saturation will limit charges induced to the point electrode to values below the measured ones by up to three orders of magnitudes [51]. It is, however, possible that charge induced electrohydrodynamic convection in the high-field zone accelerates ions to such an extent to induce such high currents, provided that a sufficiently strong convection develops on a microsecond time-scale [52]. In order to evaluate the experimental current–voltage characteristics one must first solve the problem of electrohydrodynamic convection in divergent field conditions, since approximate derivations, valid for negligible fluid motion only, cannot be used.

Amongst the alternatively proposed mechanisms for streamer initiation, Dumitrescu *et al* suggest a boiling mechanism where conduction currents induce a local heating if emitted from a microregion on the point anode [14], whereas Lewis suggests that the primary steps of any streamer initiation may be an electromechanical and highly field-dependent formation of sub-microscopic cavities [53]. It has

also been pointed out that pressure reduction induced by both the electrohydrodynamic motion [22] and Coulomb repulsion between unipolar charges [54], can be responsible for, or at least assist the formation of a gas phase.

5. Conclusion

With a point anode, probabilities for streamer initiation vary only with the additive 1-methylnaphthalene, requiring higher initiation voltages with increasing concentration. Moreover, conduction currents prior to streamer initiation were always observed, and increased to some extent with the additives N,N-dimethylaniline and 1-methylnaphthalene. With a point cathode, effects of additives on streamer initiation were not observed, and conduction currents of measurable magnitudes were less frequent. In both point polarities, the transient currents may be induced by ions left behind avalanches that are not sufficiently developed to initiate streamers. The differences between positive and negative point polarity are qualitatively explained by the stochastic event of having a starting electron available and suitable positioned in the high-field zone.

References

[1] Goldman M and Sigmond R S 1982 *IEEE Trans. Electr. Insul.* **17** 90–105
[2] Sigmond R S 1984 *J. Appl. Phys.* **56** 1355–70
[3] Berger N, Randoux M, Ottmann G and Vuarchex P 1997 *Électra* **171** 33–56
[4] Hall J F 1993 *IEEE Trans. Power. Deliv.* **8** 376–85
[5] Beroual A, Zahn M, Badent A, Kist K, Schwabe A J, Yamashita H, Yamazawa K, Danikas M, Chadband W G and Torshin Y 1998 *IEEE Electr. Insul. Mag.* **14** 6–17
[6] IEC Standard 60422 2002 Supervision and maintenance guide for mineral insulating oils Electrical Equipment 3rd edn (Geneva: International Electrotechnical Commission)
[7] Lundgaard L E, Hestad Ø and Ingebrigtsen S 2005 *Proc. Symp. on Nordic Insulation (NORD-IS, Trondheim)* pp 83–7
[8] Lundgaard L E, Linhjell D, Berg G and Sigmond R S 1998 *IEEE Trans. Dielectr. Electr. Insul.* **5** 388–95
[9] Forster E O, Mazzetti C and Pompili M 1990 *L'Energia Elettrica* **1** 1–19
[10] Denat A, Bonifaci N and Nur M 1998 *IEEE Trans. Dielectr. Electr. Insul* **5** 382–7
[11] Yamashita H, Yamazawa K and Wang Y S 1998 *IEEE Trans. Dielectr. Electr. Insul.* **5** 396–401
[12] Gournay P and Lesaint O 1993 *J. Phys. D: Appl. Phys.* **26** 1966–74
[13] Lesaint O and Tobazéon R 1988 *IEEE Trans. Electr. Insul.* **23** 941–54
[14] Dumitrescu L, Lesaint O, Bonifaci N, Denat A and Notingher P 2001 *J. Electrost.* **53** 135–46
[15] Lesaint O and Gournay P 1994 *IEEE Trans. Dielectr. Electr. Insul.* **1** 702–8
[16] Lesaint O and Gournay P 1994 *J. Phys. D : Appl. Phys.* **27** 2111–16
[17] Qotba R, Aitken F and Denat A 2005 *IEEE Proc. Int. Conf. Dielectric. Liquids (Coimbra)* pp 115–18

[18] FitzPatric G J, McKenny P J and Forster E O 1990 *IEEE Trans. Electr. Insul.* **25** 672–82
[19] Chadband W G 1980 *J. Phys. D: Appl. Phys.* **13** 1299–307
[20] Devins J C, Rzad S J and Schwabe R J 1981 *J. Appl. Phys.* **52** 4531–45
[21] Beroual A and Tobazéon R 1986 *IEEE Trans. Electr. Insul.* **21** 613–27
[22] Tobazéon R 1994 *IEEE Trans. Dielectr. Electr. Insul.* **1** 1132–47
[23] Schmidt W F 1984 *IEEE Trans. Electr. Insul.* **19** 389–418
[24] Denat A 2006 *IEEE Trans. Dielectr. Electr. Insul.* **13** 518–25
[25] Lewis T J 1985 *IEEE Trans. Electr. Insul.* **20** 123–32
[26] Gournay P and Lesaint O 1994 *J. Phys. D: Appl. Phys.* **27** 2117–27
[27] Berg G 1995 Physics of electrical breakdown of transformer oil *Doctoral Dissertation*, University of Trondheim, Norwegian Institute of Technology, ISBN 82-7119-878-5
[28] Hebner R E 1988 Measurements of electrical breakdown in liquids *The Liquid State and its Electrical properties* (*NATO Advanced Study Institute, Ser. B*: *Physics* vol 193) ed E E Kunhardt *et al* (New York: Plenum) pp 519-37
[29] Sigmond R S 1998 *Proc. 11th Symp. on Elementary Processes and Chemical Reactions in Low Temperature Plasma (Bratislava)* p 256
[30] Fotino M 1993 *Rev. Sci. Instrum.* **64** 159–67
[31] Wilhelm E and Battino R 1973 *J. Chem. Thermodyn.* **5** 117–20
[32] IUPAC-NIST Solubility Database, Standard Reference Database 106, http://srdata.nist.gov/solubility/
[33] Lide D R 2004 *Handbook of Chemistry and Physics* 84th edn (Boca Raton, FL: CRC) pp 10/181–198
[34] Hunter S R and Christophorou L G 1984 *J. Chem. Phys.* **80** 6150–63
[35] Collins P M, Christophorou L G, Chaney E L and Carter J G 1970 *Chem. Phys. Lett.* **4** 646–50
[36] Christophorou L G and Blaunstien R P 1969 *Radiat. Res.* **37** 229–45
[37] Tobita S, Meinke M, Illenberger E, Christophorou L G, Baumgartel H and Leach S 1992 *J. Chem. Phys.* **161** 501–8
[38] Bakale G, Gregg E C and McCreary R D 1977 *J. Chem. Phys.* **67** 5788–94
[39] Forster E O, Mazzetti C, Pompili M and Cecere R 1991 *IEEE Trans. Electr. Insul.* **26** 749–54
[40] Shockley W 1938 *J. Appl. Phys.* **9** 635–6
[41] Ramo S 1939 *Proc. I R E* **27** 584–5
[42] Coelho R and Debeau J 1971 *J. Phys. D : Appl. Phys.* **4** 1266–80
[43] Denat A, Gosse J P and Gosse B 1988 *IEEE Trans. Electr. Insul.* **23** 545–54
[44] Kattan R, Denat A and Lesaint O 1989 *J. Appl. Phys.* **66** 4062–6
[45] Kattan R, Denat A and Bonifaci N 1991 *IEEE Trans. Electr. Insul.* **26** 656–62
[46] Lewis T J 1994 *IEEE Trans. Dielectr. Electr. Insul.* **1** 630–43
[47] Kim M and Hebner R E 2006 *IEEE Trans. Dielectr. Electr. Insul.* **13** 1254–60
[48] Haidara M and Denat A 1991 *IEEE Trans. Electr. Insul.* **26** 592–7
[49] Halpern B and Gomer R 1965 *J. Chem. Phys.* **43** 1069–70
[50] Halpern B and Gomer R 1969 *J. Chem. Phys.* **51** 1048–56
[51] Sigmond R S 1986 *J. Electrost.* **18** 249–72
[52] Atten P 1996 *IEEE Trans. Dielectr. Electr. Insul.* **3** 1–17
[53] Lewis T J 1998 *IEEE Trans. Dielectr. Electr. Insul.* **5** 306–15
[54] Sueda H and Kao K C 1982 *IEEE Trans. Electr. Insul.* **17** 221–7

Paper 2

Effects of additives on prebreakdown phenomena in liquid cyclohexane: II. Streamer propagation

Stian Ingebrigtsen, Lars E. Lundgaard and Per-Olof Åstrand

2007

Effects of additives on prebreakdown phenomena in liquid cyclohexane: II. Streamer propagation

S Ingebrigtsen[1], L E Lundgaard[2] and P-O Åstrand[1]

[1] Department of Chemistry, Norwegian University of Science and Technology,
N-7491 Trondheim, Norway
[2] Department of Electric Power Technology, SINTEF Energy Research, N-7465 Trondheim,
Norway

E-mail: stian.ingebrigtsen@sintef.no

Abstract

Streamer propagation in cyclohexane with various additives have been
studied with fast impulses applied to a point-to-plane gap. The additives are
perfluoro-*n*-hexane, *N,N*-dimethylaniline, 1-methylnaphthalene,
di-*n*-propylether, 1,1-difluorocyclopentane and 1,4-benzoquinone,
representing molecules with different electrochemical properties. We have
used shadowgraphic imaging and a differential charge-measurement
technique with a sensitivity of 0.1 pC to integrate currents induced to the
point electrode during streamer propagation. The propagation is to various
degrees facilitated by the additives. Perfluoro-*n*-hexane affects point
cathode streamers, *N,N*-dimethylaniline and di-*n*-propylether affect point
anode streamers, while 1-methylnaphthalene and 1,4-benzoquinone affect
both point anode and point cathode streamers. 1,1-difluorocyclopentane is
the only additive without a measurable effect in either point polarity. Largest
effects are found for perfluoro-*n*-hexane, *N,N*-dimethylaniline and
1-methylnaphthalene, which are the only additives to produce a visible
change in streamer appearances. In these cases, filaments become thinner
and fewer, while propagating faster and sometimes further. The results
follow expectations, considering point cathode streamers to be governed
mainly by injection of thermal electrons from a gaseous phase, and point
anode streamers to be governed mainly by more energetic electrons,
extracted from the liquid at higher electric fields.

(Some figures in this article are in colour only in the electronic version)

1. Introduction

Dielectric liquids are used as electrical insulators in
electrotechnical applications [1]. However, the insulating
properties of insulators are quickly reduced when the electric
field exceeds a critical value. Shortly before an electric
breakdown occurs, conductive channels of ionized gas,
'streamers', initiate at the location of the highest electric
field and propagate through the insulating material until
the electrode gap is bridged. This 'prebreakdown process'
is vital to our understanding of dielectric performance of

materials and insulation systems. The understanding of
the processes originates from models developed for gaseous
discharges [2, 3]. However, the phenomena in liquids
involve mechanisms which are not yet fully understood
[4–11]. In particular, fundamental parameters describing high-
field interactions between energetic electrons and the liquid
molecules are not available. The ability of a liquid to withstand
electric stress is influenced by its molecular structure, where
conditions under which electrostatic energy is converted to
localized heat plays a role. Electron multiplication by
consecutive collisional ionizations provides an intense release

of energy, and we consider this to be the main mechanism behind initiation and propagation of streamers in liquids.

Experiments to build empirical knowledge and to verify theories on the subject have been performed for several different liquids [12]. Results have been analysed with respect to molecular parameters such as molecular weight and chain length [13], molecular branching and structure, molecular double and triple bounds [14, 15], special atoms or functional groups within the molecule [14, 16] and liquid bulk parameters such as viscosity [17–19], boiling point [17, 20], conductivity [21] and permittivity [13, 21]. Several studies have also shown that adding small amounts of molecules with specific electrochemical properties can drastically change the behavior of streamers [3, 4, 22–24]. Starting with the pioneering work of Devins [3], it has generally been demonstrated that molecules with electron-attaching capabilities such as perfluoro-*n*-hexane and carbontetrachloride encourage faster propagation velocities and thinner structures for point cathode initiated streamers, while the same effects are not observed for point anode initiated streamers [3]. Conversely, additives with low ionization potentials, such as *N,N*-dimethylaniline and pyrene, have been found to speed up point anode initiated streamers [3].

We have studied the role of additives with different electro-chemical properties on propagation of streamers generated in a point-to-plane gap, using both positively and negatively charged point electrodes. The additives were perfluoro-*n*-hexane, *N,N*-dimethylaniline, 1-methylnaphthalene, di-*n*-propylether, 1,1-difluorocyclopentane and 1,4-benzoquinone, representing the range from trace impurities up to larger fractions of the samples. As compared with cyclohexane, perfluoro-*n*-hexane, 1-methylnaphthalene and 1,4-benzoquinone are known to more easily attach electrons, while *N,N*-dimethylaniline and 1-methylnaphthalene more easily become ionized [25]. We have earlier investigated the effects of the same additives on streamer initiation [25]. Considering the varying energetic conditions for which electrons exist during streamer propagation in negative and positive point polarity, we expect for each case a significant influence of, respectively, electron attachment and ionization processes. Experimentally we have studied macroscopic features of streamer propagation, such as streamer dimensions, shape and charge. This combination of optical and electrical measurements represents today the best diagnostic technique for identifying propagation characteristics of streamers.

2. Experiment and measuring techniques

The experimental setup and procedures for sample preparation have been described in an earlier paper [25]. High-voltage rectangular pulses were applied to the plane electrode of a 10 mm point-to-plane gap, and the streamers initiated were studied with a shadowgraphic depiction technique and by measuring the charge induced on the point electrode. The magnitude of the high-voltage pulses has been varied in steps of 1 kV, and about 30 streamers were recorded at each voltage level with a minimum intermittent delay of 3 min. The experiments were conducted at room temperature and ambient pressure.

The streamers studied all stopped propagating before the high-voltage pulse was quenched and before reaching the opposite electrode. A digitized shadowgraphic image was taken at the moment of maximum streamer extension into the gap. From this image, both the radial stopping length of the furthest propagating region (filament) and the area of the streamer shadow could be obtained. The average streamer propagation velocity was estimated from the stopping length and the observed duration of the charge injection. As the measured length is taken from the projection of the streamer onto the image plane, it is not the real length unless the streamer has a spherical-like distribution. An additional scatter for this parameter is therefore expected. A digital Fourier-bandpass filter is used to remove image noise, and a threshold function is used to subtract and to measure the area of the shadow. The shadow area correlates with streamer volume and with the number of streamer filaments; however, the feasibility of this parameter relies on a low degree of filament overlap in the image.

Streamer events were measured as time-resolved oscillograms of charge stored on a capacitor connected to the point electrode, where displacement currents were suppressed by a differential technique described earlier [25]. A sudden increase in the charge readings corresponds to the initial growth of a streamer. Average streamer currents have been calculated from the slope of streamer charge versus time.

Experimental results are presented in plots with average values and standard deviations. Continuous lines, either polynomically fitted to all data or interpolated between a number of averaged values, serve as trend-lines to improve the readability of the plots.

3. Results

3.1. Streamer propagation

3.1.1. Point anode. Streamers from a point anode in pure cyclohexane have an irregular (filamentary) shape at all voltages, in accordance with what is generally observed for slow streamers in cyclohexane [26–28]. The shape resembles a bush-structure growing in a radial direction from the tip of the point electrode. Adopting conventional terminology, the streamers can be classified somewhere between 'bush-like' and filamentary 'tree-like' [26, 28]. An increase in voltage increases both the number and the length of the main branches (filaments) originating from the point and also the number of secondary side branches. The range of average filament diameters varies, decreasing from within 20–50 μm to within 15–30 μm as voltage is raised from 9 to 16 kV. A 'fast' streamer type with propagation limited to a few main filaments is expected for voltages above a 'propagation voltage', characteristic for the liquid [28–30]. Values at both 14.5 and 30 kV have been reported for cyclohexane [26, 28, 31]. Since a 'fast' streamer at some point during the propagation transforms into a 'slow' one [23], it is not revealed by taking images of fully developed streamers. However, we obtained an onset of 'fast' streamers for voltages above ∼18 kV by also taking some images during the first rather than the last part of the streamer development.

There was no noticeable effect from reducing the content of gas and water in cyclohexane. However,
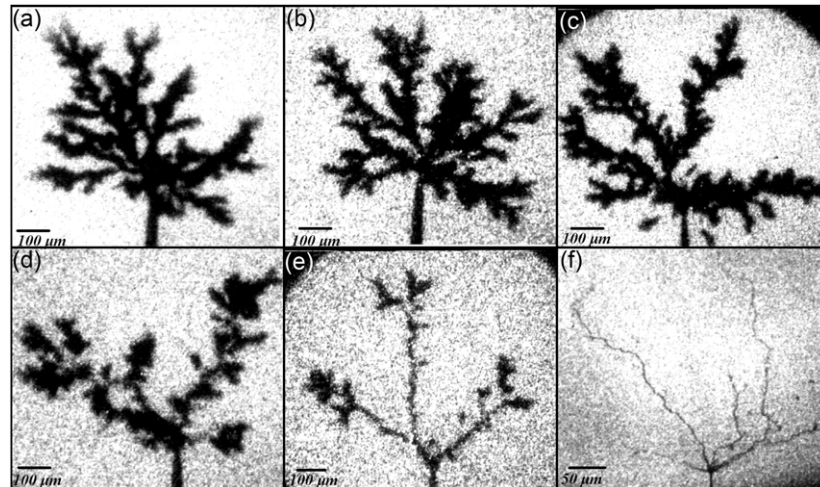
Figure 1. Shadowgraphic images of point anode streamers in cyclohexane with additive *N,N*-dimethylaniline for an applied voltage $U = 16$ kV, (*a*) 'from bottle', (*b*) dried/degassed, (*c*) 0.1 mg g^{-1} (*d*) 1.0 mg g^{-1}, (*e*) 10 mg g^{-1}, (*f*) 50 mg g^{-1}.
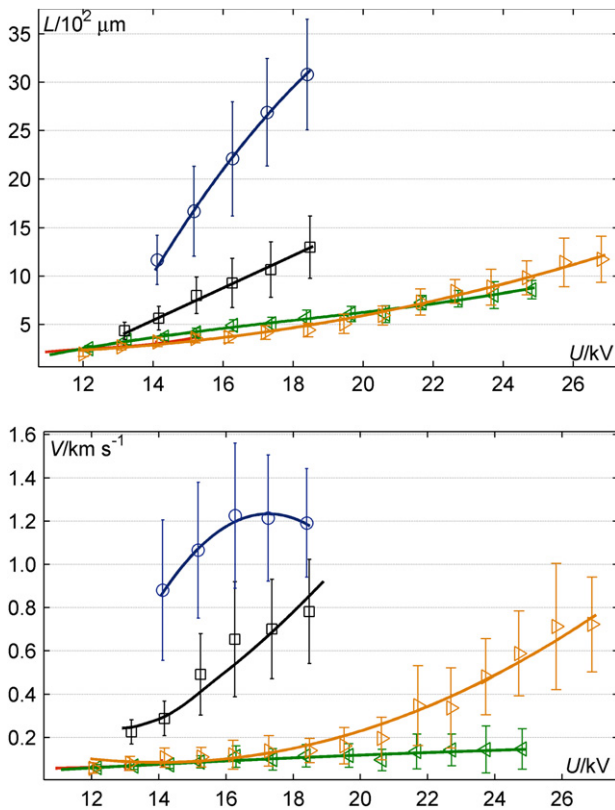
Figure 2. Stopping lengths and mean velocities of point anode streamers in cyclohexane with additive *N,N*-dimethylaniline, (◁) 0.1 mg g^{-1}, (▷) 1.0 mg g^{-1}, (□) 10 mg g^{-1}, (○) 50 mg g^{-1}.

Figure 3. Stopping lengths and mean velocities of point anode streamers in cyclohexane with additive 1-methylnaphthalene, (△) 0 mg g^{-1}, (◁) 0.1 mg g^{-1}, (▷) 1.0 mg g^{-1}, (□) 10 mg g^{-1}, (○) 50 mg g^{-1}.

N,N-dimethylaniline and 1-methylnaphthalene significantly changed the appearances of point anode streamers, as shown for *N,N*-dimethylaniline in figure 1. The additives induced changes in filament diameters, branching and propagation distance. Depending on the voltage, we could distinguish one or sometimes two main filaments with several and relatively much shorter side branches at 1.0 mg g^{-1}. With concentration increasing up to 50 mg g^{-1}, the number of side branches decreased and the main filaments propagated further. At

the same time, filament diameters were significantly reduced, ranging from approximately 10 to below 5 μm. The filaments, moreover, got a smoother shape with fewer secondary branches, opposite to the effect reported for the aromatic additive, pyrene, in cyclohexane [23]. As seen in figures 2 and 3, average streamer velocities increase with additive concentration reaching the velocity of sound in cyclohexane (1280 m s^{-1}) [32] for the two highest concentrations. Effects
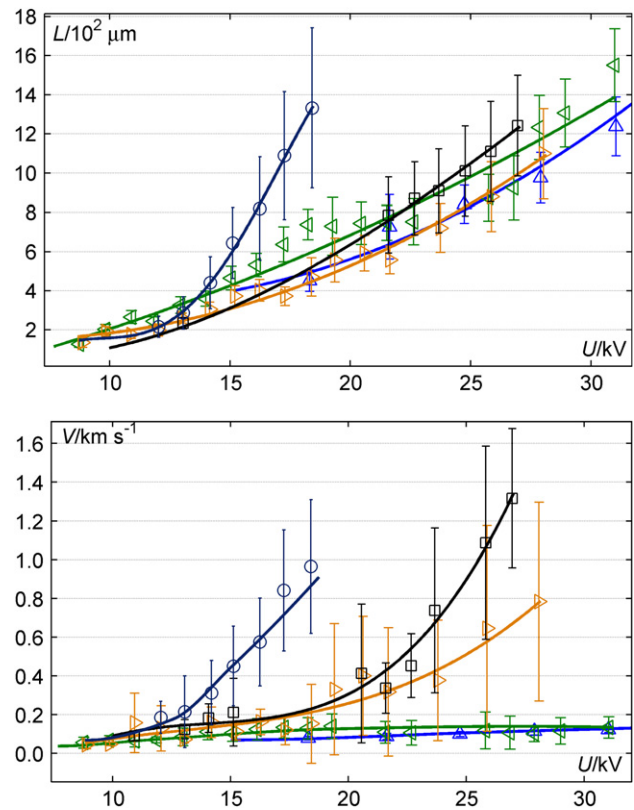
Figure 4. Shadowgraphic images of point cathode streamers in cyclohexane with additive perfluoro-*n*-hexane for an applied voltage $U = 16$ kV, (*a*) 'from bottle', (*b*) dried/degassed, (*c*) 0.1 mg g^{-1} (*d*) 1.0 mg g^{-1}, (*e*) 10 mg g^{-1}, (*f*) 50 mg g^{-1}.
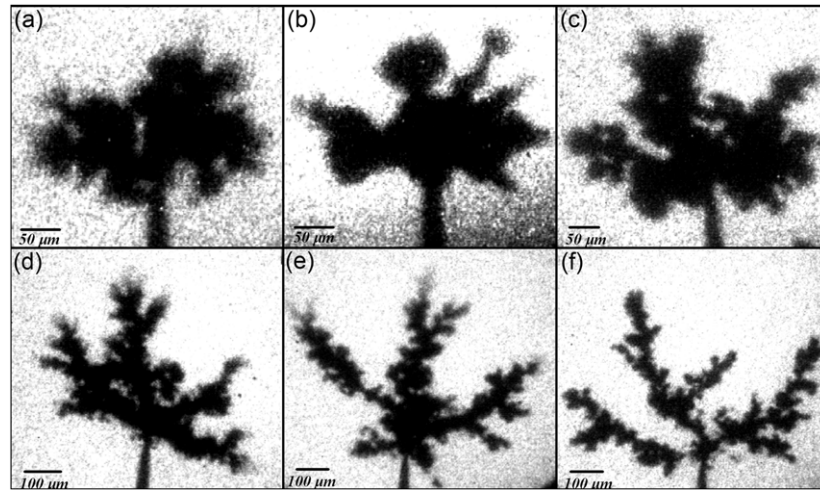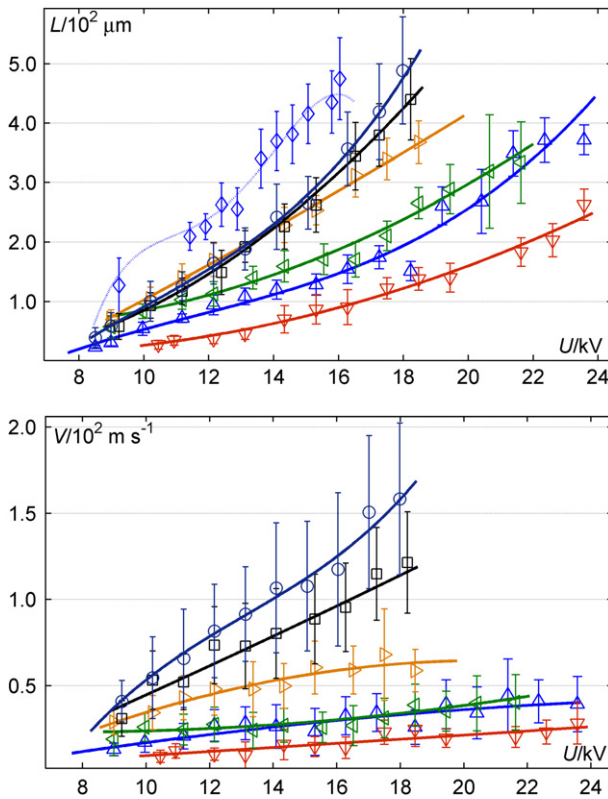

Figure 5. Stopping lengths and mean velocities of point cathode streamers in cyclohexane with additive perfluoro-*n*-hexane, ($\triangledown$) dried/degassed, ($\triangle$) 'from bottle', ($\triangleleft$) 0.1 mg g^{-1}, ($\triangleright$) 1.0 mg g^{-1}, ($\square$) 10 mg g^{-1}, ($\bigcirc$) 50 mg g^{-1}, ($\diamond$) reference plot for point anode streamers without additives.

Figure 6. Total charge and mean current of *point anode* streamers in cyclohexane with additive *N,N*-dimethylaniline, (- - - -) 0 mg g^{-1}, ($\triangledown$) 0.01 mg g^{-1}, ($\triangleleft$) 0.1 mg g^{-1}, ($\triangleright$) 1.0 mg g^{-1}, ($\square$) 10 mg g^{-1}, ($\bigcirc$) 50 mg g^{-1}.

of *N,N*-dimethylaniline and 1-methylnaphthalene on streamer velocity differ in that the dependence on voltage reduces for the former, and sonic streamers are observed even at the lower voltages. When streamers become less spherical with fewer and further propagating filaments, measured values for length and velocity become more scattered.

We could not distinguish visible effects on the streamer structures for positive point polarity by the other additives

(figures not shown). However, for voltages above some threshold voltage ($\sim$20 kV) and for the highest concentrations of 1,4-benzoquinone and di-n-propylether, average streamer velocities increase more rapidly.

3.1.2. Point cathode. Streamers originating from a point cathode in pure cyclohexane resemble the profile given by Yamashita *et al* [26]. At low voltages the streamers obtain
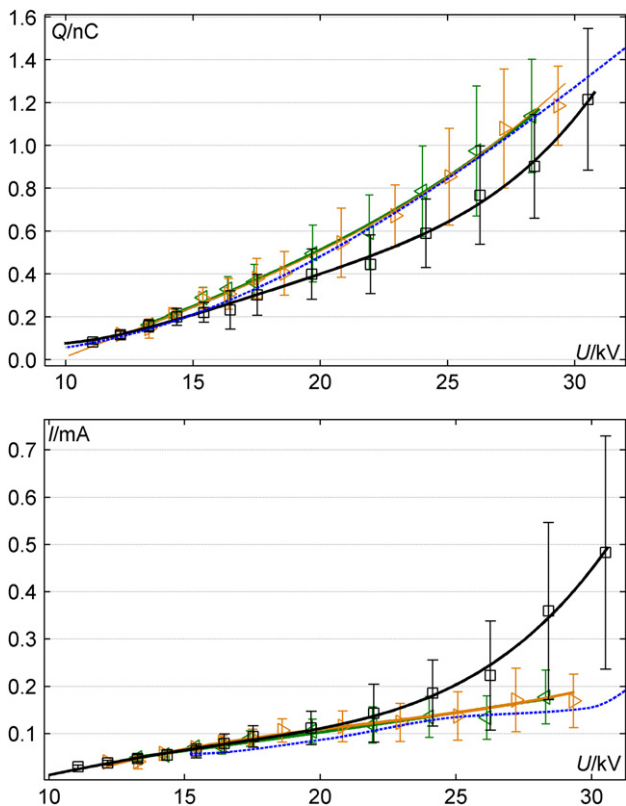
Figure 7. Total charge and mean current of point anode streamers in cyclohexane with additive di-*n*-propylether, (- - - -) 0 mg g^{-1}, (◁) 0.1 mg g^{-1}, (▷) 1.0 mg g^{-1}, (□) 10 mg g^{-1}.

Figure 8. Total charge and mean current of point cathode streamers in cyclohexane with additive perfluoro-*n*-hexane, (▽) dried/degassed, (△) 'from bottle', (◁) 0.1 mg g^{-1}, (▷) 1.0 mg g^{-1}, (□) 10 mg g^{-1}, (○) 50 mg g^{-1}. (◇) reference plot for point anode streamers without additive.

an elliptical or hemispherical structure. At higher voltages (>15 kV), the shape becomes gradually more irregular with a fragmented circumference. Secondary 'bubbles' often originate from the vicinity of these 'cloudy' structures, and occasionally also thinner branches emerge and propagate a relatively short distance.

Reducing the content of gas and water reduced the finer details of the shadow irregularities, besides reducing the overall streamer size, see figure 4. By subsequently adding perfluoro-*n*-hexane, fragmentation increased with increasing concentration until separate and more defined and branched structures with gradually thinner filaments appeared (figure 4). This effect is comparable to the effect of increasing applied voltage. At 50 mg g^{-1}, filaments were more defined for the higher voltages and with average diameters within 15–40 μm, while propagating structures were seldom observed for the lower voltages. The filaments originated from the point electrode and propagated gradually further and faster when the concentration of perfluoro-*n*-hexane was increased, opposite to the effect of reducing the content of gas and water, see figure 5. At 50 mg g^{-1}, the streamers reached velocities similar to those for a point anode. As compared with point anode streamers, the filaments were generally more 'fragmented' but not as branched with secondary filaments, and they reached a maximum stopping length while the overall streamer shape still changed with additive concentration. Thus, streamer propagation becomes less influenced by the field enhancement due to gradually thinner and more distant filament tips [23, 33] than by the tip potential determined by the voltage drop along the filament.

With the other additives, a visible effect on the streamer structure was only distinguished for 1-methylnaphthalene (figures not shown). The effect was here similar to that described for perfluoro-*n*-hexane, but weaker and thus more difficult to separate from the general random appearances of streamers. We also found that average streamer velocities increased with increasing concentration of the two additives 1-methylnaphthalene and 1,4-benzoquinone.

3.2. Electrical measurements

3.2.1. Total charge and mean current. There is an effect from the additives on the measurements of streamer charge and current analogous to the effects on streamer length and velocity, but the measurements are less scattered. Thus, *N,N*-dimethylaniline and di-*n*-propylether affect point anode streamers (figures 6 and 7), perfluoro-*n*-hexane affects point cathode streamers (figure 8), while 1-methylnaphthalene and 1,4-benzoquinone affect both point anode and cathode streamers (figures 9–12). For both point polarities, the mean streamer current increased more or less proportional to the square root of the additive concentration. For point anode streamers, *N,N*-dimethylaniline had an overall effect 2–3 times larger than 1-methylnaphthalene, and perhaps 3–5 and 6–9 times larger than 1,4-benzoquinone and di-*n*-propylether, respectively. For point cathode streamers, perfluoro-*n*-hexane had an effect about 1.5 times larger than 1-methylnaphthalene and 1,4-benzoquinone. While point cathode streamers are
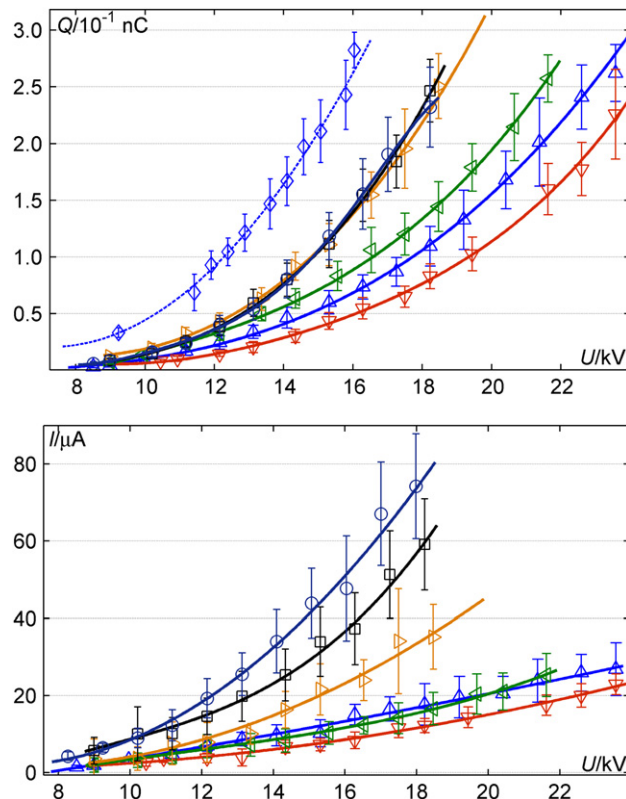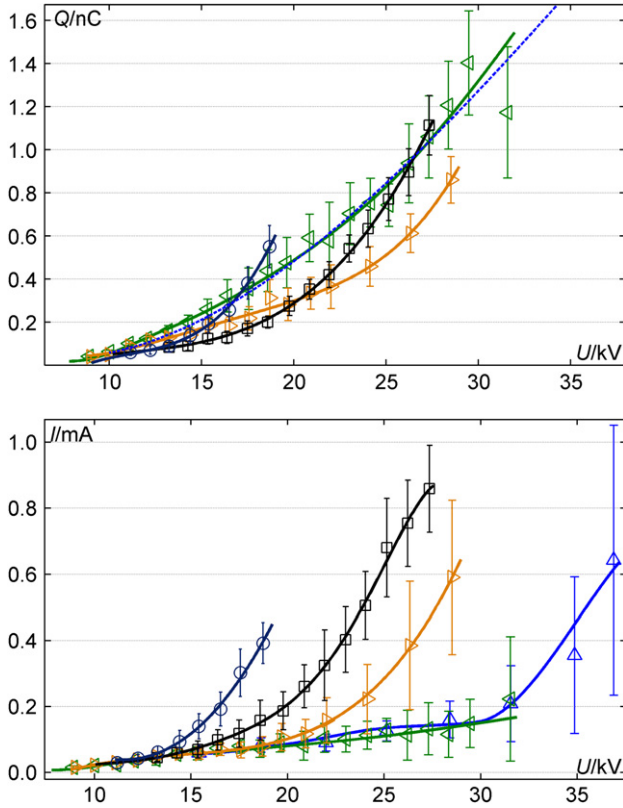
Figure 9. Total charge and mean current of point anode streamers in cyclohexane with additive 1-methylnaphthalene, ($\triangle$ and - - - -) $0 \, \mathrm{mg \, g^{-1}}$, ($\triangleleft$) $0.1 \, \mathrm{mg \, g^{-1}}$, ($\triangleright$) $1.0 \, \mathrm{mg \, g^{-1}}$, ($\square$) $10 \, \mathrm{mg \, g^{-1}}$, ($\bigcirc$) $50 \, \mathrm{mg \, g^{-1}}$.
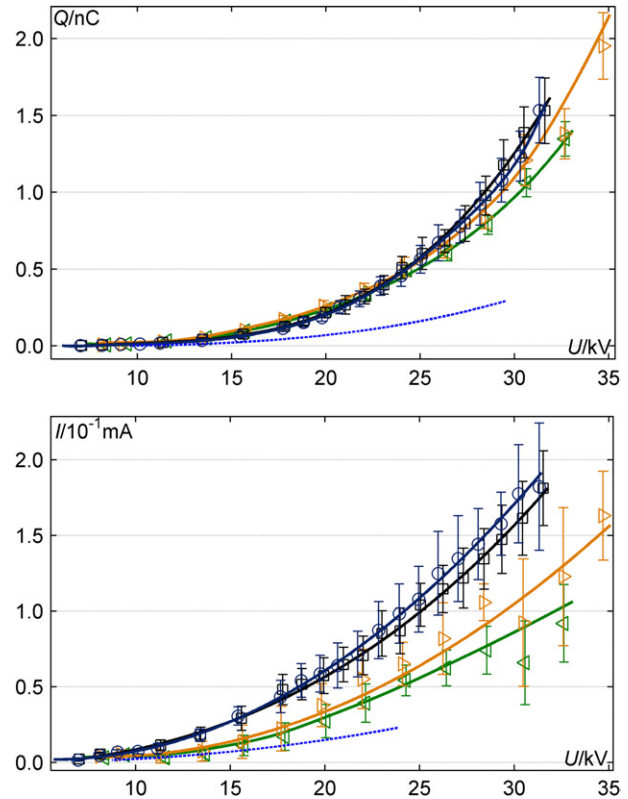

Figure 10. Total charge and mean current of point cathode streamers in cyclohexane with additive 1-methylnaphthalene, (- - - -) $0 \, \mathrm{mg \, g^{-1}}$, ($\triangleleft$) $0.1 \, \mathrm{mg \, g^{-1}}$, ($\triangleright$) $1.0 \, \mathrm{mg \, g^{-1}}$, ($\square$) $10 \, \mathrm{mg \, g^{-1}}$, ($\bigcirc$) $50 \, \mathrm{mg \, g^{-1}}$.

affected more or less equally at all voltages, the effects on point anode streamers are limited mainly to voltages above a threshold value (propagation voltage) dependent on additive and concentration. Normally, for point anode streamers, we find from the time-resolved oscillograms two current regimes with characteristic times dependent on the experimental conditions, see figure 13. Larger currents are associated with the first, corresponding to a fast propagation, for which the duration increases more rapidly when applied voltage is raised above the threshold value.

Comparing values of streamer charge and stopping length, as demonstrated in figure 14, a roughly linear correlation was found for streamers above a minimum length of around $30 \, \mu \mathrm{m}$. The nonlinearity can be reduced by plotting each streamer length against its 'capacitance', $Q U^{-1}$, as done in figure 15. The capacitances per length are found remarkably alike for all samples, $38 \pm 5 \, \mathrm{pF \, m^{-1}}$ and $42 \pm 5 \, \mathrm{pF \, m^{-1}}$ for positive and negative polarity, respectively. Similar plots have been shown previously for a mineral oil and larger electrode gaps [34], giving a capacitance per length of $30 \, \mathrm{pF \, m^{-1}}$ for positive point polarity, $20 \, \mathrm{pF \, m^{-1}}$ for negative point polarity, respectively. Also, plots of streamer length versus $Q U^{-1}$ for streamers in cyclohexane with different applied hydrostatic pressures have been presented with a general capacitance per length of around $50 \, \mathrm{pF \, m^{-1}}$ [27].

By comparing values of streamer charge and shadow area, a fairly linear correlation was obtained, in particular for point cathode streamers as shown in figure 16. Consequently,

when the total streamer charge sometimes decreased as a result of the additives, so did the volume of the ionized gas. The slopes of the plots for point anode and cathode streamers are normally 2.1 ± 0.1 and $2.4 \pm 0.3 \, \mathrm{mC \, m^{-2}}$, respectively, but increased almost linearly with the logarithm of the concentration up to values of, respectively, $6 \, \mathrm{mC \, m^{-2}}$ and $5 \, \mathrm{mC \, m^{-2}}$ for positive point polarity with additives N,N-dimethylaniline and 1-methylnaphthalene. Such relatively high values were also found when separately investigating the fast stage of point anode streamers in pure cyclohexane. For a point cathode and additive 1-methylnaphthalene, the slope increased similarly up to $4 \, \mathrm{mC \, m^{-2}}$.

3.2.2. Pulsed behaviour in charge recordings. For both point polarities, the charge injection typically started during or right after the rising flank of the applied voltage. However, a delay in the order of a few microseconds was sometimes observed for the lowest voltages. For both polarities, the increase of streamer charge was partly discontinuous, most noticeably for point cathode streamers (figure 17). The discontinuities correspond to current pulses that previously have been observed in cyclohexane using a sensitive current measurement technique [28]. For each streamer, the number of detectable current pulses, their size and the intervals between two consecutive pulses have been quantified. For both point polarities the charge of the average current pulse was 4–6% of the total streamer charge. It had a dependence on voltage and additive concentration similar to that of the total charge. With the low time resolution (20 ns) we could
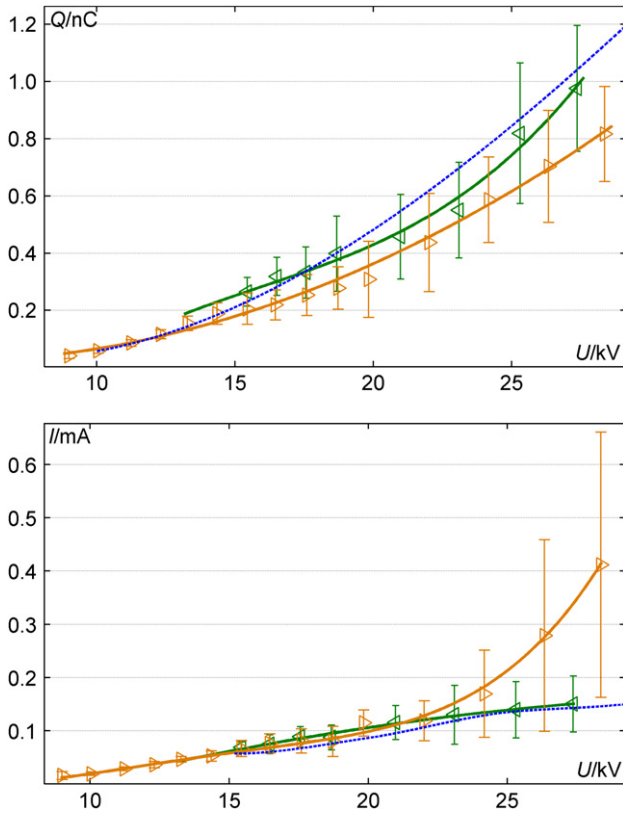
Figure 11. Total charge and mean current of point anode streamers in cyclohexane with additive 1,4-benzoquinone, (- - - -) $0\,mg\,g^{-1}$, ($\triangleleft$) $0.1\,mg\,g^{-1}$, ($\triangleright$) $1.0\,mg\,g^{-1}$.
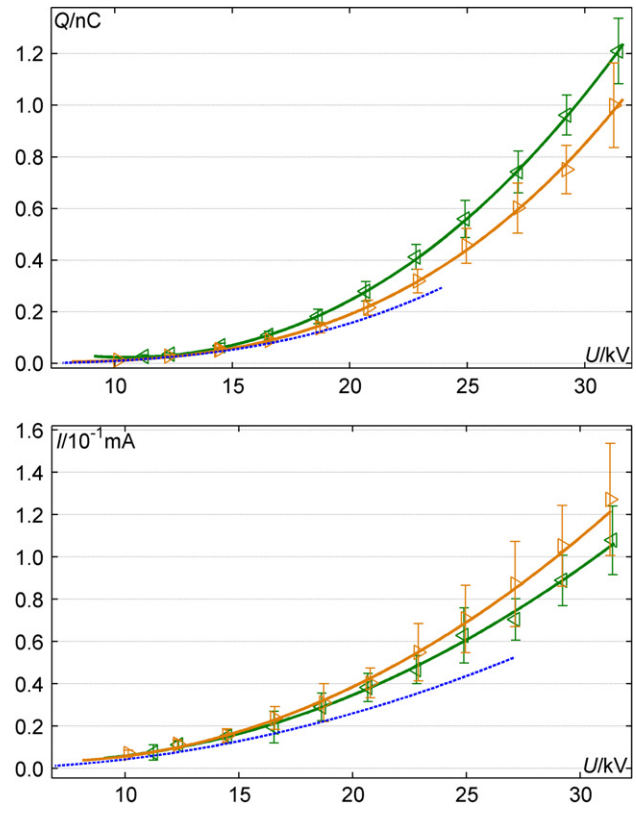
Figure 12. Total charge and mean current of point cathode streamers in cyclohexane with additive 1,4-benzoquinone, (- - - -) $0\,mg\,g^{-1}$, ($\triangleleft$) $0.1\,mg\,g^{-1}$, ($\triangleright$) $1.0\,mg\,g^{-1}$.

not resolve the pulse current, but minimum estimates are in the order of milliamperes. The magnitudes of the stepped injections for each streamer are distributed in time with gradually increasing steps towards the end of the injection. The same was observed for the intervals between two consecutive injections. In general, the repetition rate of pulsed currents is higher for positive than for negative point polarity, and the intervals between two consecutive injections vary less. We found a tendency for both point polarities that additives may increase the repetition rate in addition to the charge of pulsed currents. The effect of pulse repetition rate on average streamer propagation has been discussed previously, linking increased average currents to a more continuous propagation [35].

3.2.3. Conduction currents subsequent to streamer propagation. Succeeding the current associated with the growth of a streamer, and when the high-voltage was still applied, we measured an almost constant current due to the drift of space charge left from the streamer. Its magnitude varied almost linearly with voltage, between 50 and 800 nA for the voltage range used, and was similar for the two point polarities.

4. Discussion

4.1. Propagation mechanisms

The term 'streamer' is loosely assigned to all observable liquid prebreakdown and breakdown phenomena reported in the

literature. Streamers therefore exhibit a variety of propagation characteristics depending on the experimental conditions, and one expects a variety of mechanisms to be involved. For positive point polarity four different propagation modes are indicated from the appearances of streamer shadowgraphics, from the first mode occurring just after initiation up to the fourth mode (fast events [9]) occurring well above breakdown [36, 37]. Similarly, for negative point polarity three propagation modes are distinguished. Mainly the two first modes have been discussed in the literature. The first, slow mode ($<200\,m\,s^{-1}$) is characterized by a bubbly or bushy shape, basically consisting of vaporized liquid with low conductivity, while the second mode ($>1\,km\,s^{-1}$) is characterized by a filamentary structure of channels with a more ionized gas. With a point anode, a streamer corona mechanism is often applied similar to the mechanism for streamers in gases [2], while for point cathode streamers two complementary streamer models have been proposed. Felici suggested the first mode point cathode streamer to be a bubble-like, low conductivity vapour cavity with repetitive internal voltage collapses (partial discharges) [38]. According to this model, propagation involves bombarding the liquid phase in front of the cavity with electrons produced in the discharges, thereby inducing local vaporization by inelastic electron–molecule interactions. By balancing the electrostatic energy density to the energy required for evaporation, Felici explained vaporization of cyclohexane as being energetically possible for electric fields above $3.5\,MV\,cm^{-1}$. As evaporation in this model requires a minimum concentration of electrons in the
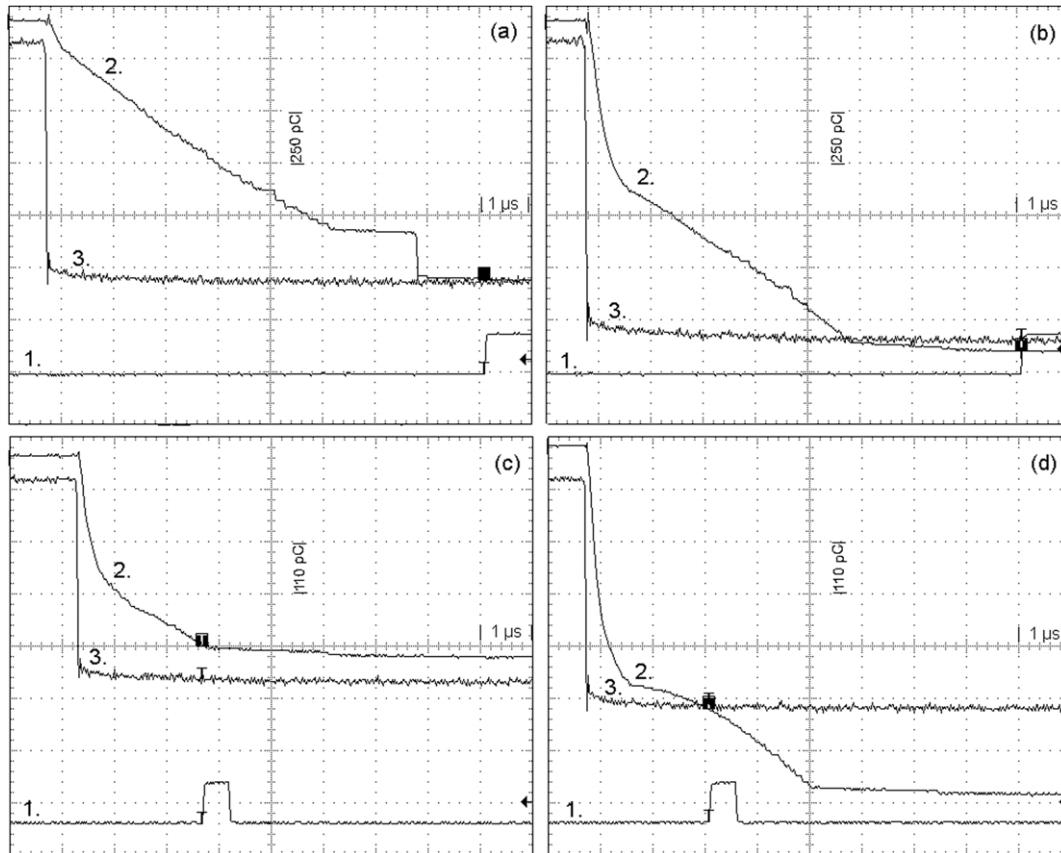
Figure 13. Oscilloscope readings showing bisected current regimes for point anode streamers: (*a*) no additive, $U = 25$ kV, (*b*) no additive, $U = 31$ kV, (*c*) 1.0 mg g^{-1} *N,N*-dimethylaniline, $U = 21$ kV, (*d*) 1.0 mg g^{-1} *N,N*-dimethylaniline, $U = 24$ kV. Each capture consists of three signals: (1) timing signal for video exposure, (2) charge signal (integrated streamer current), (3) probed high-voltage signal.

liquid, the ability of the gas discharge to supply the electrons effectively restricts streamer propagation. For the second mode of the point cathode streamer, the models by Devins [3], elaborating the consequences of liquid ionization are more relevant. Devins proposed for point cathode streamers a recursive 'two-step' model, which has been evaluated by others [4]. According to this model, electrons entering the liquid are first trapped to form a concentration of negative ions. The ionic space charge sets up an electric field which when above a critical value ionizes the liquid. This process repeats itself as electrons are readily supplied by the trailing plasma volume, and it propagates the streamer with a velocity determined by the lifetime of electrons in the respective free and trapped states. The threshold value for field ionization in cyclohexane is experimentally found to be 15 MV cm^{-1} [39].

In the streamer models referred to above, electric charge separation takes place in the gas and in the liquid phase respectively, and a new gas/liquid interface is formed. As electronic processes may take place simultaneously in both phases, they should be considered equally important. During propagation, sufficient space charge is required to maintain the total electric field at the streamer tips, either by space charge fields or by formation of a conductive filament bringing the electrode potential into the gap [40]. In the latter case, processes in the liquid phase around the streamer tip can be assumed to have a more important role due to quenching of field initiated processes within the filament. These processes

in the liquid could include collisional and field ionization [2, 3, 41], similar as for the well-established mechanisms in gases [40]. However, one can also imagine an alternating mechanism between processes in the gaseous and the liquid phases, coupled to time-varying field conditions along the filaments [9]. The pulsed nature that we have observed for the currents can be qualitatively linked to both processes.

The mechanisms of streamer propagation should also be interpreted on a molecular scale. For molecules in a liquid under high-field stress, several electronic processes may take place, described by their energy gaps and cross-sections. Single molecules may be ionized, as characterized by the ionization potential [42], or may form an anion radical as characterized by the electron affinity [43]. Furthermore, the electronic ground state may be excited, as described by the excitation energies and the corresponding oscillator strengths [42]. All these processes occur simultaneously and contribute to the overall process. It is furthermore noted that these properties depend strongly on the electric field. In addition, the thermochemistry of all the involved species (molecules, anions, cations and their excited states) will play a prominent role. Molecules will dissociate into smaller entities, which may recombine into new molecules. Although these properties may be estimated theoretically or experimentally under ideal conditions, experimental verification remains a challenge for most hydrocarbon liquids subjected to very high electric fields. The relevance for streamer propagation is not
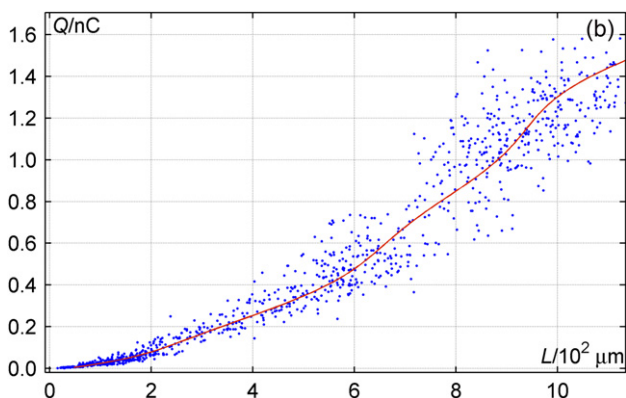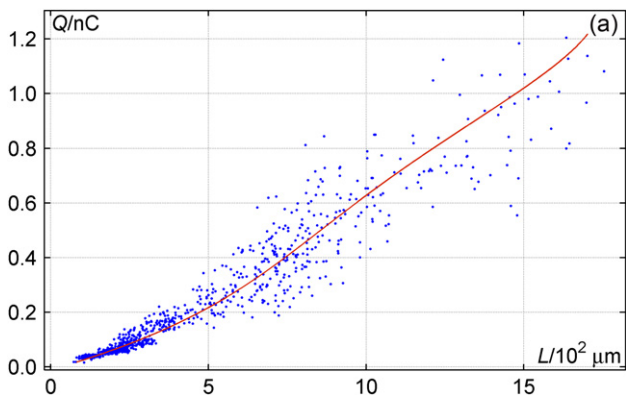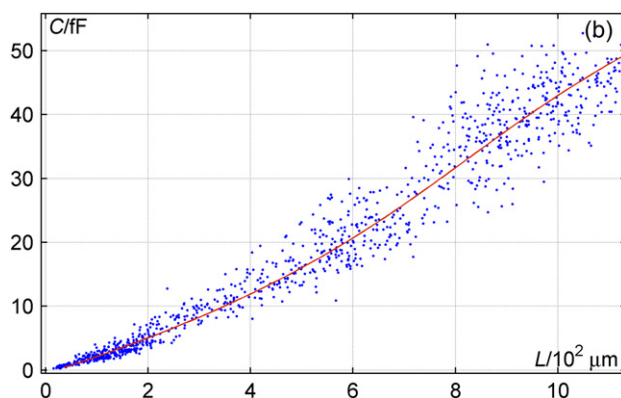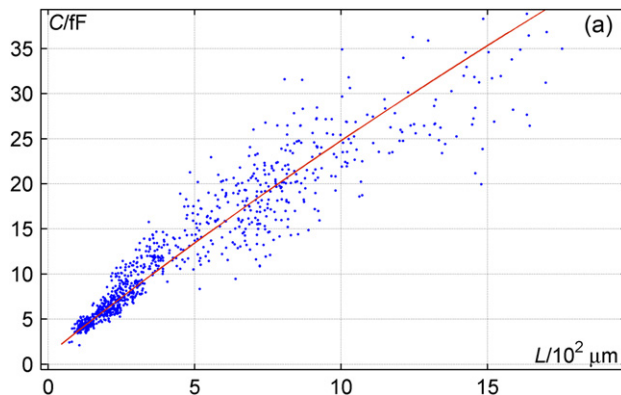
Figure 14. Total streamer charge versus stopping length, (*a*) point anode ($0.1\,\mathrm{mg\,g^{-1}}$ 1-methylnaphthalene), (*b*) point cathode ($10\,\mathrm{mg\,g^{-1}}$ 1-methylnaphthalene). Each point represents a streamer.

Figure 15. Streamer 'capacitance' versus stopping length, (*a*) point anode ($0.1\,\mathrm{mg\,g^{-1}}$ 1-methylnaphthalene), (*b*) point cathode ($10\,\mathrm{mg\,g^{-1}}$ 1-methylnaphthalene). Each point represents a streamer.

evident. However, stimulation of specific energy-dissipating mechanisms is considered important. On this basis we will in the following discuss the effect of the electrochemical environment on streamer propagation for both point polarities. As the discussion is based on macroscopic properties, often for a set of streamer filaments, we will only obtain indicative and qualitative knowledge of the specific mechanisms.

4.2. Streamer characterization and effect of additives

We have found that by adding perfluoro-*n*-hexane, 1-methyl-naphthalene and 1,4-benzoquinone to cyclohexane, larger currents for point cathode initiated streamers result. In parallel, we observe that lower voltages are required for the streamer to obtain gradually thinner and faster propagating filaments. The additives above attach thermal and near-thermal electrons [44–48], thus propagation appears to be governed mainly by electrons of 'lower' energy, injected into the liquid ahead of a gaseous structure. The field conditions under which these electrons are generated are much weaker than required for field ionization in the liquid. Since electron-attaching processes involve electronic, vibrational and rotational excitations, electron-attaching molecules lead to a more efficient and less diffusive dissipation of electric energy in the liquid phase, depending on how strongly the processes are activated. A more efficient heating, evaporation of the liquid, formation of bubbles and plasma, results. The dependence on energy of the impacting electron lies in the molecular attachment cross-section, being a measure of its

electron-accepting capacity. Negative ions resulting from both dissociative and non-dissociative attachment processes may be stable on a time-scale longer than streamer lifetimes. Thus, the observed increase in streamer stopping length, velocity and current may be partly due to enhanced space charge fields at the streamer boundary in addition to the more efficient deposition of energy. As there is no observable effect from 1,1-difluorocyclopentane, these data may suggest that the dipole moment of a molecule, and thereby the reduced molecular symmetry, is of less importance than the properties of the substituted atoms. Instead, increased fluorination, as in perfluoro-*n*-hexane, leads to an improved effect.

In general, the lifetime of delocalized electronic states and hence the electron mobility of the liquid determines the energy gained from the electric field. In mixtures containing small amounts of additives, the mobility in the solvent is considered for the electronic processes, and tabulated electron reaction rates for a given combination of solvents and solutes are utilized [49]. Relatively high rates are, for instance, reported for O_2 and CO_2 in cylohexane, and, in line with our results, an eventual presence of the atmospheric gases would contribute to the trapping of electrons. However, reaction rates are generally defined from attachment cross-sections by integration over kinetic energy and consequently serve limited use without additional knowledge of activation energies for the specific processes.

Considering the case of a positively charged point electrode, streamers are to a varying degree facilitated by the additives *N,N*-dimethylaniline, 1-methylnaphthalene,
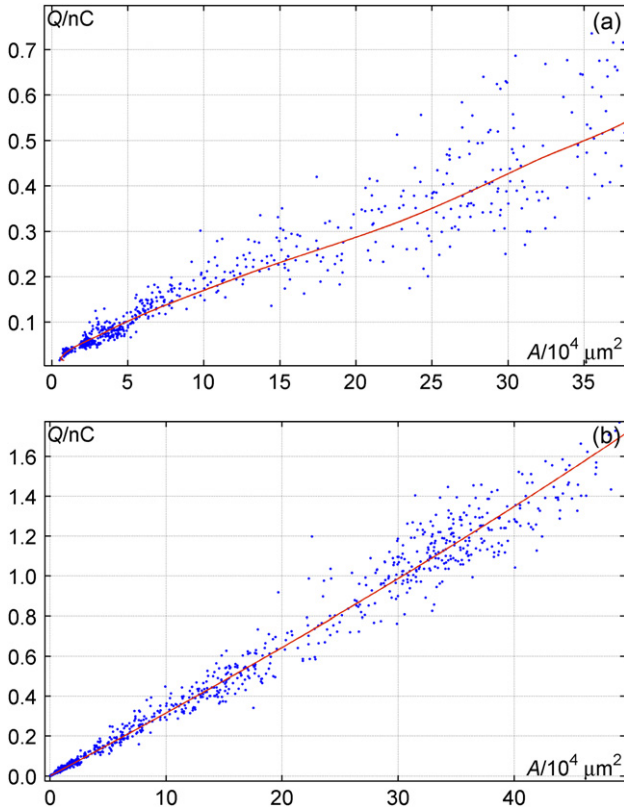
Figure 16. Total streamer charge versus shadow area, (*a*) point anode (0.1 mg g^{-1} 1-methylnaphthalene), (*b*) point cathode (10 mg g^{-1} 1-methylnaphthalene). Each point represents a streamer.

Figure 17. Oscilloscope readings showing pulsed charge behaviour for (a) point anode streamer, (b) point cathode streamer. Each capture consists of three signals: (1) timing signal for video exposure, (2) charge signal (integrated streamer current), (3) probed high-voltage signal ($U = 16$ kV).

1,4-benzoquinone and di-*n*-propylether. The first two additives exert the highest influence as both the optical and the electrical measurements suggest, while for the latter two, only a small influence is revealed exclusively by measurements of mean current. The increase in current, observed at a particular combination of applied voltage and additive concentration, stems from the prolongation of the first current regime corresponding to the fast streamer mode. If an ionization mechanism is mainly considered, in line with the relatively low ionization potentials for *N,N*-dimethylaniline and 1-methylnaphthalene [32], fast propagation is sustained during a longer period of time by more efficient ionization and more conductive filaments as two mutual amplifying features. We earlier attributed conduction currents observed prior to streamer inception to ions produced in such energetic processes [25]. *N,N*-dimethylaniline and 1-methylnaphthalene also had an observable effect in these cases. Cross-sections for collisional processes inducing ionization can provide an evaluation of the energetic conditions up to the point where the fast and slow propagation modes deactivate, but remain to be established for many liquids. However, studies of photo-ionization in liquid cyclohexane and 1-methylnaphthalene suggest optimum collisional ionization for electron energies distributed about 8.4 eV and 6.2 eV, respectively [50, 51]. Thus, electron energies associated with propagation of point anode streamers are comparably higher than for streamers from a point cathode, which explains the absent effect of perfluoro-*n*-hexane in our case. Since additives with low ionization potentials also promote photo-ionization in the
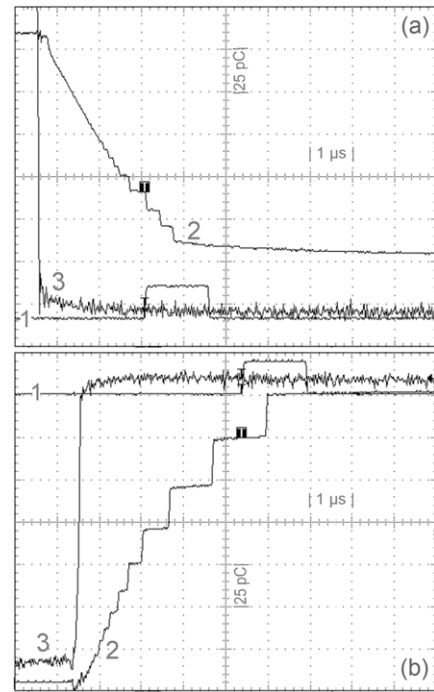
liquid ahead of the streamer, photo-ionization is a possible feedback mechanism during propagation, as proposed for point anode streamers in gases [40] and also for very fast streamers in liquids [9].

We have seen that despite the changes induced by the additives on streamer propagation, values for streamer 'capacitance', combining measurements of streamer charge, length and applied voltage, remained unaltered. The near linearity of the plots of streamer 'capacitance' versus streamer length is well predicted by a capacitance-based streamer model [33], where charge flowing into the streamer structure is equal to what would be the case for a structure with conductive filaments, bringing the electrode potential out to the tip. This model could also be adapted to less conductive streamers by considering a voltage drop along the streamer filaments. Thus, from our experimental results we conclude that average changes in streamer conductivities, as a result of the additives, must be small compared with the accuracy of the experimental method.

Intuitively, for a streamer propagating with the exchange of charge there is a close relationship between streamer current and velocity. This is supported by basic energetic and electrostatic considerations [35, 38] and is also obtained from our measurements. All filaments connected to the point electrode contribute to the measurable current during propagation, but it is difficult to establish a relation between the length of one filament and its corresponding charge. In this context, we have shown that the streamer shadow area, which relates to the total length and volume of non-overlapping filaments, better relates to the measured charge and can therefore be an informative parameter for characterizing a streamer.

5. Conclusion

We have experimentally investigated effects from additives on streamers in cyclohexane. Perfluoro-*n*-hexane facilitates point cathode streamers, *N,N*-dimethylaniline and di-*n*-propylether facilitate point anode streamers, while 1-methylnaphthalene and 1,4-benzoquinone facilitate both point anode and point cathode streamers. 1,1-difluorocyclopentane is the only additive without a measurable effect in either point polarity. The largest effects are found for perfluoro-*n*-hexane, *N,N*-dimethylaniline and 1-methylnaphthalene, which are the only additives to produce a visible change in streamer appearances. In these cases, filaments become thinner and fewer, while propagating faster and sometimes further. The results follow expectations when we consider point cathode streamers to be mainly governed by injection of thermal electrons from a gaseous phase and point anode streamers to be mainly governed by more energetic electrons, extracted from the liquid at higher electric fields. For the former, electron attachment processes will be important and influenced by the additives which effectively attach electrons, while for the latter, ionization processes will be important and influenced by the additives which are more easily ionized.

References

[1] Berger N, Randoux M, Ottmann G and Vuarchex P 1997 *Électra* **171** 33–56
[2] Chadband W G 1980 *J. Phys. D: Appl. Phys.* **13** 1299–307
[3] Devins J C, Rzad S J and Schwabe R J 1981 *J. Appl. Phys.* **52** 4531–45
[4] Beroual A and Tobazéon R 1986 *IEEE Trans. Electr. Insul.* **21** 613–27
[5] Tobazéon R 1994 *IEEE Trans. Dielectr. Electr. Insul.* **1** 1132–47
[6] Schmidt W F 1984 *IEEE Trans. Electr. Insul.* **19** 389-418
[7] Denat A 2006 *IEEE Trans. Dielectr. Electr. Insul.* **13** 518–25
[8] Lewis T J 1985 *IEEE Trans. Electr. Insul.* **20** 123–32
[9] Lundgaard L, Linhjell D, Berg G and Sigmond R S 1998 *IEEE Trans. Dielectr. Electr. Insul.* **5** 388–95
[10] Lesaint O and Gournay P 1994 *J. Phys. D: Appl. Phys.* **27** 2111–16
[11] Gournay P and Lesaint O 1994 *J. Phys. D: Appl. Phys.* **27** 2117–27
[12] Beroual A, Zahn M, Badent A, Kist K, Schwabe A J, Yamashita H, Yamazawa K, Danikas M, Chadband W G and Torshin Y 1998 *IEEE Electr. Insul. Mag.* **14** 6–17
[13] Schütte T 1994 *Proc. Nordic Insulation Symp. (Vaasa, Finland)* pp 147–60
[14] Nakao Y, Yamazaki T, Miyagi K, Sakai Y and Tagashira H 2002 *Electr. Eng. Japan* **139** 1–8
[15] Hamano N, Nakao Y, Naito T, Nakagami Y, Shimizu R, Sakai Y and Tagashira H 2002 *Proc. Int. Conf. Dielectric Liquids (Graz, Austria)* pp 119–22
[16] Nakao Y, Yamazaki T, Tagashira H, Miyagi K and Sakai Y 1999 *Proc. Int. Conf. Dielectric Liquids (Nara, Japan)* pp 261–64
[17] Watson P K, Chadband W G and Sadeghzadeh-Araghi M 1991 *IEEE Trans. Electr. Insul.* **26** 543–59
[18] Chadband W G 1991 *J. Phys. D: Appl. Phys.* **24** 56–64
[19] Jomni F, Aitken F and Denat A 2002 *Proc. Int. Conf. Dielectric Liquids (Graz, Austria)* pp 194–98
[20] McCluskey F M J and Denat A 1994 *IEEE Trans. Dielectr. Electr. Insul.* **1** 672–79
[21] Nieto-Salazar J, Lesaint O, Denat A and Robledo-Martinez A 2003 *Proc. Int. Symp. on High Voltage Engineering (Delft, The Netherlands)* p 1
[22] Nakao Y, Itoh H, Hoshino S, Sakai Y and Tagashira H 1994 *IEEE Trans. Dielectr. Electr. Insul.* **1** 383–9
[23] Lesaint O and Jung M 2000 *J. Phys. D: Appl. Phys.* **33** 1360–8
[24] Chadband W G and Sufian T M 1985 *IEEE Trans. Electr. Insul.* **20** 239–46
[25] Ingebrigtsen S, Lundgaard L E and Åstrand P-O 2007 *J. Phys. D: Appl. Phys.* **40** 5161–9
[26] Yamashita H, Yamazawa K and Wang Y S 1998 *IEEE Trans. Dielectr. Electr. Insul.* **5** 396–401
[27] Costeanu L and Lesaint O 2002 *Proc. Int. Conf. on Electrical Insulation and Dielectric Phenomena (Cancun, Mexico)* pp 256–59
[28] Gournay P and Lesaint O 1993 *J. Phys. D: Appl. Phys.* **26** 1966–74
[29] Frayssines P E, Bonifaci N, Denat A and Lesaint O 2002 *J. Phys. D: Appl. Phys.* **35** 369–77
[30] Lesaint O and Gournay P 1994 *IEEE Trans. Dielectr. Electr. Insul.* **1** 702–8
[31] Denat A, Bonifaci N and Nur M 1998 *IEEE Trans. Dielectr. Electr. Insul.* **5** 382–87
[32] Lide D R 2004 *Handbook of Chemistry and Physics* 84th edn (Boca Raton, FL: CRC Press)
[33] Massala G and Lesaint O 1998 *IEEE Trans. Dielectr. Electr. Insul.* **5** 371–81
[34] Massala G and Lesaint O 2001 *J. Phys. D: Appl. Phys.* **34** 1525–32
[35] Beroual A 1993 *J. Appl. Phys.* **73** 4528–33
[36] Hebner R E 1988 Measurements of electrical breakdown in liquids *The Liquid State and its Electrical Properties (NATO Advanced Study Institute, Series B: Physics* vol 193) ed E E Kunhardt *et al* (New York: Plenum) pp 519–37
[37] Lesaint O and Massala G 1998 *IEEE Trans. Dielectr. Electr. Insul.* **5** 360–70
[38] Felici N J 1988 *IEEE Trans. Electr. Insul.* **23** 497–503
[39] Denat A, Gosse J P and Gosse B 1988 *IEEE Trans. Electr. Insul.* **23** 545–54
[40] Goldman M and Sigmond R S 1982 *IEEE Trans. Electr. Insul.* **17** 90–105
[41] Lundgaard L E, Linhjell D and Berg G 2001 *IEEE Trans. Dielectr. Electr. Insul* **8** 1054–63
[42] Lipsky S 1981 *J. Chem. Educ.* **58** 93–101
[43] Christophorou L G 1980 *Environ. Health Perspectives* **36** 3–32
[44] Hunter S R and Christophorou L G 1984 *J. Chem. Phys.* **80** 6150–63
[45] Spyrou S M, Sauers I and Christophorou L G 1983 *J. Chem. Phys.* **78** 7200–16
[46] Collins P M, Christophorou L G, Chaney E L and Carter J G 1970 *Chem. Phys. Lett.* **4** 646–50
[47] Christophorou L G and Blaunstien R P 1969 *Radiat. Res.* **37** 229–45
[48] Tobita S, Meinke M, Illenberger E, Christophorou L G, Baumgartel H and Leach S 1992 *J. Chem. Phys.* **161** 501–8
[49] Tabata Y, Ito Y and Tagawa S 1991 *CRC Handbook of Radiation Chemistry* (Boca Raton, FL: CRC Press) pp 411–15
[50] Casanovas J, Grob R, Delacroix D, Guelfucci J P and Blanc D 1981 *J. Chem. Phys.* **75** 4661–8
[51] Holroyd R A, Preses J M, Boettcher E H and Schmidt W F 1984 *J. Phys. Chem.* **88** 744–49

Paper 3

Effects of Electron-Attaching and Electron-Releasing Additives on Streamers in liquid Cyclohexane

Stian Ingebrigtsen, Hans Sverre Smalø, Per-Olof Åstrand, and Lars E. Lundgaard

2008

Submitted

Effects of Electron-Attaching and Electron-Releasing Additives on Streamers in liquid Cyclohexane

S. Ingebrigtsen, H.S. Smalø, P.-O. Åstrand
Department of Chemistry
Norwegian University of Science and Technology (NTNU)
7491 Trondheim, Norway

and **L.E. Lundgaard**
Department of Electric Power Technology
SINTEF Energy Research
7465 Trondheim, Norway

ABSTRACT

The effects of electron-attaching and electron-releasing additives in cyclohexane on the initiation and propagation of positive and negative streamers have been studied quantitatively. Fast impulses (<20 ns, <40 kV) were applied on a 10 mm point-to-plane gap and studied by shadowgraphic imaging and a differential charge measurement technique. The properties of both positive and negative streamers depend on the specific electronic characteristic of the additives. Electron-attaching additives facilitate the propagation of negative streamers, whereas the most effective electron-releasing additives reduce initiation voltages and facilitate the propagation of positive streamers. Depending on the reactivity and concentration of the additives, streamer filaments become thinner and fewer while propagating faster and further. The Townsend–Meek theory for streamer inception in gases has been adapted to a solution and applied to analyze the voltage dependence of the positive streamer propagation. Results show a quantitative dependency on the ionization potential and concentration in agreement with experimental trends.

Index Terms — Prebreakdown, streamer, charge, cyclohexane, additives, electron attachment, impact ionization.

1 INTRODUCTION

LIQUIDS are used as electric insulation in transformers and other electric equipment [1]. When new liquids are introduced it is important to know their dielectric performance. The ability of a liquid to withstand electric stress is influenced by its chemical composition since it influences the conversion of electrostatic energy into heat. Heating leads to evaporation and the formation of plasma channels that can bridge the electrode gap and cause electric breakdown. Prebreakdown processes in molecular liquids are not understood as well as in gases due to limited knowledge concerning electronic high-field processes at an atomistic scale in the condensed phases.

In an earlier paper [2], we have discussed how streamers starting from a point-cathode propagate faster and further in the presence of electron scavenger additives as compared to dried and degassed cyclohexane. Propagation lengths, velocities and currents increased. This was partly attributed to fields enhanced by space charge at the streamer extremity, and partly to a more efficient and less diffusive deposition of electric energy. For streamers starting from a point-anode, either a "slow" or a "fast" propagation mechanism dominates, depending on the electric field strength. Additives with low ionization potential effectively reduce electric fields required for fast propagation [2].

Electronic processes relevant for streamer initiation and propagation are influenced by the density and the nature of the medium in which the processes occur [3,4]. For liquids, phenomenological "theories" have been developed for different ranges of electron energies [3,5]. Depending on whether the conducting state energy for quasi-free electrons in liquids, V_0, is above or below the vacuum level, excess electrons are classified as either *localized* or *delocalized* [3]. In the delocalized state, electrons can be pictured as free particles interacting with liquid molecules by collisions. In the localized state, electrons are localized either in preexisting "traps" in the liquid, or in "traps" formed by polarization interaction between the electron and the liquid molecules. The measured value of V_0 in cyclohexane is 0.01 eV [6], thus cyclohexane represents an intermediate case. Excess electrons are here considered partly localized and partly delocalized in an equilibrium governing their behavior and response to an applied electric field or hydrostatic pressure [7]. At electric fields exceeding a certain level (e.g. 1 kV/mm), a shift

towards more delocalized electrons causes a superlinear field dependence in the electron mobility [3]. This field dependence is difficult to assess experimentally and theoretically at higher electric fields ($>10^2$ kV/mm) [8]. The uncertainty stemming from this is basis for one of the controversies in the field of prebreakdown mechanisms in molecular liquids, namely whether or not quasi-free electrons can have sufficient kinetic energy to ionize the molecules by impact.

We have experimentally studied streamer initiation and propagation in liquid cyclohexane with 15 additives with different electrochemical properties. A point-to-plane electrode gap was studied using step voltages of positive and negative polarity. Voltages were varied from levels well below initiation to levels below breakdown. Thus, only lower streamer modes were activated. Cyclohexane have been used as base liquid since it is a simple and well-described alkane and may serve as a simple model liquid for insulating oils. Cyclohexane is also a good solvent and allows quasi-free electrons to exist long enough to react with the additives [6].

A more detailed investigation for a few of the additives has been reported previously [2]. The present paper focuses on quantitative effects of the additives on streamer initiation and propagation, and attempts to explain old and new experimental results in terms of molecular properties and simple models for streamer propagation. Our basis has primarily been existing data describing gas phase molecules and reactions. The validity for these data in the liquid phase is discussed. Experimental results have been based on macroscopic properties averaged over a large number of measurements. Results for positive and negative point polarity have been presented in different ways to better demonstrate effects of additives.

2 EXPERIMENT

The experimental setup and procedures for sample preparation has been described previously [2,10]. High-voltage rectangular pulses were applied to the plane electrode of a 10 mm point-plane gap. Streamers were studied with a shadowgraphic depiction technique and by measuring charge induced on the point electrode. The pulse voltage level was varied in 1 kV steps with 3 minutes intermittent delays, and at least 30 streamers were recorded at each level. The point radii were in the 1.3–1.5 μm range, and checked with a microscope before and after each series. In contrast to our earlier procedure [10], the same point electrode was now kept as long as possible until a significant change in the point radii was observed due to either erosion or accidents. Degassed and dried cyclohexane of the type Merck LiChrosolv® with a purity of 99.9% was used in the experiments [10]. The streamers stopped propagating mid-gap before the high voltage pulse was quenched. A digitized shadowgraphic image was taken when the streamer reached maximum extension, using a single-shot intensified CCD camera. From the images we have obtained the maximum extension (length) of the streamer. The temporal development of charge induced during propagation was measured with a sensitive differential technique [9,10]. Charges were also measured below streamer initiation. A sudden increase in the charge corresponds to the
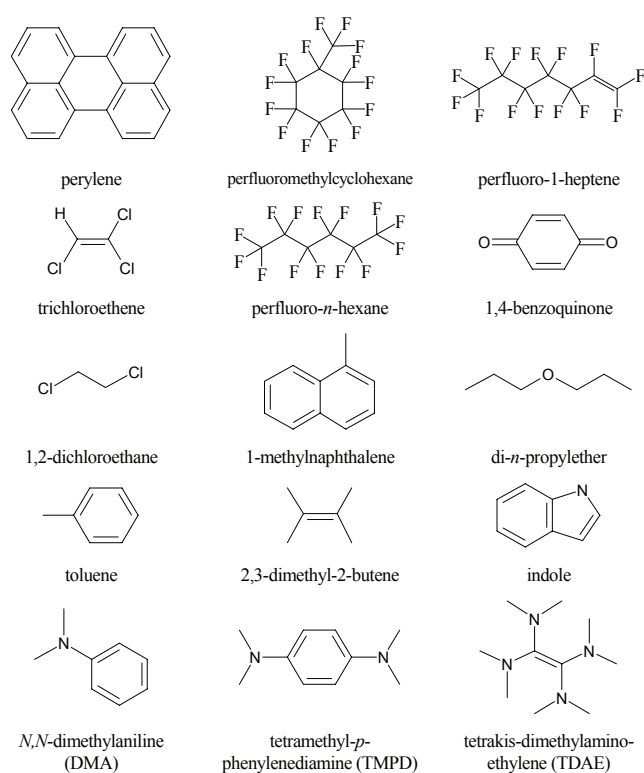
Figure 1. Molecular structure of additives.

initiation of a streamer, and the average streamer currents were derived from the slope of streamer charge versus time. Similarly, the average streamer propagation velocity was estimated from the stopping length and the duration of the charge injection. The total number of recordings for each additive concentration varied between 500–1000. Some of the results have been plotted with average values and standard deviations, including continuous trend-lines to improve the readability. The probability for streamer initiation versus voltage have been based on 60–100 impulses at each voltage level around the onset.

The electron acceptors added to cyclohexane are perylene, perfluoromethylcyclohexane, perfluoro-1-heptene, trichloro-ethene, perfluoro-n-hexane, 1,4-benzoquinone, 1,2-dichloro-ethane, and 1-methylnaphthalene, see Figure 1 and Table 1. Their mechanisms of electron scavenging are well documented in the gaseous phase and shown to follow a resonance scattering formalism [11]. The molecules 1,2-dichloroethane and trichloroethene generate intermediate parent anions which subsequently decay via various channels of dissociative attachment [11], whereas 1,4-benzoquinone and perylene attach electrons to electronically excited states, producing long-lived anions [11-13]. Electron attachment to perfluoro-n-hexane, perfluoromethylcyclohexane and perfluoro-1-heptene result both in long-lived parent and fragmented anions [14,15], indicating several possible negative ionic states. The electron donors added are, in order of decreasing gas-phase ionization potentials [16,17], di-n-propylether (9.27 eV), toluene (8.82 eV), 2,3-dimethyl-2-butene (8.27 eV), 1-methylnaphthalene (7.97 eV), indole (7.76 eV), N,N-dimethylaniline (7.12 eV),
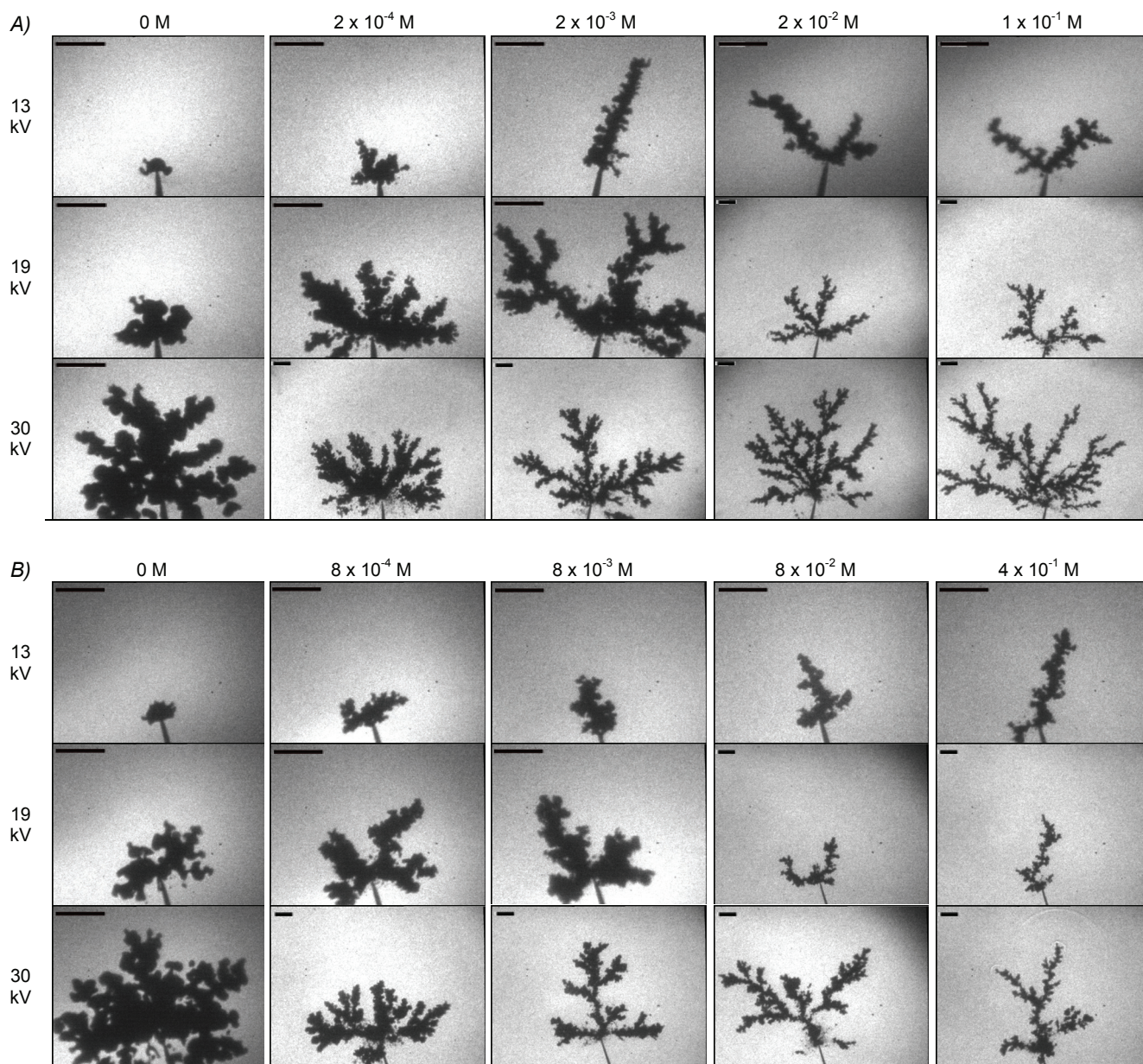
Figure 2. Shadowgraphic images of fully developed *negative streamers* in cyclohexane with (A) perfluoromethylcyclohexane and (B) 1,2-dichloroethane. Concentration dependencies are shown along rows, voltage dependencies along columns. A 250 μm scale is added to each image.

perylene (6.96 eV), tetramethyl-*p*-phenylenediamine (6.75 eV) and tetrakis-dimethylamino-ethylene (6.11 eV), see Figure 1. By comparison, the gas-phase ionization potential for cyclohexane is 9.86 eV, and for the remaining additives in the range 9.5 to 12 eV [16]. The aromatic molecules 1-methylnaphthalene and perylene have both electron-scavenging (Table 1) and electron-releasing properties. Either property can be activated depending on the energetic state of the interacting electron.

The range of additive concentrations spans from trace impurities (~100 ppm) to higher concentrations (~5 %), except for 1,4-benzoquinone and perylene which we only managed to dissolve in low concentrations (<1 ‰). The additives had purities better than 97–99%, and were dissolved without further processing. All additives were studied with both positive and negative point electrodes.

3 RESULTS

3.1 NEGATIVE STREAMERS

Effects on streamer appearances from increasing scavenger concentration follow the scheme previously reported for perfluoro-*n*-hexane [2], and is shown in Figure 2 for perfluoromethylcyclohexane and 1,2-dichloroethane. The degree of fragmentation increases with increasing concentration until separate and more defined and branched structures with gradually thinner filaments appear. Streamers propagate further and faster with increasing concentration [2], the effect being comparable to the effect of increasing applied voltage. Differences between the different scavengers are at first sight difficult to separate from the general random appearances, whereas effects from the molecules that were not

3

Figure 3. Cube root of total charge versus voltage for *negative streamers* in cyclohexane with *perfluoromethylcyclohexane*, ($\triangle$) 0 M, ($\triangleleft$) 2 x 10⁻⁴ M, ($\triangleright$) 2 x 10⁻³ M, ($\square$) 2 x 10⁻² M, ($\circ$) 1 x 10⁻¹ M.
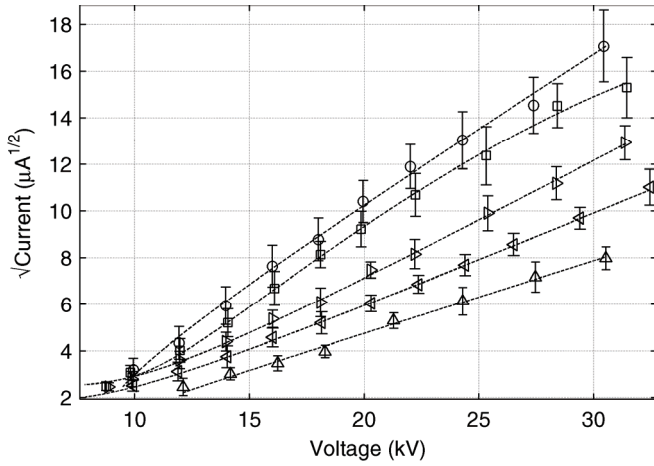
Figure 4. Square root of mean current versus voltage for *negative streamers* in cyclohexane with *perfluoromethylcyclohexane*, ($\triangle$) 0 M, ($\triangleleft$) 2 x 10⁻⁴ M, ($\triangleright$) 2 x 10⁻³ M, ($\square$) 2 x 10⁻² M, ($\circ$) 1 x 10⁻¹ M.

originally considered to be electron scavengers could be distinguished only for tetrakis-dimethylaminoethylene (TDAE). Perfluoromethylcyclohexane and 1,2-dichloroethane span the relatively small range of effects of scavengers. Compared to pure cyclohexane, the propagation length and velocity for ~0.1 M perfluoromethylcyclohexane (Figure 2A) at 30 kV increased by a factor of 2.1 and 11, respectively. Similarly for ~0.1 M 1,2-dichloroethane (Figure 2B), propagation length and velocity increased by a factor of 1.6 and 7.9, respectively. Occasionally, the streamers had not fully stopped when photographed. Consecutive shock waves originating from the tips of the most filamentary streamers could then be observed (Figure 2B, last image). This indicates a stepped propagation.

As shown in Figures 3 and 4, asymptotic concentration dependencies are observed for streamer charge and average currents (i), where the latter is more affected by the concentration. Effects are observed even at trace concentrations. At the highest concentration, average currents become comparable to those of positive streamers [2]. For each concentration, the total charge is proportional to the cube of the voltage, while the average current is proportional to the square of the voltage. Consequently, the duration of the
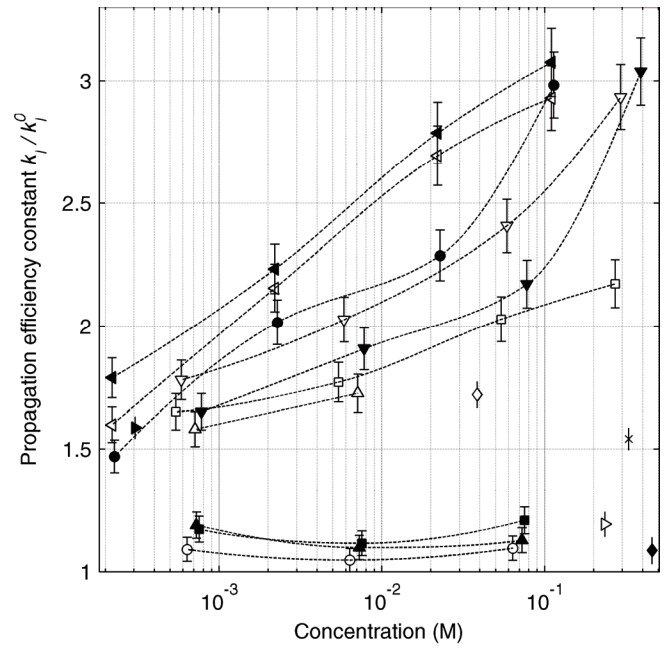
Figure 5. Normalized propagation efficiency constant and dependence on additive and concentration, ($\blacktriangleright$) perylene, ($\blacktriangleleft$) perfluoro-1-heptene, ($\triangleleft$) perfluoromethylcyclohexane, ($\bullet$) perfluoro-*n*-hexane , ($\triangledown$) trichloroethene, ($\blacktriangledown$) 1,2-dichloroethane, ($\square$) 1-methylnaphthalene, ($\triangle$) 1,4-benzoquinone, ($\lozenge$) TDAE, ($\times$) indole, ($\blacksquare$) di-*n*-propylether, ($\blacktriangle$) di-fluorocyclopentane, ($\circ$) DMA, ($\triangleright$) TMPD, ($\blacklozenge$) 2,3-dimethyl-2-butene. Includes experimental data from [1].

propagation becomes more or less proportional to the applied voltage (U). We have earlier attributed the increase in mean streamer current to an increase both in the repetition rate and the size of transient current pulses associated to the streamer event (bipolar conduction) [2]. Electrical measurements presented for perfluoromethylcyclohexane can represent the trends for all electron scavengers used. Most interesting is perhaps the increase in average streamer current, and therefore the increase in power consumption,

$$\overline{W}_{el} = U \cdot \bar{i} = U \cdot k_I U^2 = k_I U^3 \tag{1}$$

The constant k_I represents the propagation efficiency, and is an empirical function of scavenger type and concentration. This constant is presented for several electron-attaching and electron-releasing additives in Figure 5. Here, it has been normalized against the efficiency constant in pure cyclohexane. An almost linear increase with the logarithm of scavenger concentration can be derived over some interval. Perfluoromethylcyclohexane and perfluoro-1-heptene show the largest increase, whereas in the other end we find 1,4-benzoquinone, 1-methylnaphthalene and 1,2-dichloroethane. Note that k_I deviates sharply above the linear trend for the highest concentration of 1,2-dichloroethane. In the middle we find trichloroethene and perfluoro-*n*-hexane, also here with a sharper increase in k_I at the highest concentration. Of the molecules not originally considered to be electron scavengers, only TDAE and indole increase k_I above the level separating effects from non-effects ($k_I / k^0_I > 1.2$). Concentration dependencies for TDAE and indole have not been investigated.

4
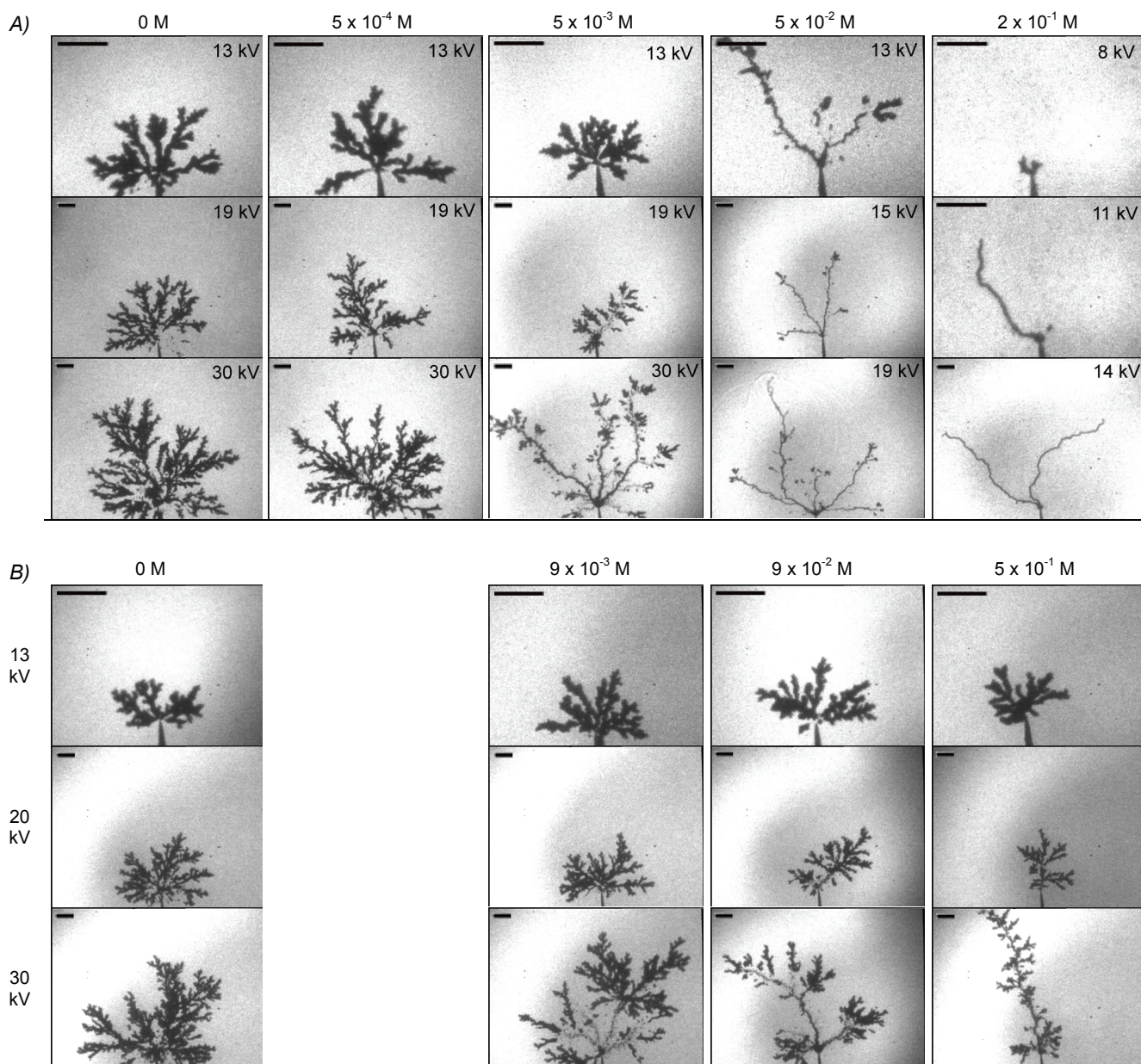
Figure 6. Shadowgraphic images of fully developed *positive streamers* in cyclohexane with (A) TMPD and (B) 2,3-dimethyl-2-butene. Concentration dependencies are shown along rows, voltage dependencies along columns. A 250 μm scale is added to each image.
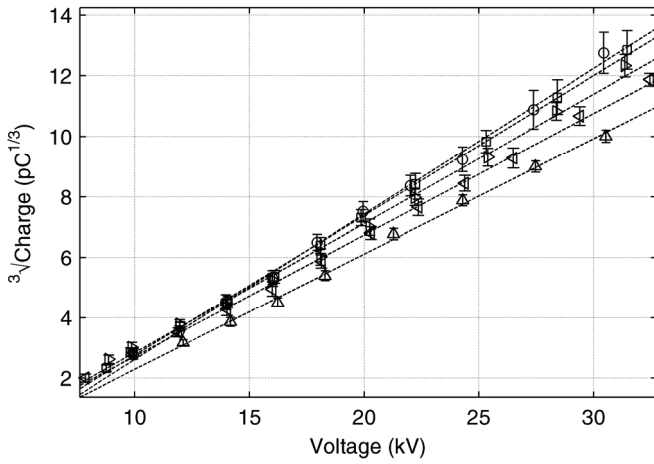
3.2 POSITIVE STREAMERS

Effects on streamer shape from increasing concentration of all the electron-releasing molecules follow the same scheme as previously reported for *N,N*-dimethylaniline and 1-methyl-naphthalene [2], and is shown in Figure 6 for tetramethyl-*p*-phenylenediamine (TMPD) and 2,3-dimethyl-2-butene solutions. Effects on streamer propagation are observed above a certain threshold voltage. At this threshold voltage, determined by the additive and concentration, streamer shapes change from "bush-like" to a filamentary "tree-like" via an intermediate state with characteristics from both. The filamentary streamers have fewer and thinner filaments than the bush-like, and they propagate considerably further from the point. We could not distinguish effects on the streamer shape from molecules not considered to be electron-releasers.

As previously shown [2], oscillograms display two almost distinct current regimes with characteristic times dependent on the experimental conditions. Larger average currents were measured during the first regime, corresponding to the "tree-like" propagation mode. For low voltages the duration of this high-current regime was very short, but increased rapidly when the voltage was raised above the threshold level.

The threshold, originally called the "propagation voltage" [18], may be defined in several ways. The streamer shapes seen during the initial streamer propagation in pure cyclohexane suggests an onset of the faster propagation mode for voltages at about 19 kV, while the occurrence of the 'fast' current regime seen from oscillograms suggests a higher onset at about 25 kV. Finally it can be derived from the deflection
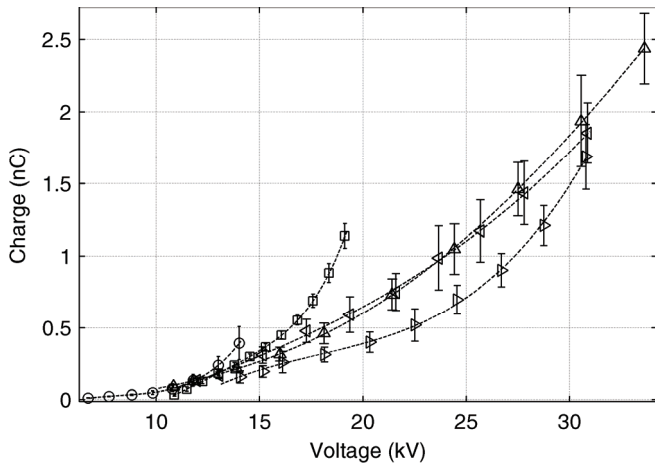
Figure 7. Total charge of *positive streamers* in cyclohexane with *TMPD*, ($\triangle$) 0 M, ($\triangleleft$) 5 x 10^{-4} M, ($\triangleright$) 5 x 10^{-3} M, ($\square$) 5 x 10^{-2} M, ($\circ$) 2 x 10^{-1} M.

Figure 9. Propagation voltage versus additive and concentration, ($\square$) di-*n*-propylether, ($\blacktriangleright$) toluene, ($\blacktriangleleft$) 2,3-dimethyl-2-butene, ($\blacksquare$) 1,4-benzoquinone [1], ($\circ$) 1-methylnaphthalene [1], ($\triangledown$) indole, ($\bullet$) DMA [1], ($\blacktriangle$) TMPD, ($\triangleleft$) TDAE.

Figure 8. Mean current of *positive streamers* in cyclohexane with *TMPD*, ($\triangle$) 0 M, ($\triangleleft$) 5 x 10^{-4} M, ($\triangleright$) 5 x 10^{-3} M, ($\square$) 5 x 10^{-2} M, ($\circ$) 2 x 10^{-1} M. Propagation voltages are defined at the initial deviation from the $\triangle$-line.

Figure 10. Stopping lengths of *positive streamers* with additives ($\triangleleft$) 2 x 10^{-1} M TMPD, ($\square$) 3 x 10^{-1} M Indole, ($\triangleright$) 6 x 10^{-2} M DMA [1], ($\circ$) 6 x 10^{-2} M Indole, ($\triangledown$) 5 x 10^{-1} M 2,3-dimethyl-2-butene. The initial deviations from the solid line (pure cyclohexane) correspond to the propagation voltages.

point in the average current-voltage characteristics, giving an onset between 33 to 36 kV [2]. The two techniques mentioned first are more appropriate for studying the beginning of the transition regime between a slow and a fast mode, whereas the end of the transition is better characterized using the latter technique, see Figure 8 for the TMPD solutions. The propagation voltages derived from average current-voltage profiles vary with additive and concentration as shown in Figure 9, and correlate well with the shadowgraphic images of the streamers (e.g. Figure 6). There were no observable effects on the propagation voltage at trace concentrations (10–100 ppm), but for higher concentrations a systematic reduction with increasing concentration and decreasing gas-phase ionization potential took place. The 1,4-benzoquinone solutions behaved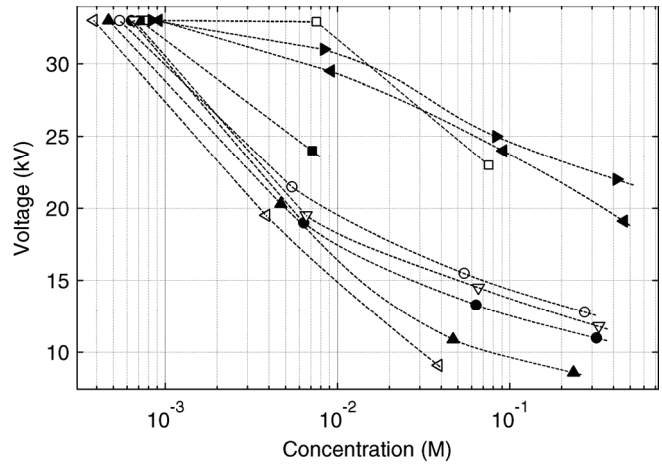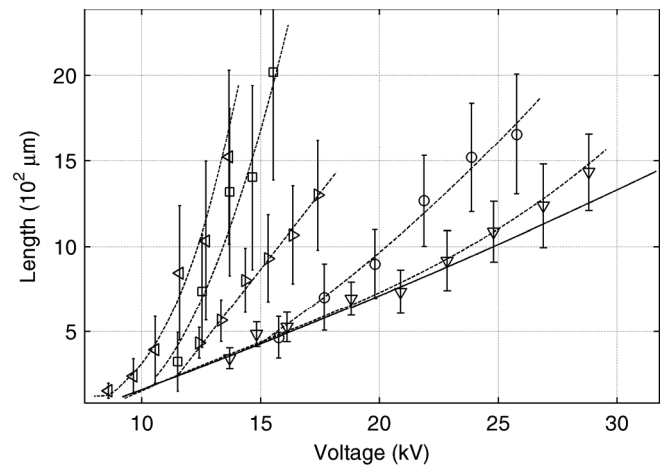 differently from expected since the propagation voltage was reduced despite the ionization potential being just above that of cyclohexane (I_g = 10.0 eV).

Note from Figure 7 that the total streamer charge can be smaller than for pure cyclohexane at voltages about the propagation voltage. This is most easily observed for liquids having a wide transition regime, as previously demonstrated for 1-methylnaphthalene in cyclohexane [1]. It illustrates the combined effects of the reduced number of and increased

lengths of filaments, as charge correlates to the sum of the lengths of all filaments [1].

Above the propagation voltage, there is an almost linear increase in mean current with voltage, see Figure 8. The slope varies in the range 70–110 μA/kV, but does not correlate to ionization potentials or additive concentrations. There is an almost linear dependence between these currents and the mean streamer propagation velocities [1], but the dependence is not significantly affected by additive or concentration.

As shown in Figures 6 and 10, the voltage dependence of the streamer propagation length is related to the propagation voltage. The extent of this relationship can be illustrated with two solutions having a relative large difference in propagation voltages: A 0.2 M TMPD solution with a propagation voltage of about 9 kV showed at 14 kV a 4 times increase in propagation length and a 11.5 times increase in mean velocity, relative pure cyclohexane. In contrast, a 0.5 M 2,3-dimethyl-2-butene solution with a comparatively high propagation voltage of about 19 kV, showed at 30 kV only a 1.2 times increase in propagation length and a 3.5 times increase in mean velocity.
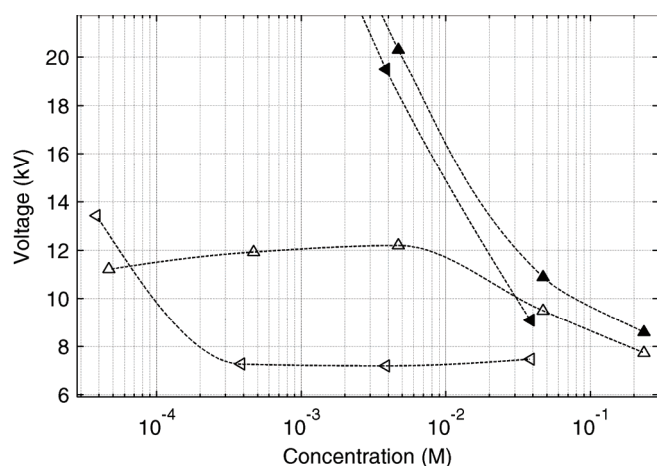
Figure 11. *Positive streamer* initiation voltages (open symbols) and propagation voltages (filled symbols) versus concentration of TMPD (△) and TDAE (◁).

3.3 STREAMER INITIATION

For voltages about the onset level for streamers, the regularity of initiations in a sequence of measurements often varied in such a way that streamer initiations were mainly confined to some parts of the sequence. This was most prominent for positive point polarity, where 50% initiation voltage reproducibility lies typically within 2 kV for the same point electrode, compared to 1 kV for point cathodes. No systematic influence from additive type or from concentration have been seen for initiation voltages varying in the low range 11–14 kV for point anodes, and in the range 7–9 kV for point cathodes. We previously reported a systematic increase with increasing concentration of 1-methylnaphthalene solutions in the higher range of 8–13 kV for point anodes, but suspected this to be due to a "conditioning" effect after replacing the point electrode [10]. By using the same point electrode for different solutes, we find a statistically better agreement between each reference measurement. Systematic influence of additive concentrations on initiation voltages were only observed with a point anode for TMPD and TDAE solutions. As shown in Figure 11, their concentration dependencies differ, whereas in both cases initiation voltages at the highest concentration drop to within 7.5–8 kV. Propagation voltages derived from average current-voltage characteristics were only 1–2 kV higher. At these low voltages it is difficult to separate the two propagation modes from shadowgraphic images. Reference measurements were done before and after these additives in order to verify that the tip conditions remained the same.

4 DISCUSSION

4.1 NEGATIVE STREAMERS

Felici has suggested that the first mode negative streamer is a bubble-like, low conductivity vapor cavity with repetitive internal voltage collapses (partial discharges) [19]. Accordingly, propagation involves bombarding the liquid phase in front of the cavity with electrons produced in the discharges, thereby inducing local vaporization by inelastic collisions in the liquid. For a second and faster stage, some models elaborate the consequences of ionization in the liquid [20,21]. Devins *et al.* have proposed a recursive "two-step" process for negative streamers [21]. According to their model, electrons entering the liquid are first trapped, forming negative ions. This space charge gives an electric field which ionizes the liquid above a critical field. This process repeats itself as electrons are readily supplied by the trailing plasma channel, driving the streamer with a velocity determined by the characteristic times for each step. The pulsed nature we observe for the streamer currents can qualitatively be linked to the rate of streamer growth in both models [2]. In both cases, instantaneous evaporation from high-energy density electron injections to the liquid would cause the consecutive shock waves as we have observed in the shadowgraphic images.

Electron attachment processes can play a role in both models. For electron-molecule interactions in the liquid, numerous vibrational and electronic energy losses occur below the ionization threshold, and are frequently associated with electron-attaching processes at near-thermal conditions. Chemical reactions may add to the energy supplied by the electron if the electron affinity of the scavenger is positive, or, in the case of dissociative attachment, if the affinity for one molecule fragment exceeds the dissociation energy. Thus, with relevance to Felici's model, electron scavengers induce a less diffusive and more efficient energy dissipation at fields far below those required for ionization. With relevance for Devins' model, electrons penetrate and spread less into the liquid, and anions become more concentrated, thereby producing stronger space-charge fields at the streamer perimeter. Neither model can directly predict effects of electron-attaching additives due to the simplified and quite qualitative nature. A more comprehensive model should take into account electrohydrodynamic instabilities occurring at the charged bubble surface. The instabilities will enhance the electric field and make propagation more probable along these locations [22].

Throughout the course of streamer propagation, electrons enter the liquid phase under strongly varying electric field conditions, and one must consider the scavenging of both non-thermal ("hot") and thermal electrons. If *non-thermal electrons* are captured by the electron scavengers during times shorter than their thermalization-time, a gas-kinetic process can be considered taking place in the liquid. This is based on scattering cross-sections for near-thermal electrons in gaseous and liquid alkanes, both being reasonably close to the geometrical values [3]. For *thermal electrons* in different solvents, attachment rates to specific scavenger impurities correlate to V_0 of the solvents analogously to what would be the dependence on electron mean kinetic energy in the vapors. Thus, a gas *inspired* description of the electron attachment mechanism has been proposed for these cases [3,23]. Particular for the transition from a gas to a liquid are the changes in reaction-energy and stability of ions against auto-detachment or dissociation [3]. However, accurate knowledge of the changes in magnitude and energy dependence on electron attachment processes is lacking.

The attachment rate constant k_0 of reactants in the

condensed phase is generally expressed as [3],

$$k_0^{-1} = k_d^{-1} + k_a^{-1} \qquad (2)$$

where k_d is the rate at which the electron and additive molecules "collide", and k_a the rate at which the attachment reaction occurs. For the scavenging of thermal electrons in a low mobility liquid such as cyclohexane, the rate-determining step is considered to be the diffusive motion of the electron rather than the final capture process ($k_d \ll k_a$). In such cases, electron attachment would depend mainly on the medium through its effect on electron mobility (as long as the negative ionic states exists at thermal energies), and less affected by the electron-attaching properties of the scavenger. However, a weak increase in k_0 with increasing dipole moment was found for different nitro-compound scavengers in cyclohexane, but was attributed to an increase in k_d through the effect of long-range attractive dipole and induced-dipole forces [24]. The above is generally valid for thermal electrons in low mobility liquids at "normal" field conditions. Field-enhanced attachment has been found to coincide with the onset of the superlinear field dependence referred to earlier in our introduction [3]. Possibly, the attachment process would cease to be diffusion limited at some critical electric field, but little data exists.

The peak values of gas-phase attachment cross-sections and their respective resonance energies have been listed in Table 1 for the different electron scavengers used in our study. In order to compare the scavengers on an equal basis, we have for each molecule assumed a gas-like attachment mechanism and calculated attachment rates k_a from the relation [11],

$$k_a = \left(\frac{2}{m_e}\right)^{0.5} \int_0^\infty \sigma_a(\varepsilon) f_e(\varepsilon) \varepsilon^{0.5} d\varepsilon \qquad (3)$$

using experimental cross-sections $\sigma_a(\varepsilon)$, and a hypothetical electron energy distribution $f_e(\varepsilon)$ in liquid cyclohexane. Here, we have used two Maxwellian energy distributions with mean electron energies at 1.5 eV (epithermal) and 0.1 eV ("thermal" [3]). Values are listed in Table 1, including experimental rates for perfluoromethylcyclohexane and 1,4-benzoquinone in cyclohexane, reported for thermal and non-thermal conditions respectively [6,25]. For 1-methylnaphthalene, cross-sections were not available at these energies. The range of attachment rates is about three orders of magnitudes for each energetic case, but their relative magnitudes depend on the electron mean energy. It is thus difficult to directly relate these data to our experimental results. However, there is an approximate correlation, e.g. if one compares the propagation efficiency constant k_I in Figure 5 with cross-sections arranged in decreasing order in Table 1. Effects of increasing the attachment cross section by three orders of magnitudes are comparable to the effects of increasing the scavenger concentration by the same factor. This is in accordance with an electron attachment mechanism. The asymptotic concentration dependence should be further investigated within the framework of a model for negative streamer

Table 1. Experimental peak values for electron attachment cross-section σ_a and corresponding electron energy ε_a, estimated attachment rate per scavenger molecule k_a and experimental rate in cyclohexane solvent k_a^{exp}.

Electron Scavenger	σ_a (cm^2)	ε_a (eV)	$k_{a\ \varepsilon=0.1\ eV}$ (cm^3 s^{-1})	$k_{a\ \varepsilon=1.5\ eV}$ (cm^3 s^{-1})	k_a^{exp} (cm^3 s^{-1})
[a] Perylene	$1.3 \cdot 10^{-14}$	0.70	$4.2 \cdot 10^{-10}$	$5.5 \cdot 10^{-6}$	
[b] Perfluoro methylCH	$1.1 \cdot 10^{-14}$	0.07	$1.5 \cdot 10^{-09}$	$9.5 \cdot 10^{-7}$	[f] $5.8 \cdot 10^{-10}$
[b] Perfluoro-1-heptene	$1.4 \cdot 10^{-15}$	0.25	$2.5 \cdot 10^{-10}$	$1.8 \cdot 10^{-7}$	
[c] Trichloro-ethene	$7.8 \cdot 10^{-16}$	0.77	$7.5 \cdot 10^{-11}$	$1.8 \cdot 10^{-7}$	
[d] Perfluoro-n-hexane	$2.6 \cdot 10^{-16}$	1.20	$3.0 \cdot 10^{-10}$	$1.7 \cdot 10^{-7}$	
[e] Benzo-quinone	$6.7 \cdot 10^{-17}$	2.10		$1.4 \cdot 10^{-8}$	[g] $6.5 \cdot 10^{-9}$
[c] Dichloro-ethane	$9.3 \cdot 10^{-18}$	0.36	$1.5 \cdot 10^{-12}$	$3.4 \cdot 10^{-9}$	
[a] Methyl-naphthalene	$\sim 10^{-17}$	7.90			

[a]Ref. [13], [b]Ref. [14], [c]Ref. [11], [d]Ref. [15], [e]Ref. [12], [f]Ref. [6], [g]Ref [25].

propagation, e.g. the "two-step" model by which the overall propagation rate becomes less dependent on the step involving electron trapping. Alternatively, there may be other non-linearities resulting from increasing scavenger concentration orders of magnitudes above the expected ppm concentration of electrons in the liquid. Diffusion limitations in cyclohexane may furthermore contribute to the asymptotic dependence on cross-section or attachment rates for the strongest scavengers.

Experimental and calculated electron affinities for the different additives have been presented elsewhere [17]. Here, electron affinities reported for the scavengers used in our study span from positive to negative values, and we cannot find any correlation between the experimental streamer propagation efficiency constant k_I and the values of the affinities. A detailed study of electron attachment in gases has already shown that the electron affinity is not a good absolute parameter for the electron accepting capacity of a molecule [26]. Moreover, a general correlation between electron affinities and electron attachment cross-sections does not exist. Thus, the electron attachment cross-section for gas-phase reactions still represents the best molecular descriptor for negative streamer propagation in electron-accepting solutes.

4.2 POSITIVE STREAMERS

The observed duality of positive streamer propagation is well known, and often denoted the 1st and 2nd mode, respectively. It has been suggested that processes responsible for the continuous formation of the gas/liquid interface of the streamer occur both within the gaseous void and in the liquid [27]. The slow mode has been associated with a mechanism in the gas as it is readily quenched by high hydrostatic pressures [27]. During the fast mode, processes in the liquid are considered primary and the dynamics of the gas channel secondary, but a model compatible to this duality does not exist. Electronic processes are considered important, but there

is a discrepancy in the literature concerning the origin of excess electrons in the liquid. Both field ionization [21] and impact ionization [28] have been invoked as main contributors. Impact ionization in the liquid requires one seeding electron formed by e.g. field-ionization. During initiation and initial propagation of streamers in cyclohexane, the high electric fields are able to facilitate charge generation in the liquid, either from impact ionization processes at fields > 2 MV/cm or from field ionization processes at fields > 15 MV/cm [29]. In order for these processes to remain active in the regions of rapidly decaying Laplacian fields, the total electric field must be maintained by local unipolar space charges at the streamer tips or by a conductive filament carrying the electrode potential to the tip. According to the Townsend–Meek avalanche-to-streamer criterion for gases in non-uniform fields [30], the electric field should be sufficiently high over a certain distance to allow the formation of a minimum charge concentration by impact ionization. This criterion may have found its analogy in liquids through the identification of a critical "electrostatic radius" and a critical voltage for propagation of fast mode streamers [18,31]. According to the experimental results of this and previous studies [2,32], the propagation voltage is liquid-specific and moreover reduced when the concentration of an easily ionized additive is increased. It is believed that molecular additives with reduced ionization potentials increase the rate at which electrons are produced, fulfilling the Meek criterion in weaker field conditions. The Townsend-Meek avalanche-to-streamer criterion reads,

$$\int_0^d \alpha\left[E\left(x\right)\right]dx = C \tag{4}$$

where α is the Townsend impact ionization coefficient, E is the local electric field, x is the distance from the point electrode, and C is the Meek constant. The size of the corona region area is defined by the integration limit d. The exact expression for $\alpha(E)$ in liquids is nontrivial. Approximate analytical expressions have been evaluated for rare gas liquid such as xenon and argon [33,34]. For cyclohexane and propane, α has been experimentally obtained by comparing avalanche current pulses in high-pressure gas phase with those in the liquid phase [35]. The Townsend coefficient in liquids is empirically expressed as [36],

$$\alpha\left(E\right) = A\,\exp\left(-\frac{B}{E}\right) \tag{5}$$

where A and B are constants characteristic for the liquid. The field-dependence incorporates all field-effects, e.g. increase in electron energy and field-lowering of molecular ionization potentials. Experimental data in purified cyclohexane give $A = 2 \times 10^6$ cm^{-1} and $B = 30$ cm/MV [35], and allow us to evaluate C for a propagation voltage and a streamer tip radius of respectively 33 kV and 6 μm, which is believed relevant for this study [18]. For C we obtained a value of 23 by numerical integration of equation (5) from the point electrode along the

axial direction until the field is below critical. The axial electric field in the 10 mm point-to-plane gap was analytically calculated [37]. The form of equation (5) is inherited from the expression for the Townsend coefficient in gases, in which case there exists an empirical relation between B and the ionization potential I_g of the gas [38],

$$B \sim I_g \tag{6}$$

Intuitively, for an additive dissolved in a base liquid, the Townsend coefficient takes the form,

$$\alpha\left(E\right) \sim C_A\,P_A\left(E,I_A\right) + C_B\,P_B\left(E,I_B\right) \tag{7}$$

where C_A, C_B, I_A and I_B, are the concentrations and ionization potentials of additives and base molecules respectively, while P_A and P_B are the probabilities of ionization at each electron-molecule impact. These probabilities are proportional to the probabilities of having an electron with energy above the respective ionization potential I_A and I_B. P would then take the form of a cumulative distribution with respect to electron energy. We assume that the influence of additive concentration on the electron energy distribution is negligible, and moreover that the distribution is exponentially decaying (e.g. the high-energy tail of the Maxwell distribution). For zero-field conditions this gives,

$$\frac{P_A}{P_B} = \exp\left[-k_1\left(I_A - I_B\right)\right] \tag{8}$$

Next, we assume equation (8) to hold even when an electric field is applied. Thus, we use a field dependence for P_A and P_B similar to that of the empirical Townsend coefficient in pure cyclohexane in equation (5),

$$\alpha\left(E\right) = A\left[C_A\exp\left(-\frac{B}{E} - k_1\left(I_A - I_B\right)\right) + \left(1 - C_A\right)\exp\left(-\frac{B}{E}\right)\right] \tag{9}$$

In order to predict the propagation voltages, V_P, we have then numerically solved the Meek integral in equation (4) along the point-plane symmetry axis for different k_1 values,

$$\int_0^d \alpha\left[E\left(V_p\right), I_A, I_B, C_A, k_1\right]dx = 23 \quad \Rightarrow \quad V_p\left(I_A, I_B, C_A, k_1\right) \tag{10}$$

By setting $k_1 \approx 2.8$, it is possible to approximately reproduce the experimental reduction in propagation voltages caused by either increasing C_A or by decreasing I_A below that of cyclohexane, see Figure 12. Compared to the experimental values, simulated results predict a less sudden decrease in V_p in the concentration range $10^{-4} – 10^{-2}$ M for the strongest electron releasers. Experimental changes of V_p in this range are not easily determined due the gradual changes in average streamer characteristics. We thus expect to have experimentally over-estimated propagation voltages at the lowest concentrations used.

9
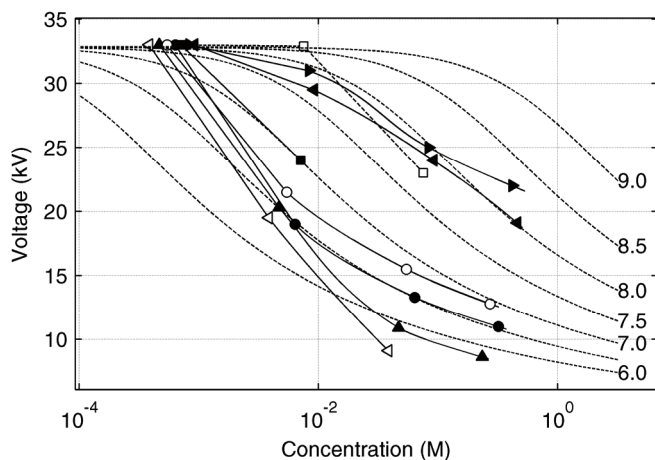
Figure 12. Propagation voltages versus additive concentration, (---) calculated for ionization potentials in steps of 0.5 eV from 6 to 9 eV, (—) experimental values: (□) di-*n*-propylether (9.27 eV), (►) toluene (8.82 eV), (◄) 2,3-dimethyl-2-butene (8.27 eV), (■) 1,4-benzoquinone (10.0 eV), (○) 1-methylnaphthalene (7.97 eV), (●) DMA (7.12 eV), (▲) TMPD (6.75 eV), (◁) TDAE (6.11 eV).

Our empirical model may be improved by including solvation and field effects for the ionization potential. Whereas ionization potentials for gas phase molecules can be calculated in good agreement with their experimental values [17], the reduction in ionization potential for a molecule in cyclohexane solvent may be estimated from,

$$I_{\mathrm{L}} - I_{\mathrm{g}} = P^{+} + V_{0} \qquad (11)$$

where I_{g} and I_{L} are the ionization potentials of the gas and liquid phase respectively, and P^{+} is polarization energy of the positive ion placed in the medium [3]. Calculations of the solvent effect on the ionization potential based on the polarized continuum model (PCM) [39] have been presented elsewhere [17], with the main conclusion that the ionization potential of the additives are typically reduced by an amount similar to the calculated difference in the ionization potential between gaseous and liquid cyclohexane. Consequently, for each additive, $I_{\mathrm{B}} - I_{\mathrm{A}}$ in equation (9) will not be significantly changed when going from gas to liquid. An investigation of the influence of electric fields on the potential difference above remains. A field-lowering of the ionization potential is in fact the proposed mechanism for field-enhanced electronic conduction in both solid and liquid dielectrics [40]. Accordingly, the potential barrier for electron escapes is lowered in the field direction by an amount proportional to the field magnitude.

For voltages exceeding the propagation voltage, the ionization region moves into the gap during the 2nd mode streamer propagation, analogous to the mechanism in gases [41]. Depending on the streamer conductivity and the critical field-conditions for avalanche growth, the value of the Meek-integral in equation (4) eventually falls below C, and the 2nd mode ceases to propagate. The streamer conductivity and the critical field are both related to the ionization rate. Thus, the propagation voltage and the length of 2nd mode streamers at elevated voltages are related, as shown in Figure 10.

4.3 STREAMER INITIATION

It is difficult to assess effects of additives on the initiation voltage by comparing inception from one experiment to another since the initiation probabilities varied with time. This merely demonstrates that the streamer events were not independent of each other and therefore not binomially distributed. The intermittent delay of 3 minutes between each impulse voltage may have been too short compared to the charge relaxation time in liquid cyclohexane $\varepsilon/\sigma \approx 30$ minutes (ε being the permittivity and σ the low-field conductivity as measured with an IRLAB® conductance meter).

We have previously suggested that transient currents observed for both point polarities around the onset of streamers are induced by ions created by avalanches in the liquid which did not develop into streamers [10]. Support for the hypothesis of avalanches can be found for the behavior of positive streamers. The initiation voltages dropped significantly when adding molecules with sufficiently low ionization potentials (i.e. TMPD and TDAE). These results are qualitatively in agreement with the effect of reduced ionization potentials on the ionization coefficient in equation (9). Indeed, the convergence shown in Figure 11 between initiation voltages and the more loosely defined propagation voltages coincides with our hypothesis that streamer initiation and 2nd mode propagation is due to the same mechanism. In other words, the fast mode extends from initiation until the slower mode completes the propagation. At low voltages only the slow mode will be observable, hence the label "1st mode". Initiation voltages for negative streamers are not equally affected by electron donors, though an avalanche mechanism is known to be responsible for their initiation [29]. Thus, streamer initiation voltages at 7–8 kV seem to represent a lower bound for the initiation voltages for both point polarities. For voltages below this level, the distance within which the field is above the critical value reduces much faster than an obtainable increase in the ionization frequency.

5 CONCLUSION

First, this experimental study has confirmed what could be anticipated from earlier experimental evidence reported in the literature. For voltages below the breakdown level, negative streamers are accelerated solely by electron-attaching additives, whereas additives that are ionized more easily than the base liquid accelerate streamers from a point anode. Secondly, we have obtained quantitative correlations between the electronic properties of the additives studied and the speed and length of propagation of streamers. For negative streamers, the propagation efficiency at all voltages has an asymptotic dependence on both the electron scavenging efficiencies and concentrations of additives, even for trace concentrations. This is due to an additional localization of space charge and energy. Gas-phase electron attachment cross-sections rather than electron affinities have been used to characterize the electron-scavenger molecules. For positive streamers, the transition from the slow to the faster mode of propagation is shifted towards lower voltages by increasing concentrations and decreasing ionization potentials of

electron-releasing additives. Trace concentrations have no observable effects here. At voltages above the propagation voltage, significantly more elongated streamers results. The Townsend–Meek theory for streamer inception in gases can be adapted to liquid conditions to analyze the voltage dependence of positive streamer propagation. Results support the hypothesis that impact ionization takes place in the liquid phase outside a positive streamer. The reduction of streamer initiation voltages with the most effective electron donors suggests that the same process takes place during streamer initiation with a point anode.

There is a need of data concerning fundamental electronic processes in dielectric liquids subject to electric fields. These may be obtained from ab initio calculations for molecules of interest, and verified with data obtained empirically under well-controlled experimental conditions.

REFERENCES

[1]   N. Berger, M. Randoux, G. Ottmann, and P. Vuarchex, "Rewiev on insulating liquids," Electra, Vol. 171, pp. 33-56, 1997.

[2]   S. Ingebrigtsen, L. Lundgaard, and P-O. Åstrand, "Effects of additives on prebreakdown phenomena in liquid cyclohexane: II. Streamer propagation," J. Phys. D: Appl. Phys., Vol. 40, pp. 5624-5634, 2007.

[3]   L. G. Christophorou, Electron-molecule Interactions and Their Applications, Vol. 2, Academic Press, San Diego, ch. 4, pp. 221-316, 1984.

[4]   L. G. Christophorou, "Electron attachment to molecules in dense gases ("quasi-liquids")," Chem. Rev., Vol. 76, pp. 409-423, 1976.

[5]   W. H. Hamill, "Dependence of specific rates for excess-electron scavenging in nonpolar liquids on electron energy," J. Phys. Chem., Vol. 85, pp. 3588-3592, 1981.

[6]   Handbook of Radiation Chemistry, CRC Press, Boca Raton, ch.7, p. 414, 1991.

[7]   W. F. Schmidt, "Electron mobility in non-polar liquids, the effect of molecular structure, temperature, and electric field," Can. J. Chem., Vol. 55, pp. 2197-2209, 1977.

[8]   W. F. Schmidt, "Electronic conduction processes in dielectric liquids," IEEE Trans. Electr. Insul., Vol. 19, pp. 389-418, 1984.

[9]   L. Dumitrescu, O. Lesaint, N. Bonifaci, A. Denat, and P. Notingher, "Study of streamer inception in cyclohexane with a sensitive charge measurement technique under impulse voltage," J. Electrost., Vol. 53, pp. 135-146, 2001.

[10] S. Ingebrigtsen, L. E. Lundgaard, and P-O. Åstrand, "Effects of additives on prebreakdown phenomena in liquid cyclohexane: I. Streamer initiation," J. Phys. D: Appl. Phys., Vol. 40, pp. 5161-5169, 2007.

[11] L. G. Christophorou, "Electron Attachment Processes" in Electron-molecule Interactions and Their Applications, Vol. 1, Academic Press, San Diego, ch. 6, pp. 477-617, 1984.

[12] P. M. Collins, L. G. Christophorou, E. L. Chaney, and J. G. Carter, "Energy dependence of the electron attachment cross section and the transient negative ion lifetime for p-benzoquinone and 1,4-naphthoquinone," Chem. Phys. Lett., Vol. 4, pp. 646-650, 1970.

[13] S. Tobita, M. Meinke, E. Illenberger, L. G. Christophorou, H. Baumgartel, and S. Leach, "Polycyclic aromatic hydrocarbons: negative ion formation following low energy (0-15 eV) electron impact," Chem. Phys., Vol. 161, pp. 501-508, 1992.

[14] L. G. Christophorou, "Negative Ions of Polyatomic Molecules," Environmental Health Perspectives, Vol. 36, pp. 3-32, 1980.

[15] S. R. Hunter and L. G. Christophorou, "Electron attachment to the perfluoroalkanes n-C_NF_{2N+2} (N=1-6) using high pressure swarm techniques," Chem. Phys., Vol. 80, pp. 6150-6163, 1984.

[16] Handbook of Chemistry and Physics, 84th ed. CRC Press, Boca Raton, ch. 10, p 181, 2004.

[17] H. S. Smalø, S. Ingebrigtsen and P.-O. Åstrand, "Calculation of ionization potentials and electron affinities for molecules relevant for streamer initiation and propagation." in preparation.

[18] O. Lesaint and P. Gournay, "Initiation and propagation thresholds of positive prebreakdown phenomena in hydrocarbon liquids," IEEE Trans. Dielectr. Electr. Insul., Vol. 1, pp. 702-708, 1994.

[19] N. J. Felici, "Blazing a fiery trail with the hounds," IEEE Trans. Electr. Insul., Vol. 23, pp. 497-503, 1988.

[20] H. M. Jones and E. E. Kunhardt, "Development of pulsed dielectric breakdown in liquids," J. Phys. D: Appl. Phys., Vol. 28, p. 178, 1995.

[21] J. C. Devins, S. J. Rzad, and R. J. Schwabe, "Breakdown and prebreakdown phenomena in liquids," J. Appl. Phys.,Vol. 52, pp. 4531-4545, 1981.

[22] P. K. Watson, W. G. Chadband, and M. Sadeghzadeh-Araghi, "The role of electrostatic and hydrodynamic forces in the negative-point breakdown of liquid dielectrics," IEEE Trans. Electr. Insul., Vol. 26, pp. 543-559, 1991.

[23] A. O. Allen, T. E. Gangwer, and R. A. Holroyd, "Chemical reaction rates of quasifree electrons in nonpolar liquids. II," J. Phys. Chem., Vol. 79, pp. 25-31, 1975.

[24] G. Bakale, E. C. Gregg, and R. D. McCreary, "Electron attachment to nitro compounds in liquid cyclohexane," Chem. Phys., Vol. 67, pp. 5788-5794, 1977.

[25] R. A. Holroyd, "Electron attachment to p-benzoquinone and photodetachment from benzoquinone anion in nonpolar solvents," J. Phys. Chem., Vol. 86, pp. 3541-3547, 1982.

[26] R. P. Blaunstein and L. G. Christophorou, "On molecular parameters of physical chemical and biological interest," Rad. Res. Rev., Vol. 3, pp. 69-118, 1971.

[27] O. Lesaint and P. Gournay, "On the gaseous nature of positive filamentary streamers in hydrocarbon liquids. I: Influence of the hydrostatic pressure on the propagation," J. Phys. D: Appl. Phys., Vol. 27, pp. 2111-2116, 1994.

[28] A. Denat, "High field conduction and prebreakdown phenomena in dielectric liquids," IEEE Trans. Dielectr. Electr. Insul., Vol. 13, pp. 518-525, 2006.

[29] A. Denat, J. P. Gosse, and B. Gosse, "Electrical conduction of purified cyclohexane in a divergent electric field," IEEE Trans. Electr. Insul., Vol. 23, pp. 545-554, 1988.

[30] J. M. Meek and J. D. Craggs, Electrical Breakdown of Gases, John Wiley & Sons, New York, 1978.

[31] P. E. Frayssines, N. Bonifaci, A. Denat, and O. Lesaint, "Streamers in liquid nitrogen: Characterization and spectroscopic determination of gaseous filament temperature and electron density," J. Phys. D: Appl. Phys., Vol. 35, pp. 369-377, 2002.

[32] O. Lesaint and M. Jung, "On the relationship between streamer branching and propagation in liquids: influence of pyrene in cyclohexane," J. Phys. D: Appl. Phys., Vol. 33, pp. 1360-1368, 2000.

[33] V. M. Atrazhev, I. T. Iakubov, and V. I. Roldughin, "The Townsend coefficient of ionization in dense gases and fluids," J. Phys. D: Appl. Phys., Vol. 9, pp. 1735-1742, 1976.

[34] N. Bonifaci, A. Denat, and V. Atrazhev, "Ionization phenomenon in high-density gaseous and liquid argon in corona discharge experiments," J. Phys. D: Appl. Phys., Vol. 30, pp. 2717-2725, 1997.

[35] M. Haidara and A. Denat, "Electron multiplication in liquid cyclohexane and propane," IEEE Trans. Electr. Insul., Vol. 26, pp. 592-597, 1991.

[36] V. M. Atrazhev, E. G. Dmitriev, and I. T. Iakubov, "The impact ionization and electrical breakdown strength for atomic and molecular liquids," IEEE Trans. Electr. Insul., Vol. 26, pp. 586-591, 1991.

[37] R. Coelho and J. Debeau, "Properties of the tip-plane configuration," J. Phys. D: Appl. Phys., Vol. 4, pp. 1266-1280, 1971.

[38] O. H. LeBlanc, Jr. and J. C. Devins, "Townsend ionization constants in N-alkanes," Nature, Vol. 188, pp. 219-220, 1960.

[39] C. J. Cramer, "Implicit Models for Condensed Phases" in Essentials of computational chemistry: theories and models, Wiley, Chichester, ch. 11, 2004.

[40] C. W. Smith and J. H. Calderwood, "The application of a classical conductivity model to dielectric liquids," Journal of Electrostatics, Vol. 12, pp. 173-178, 1982.

[41] M. Goldman and R. S. Sigmond, "Corona and insulation," IEEE Trans. Electr. Insul., Vol. 17, pp. 90-105, 1982.

Paper 4

Spectral analysis of the light emitted from streamers in chlorinated alkane and alkene liquids

Stian Ingebrigtsen, Nelly Bonifaci, André Denat and Olivier Lesaint

Spectral analysis of the light emitted from streamers in chlorinated alkane and alkene liquids

S Ingebrigtsen[1], N Bonifaci[2], A Denat[2] and O Lesaint[2]

[1] Department of Chemistry, Norwegian University of Science and Technology (NTNU)
N-7491 Trondheim, Norway

[2] INPG, CNRS and Joseph Fourier University, G2E-lab, 25 rue des Martyrs
 38042 Grenoble, France

E-mail: stian.ingebrigtsen@sintef.no

Abstract.

We have studied the time-averaged optical emission from fast positive and negative non-breakdown streamers under pulsed divergent field conditions in five chlorocarbon liquids, namely dichloromethane, 1,2-dichloroethane, tetrachloro-methane, trichloroethene, and tetrachloroethene. We have accumulated light emitted from the first 10–15 μm trail of a few thousand streamers. We have also briefly studied single breakdown arcs in tetrachloromethane. Atomic lines of hydrogen, chlorine and carbon as well as excited states of C_2 radicals (Swan bands) have been observed, and with sufficient resolution for evaluating line and band-shapes. The characteristic broadening, shift and asymmetry of atomic lines varied significantly between the liquids. Differences between the two streamer polarities were comparatively small. Densities of electrons and neutrals in the illuminated phase have been deduced from broadening of atomic lines, atomic excitation temperatures from absolute line intensities, and rotational and vibrational temperatures from the Swan bands. The gas densities of the propagating streamers were generally very high (~10% of critical) and with a high degree of ionization (~1‰). Dichloromethane and 1,2-dichloroethane produced re-illuminating streamers with densities close to atmospheric conditions, in agreement with a rapid pressure relaxation. Rotational temperatures were high and in the range 2×10^3 – 6×10^3 K for the different liquids. Results can be interpreted to suggest a partial local thermodynamic equilibrium in the streamer plasmas.

1. Introduction

Research on transient prebreakdown processes is vital to our understanding of dielectric performance of materials and insulation systems. Shortly before electrical insulating liquids suffer voltage breakdown, conductive channels of ionized gas, "streamers", initiate at the location of highest electric field and propagate through the material until the electrode gap is bridged. The streamer is a gas / plasma filled channel that initiates and rapidly develops in a region with very high electric fields. It contains electrons and molecules of vaporized and decomposed liquid. Excited and ionized species result from inelastic collisions between hot electrons and molecules or atoms, by the thermal collisions among atoms and molecules, and by photochemical reactions. During radiative relaxation, optical emission spectrometry allows us to evaluate these energetic processes and the momentary physical conditions.

Light is emitted both during streamer initiation and propagation in hydrocarbon liquids subjected to very high electric fields.[1,2] With assumptions more or less restrictive to the thermodynamic state of the ionized medium, the spectral content can inform about characteristic plasma parameters, may it be the nature of excited species, electron density or kinetic temperatures.[3] These parameters are known to vary both spatially and temporally in a streamer,[4] and more often indicate non-equilibrium (non-thermal) conditions. Ideally, one separates between light emitted from the gaseous body of the streamer, and light emitted from the high-field ionization region in the liquid around the propagating filament tip. However, for streamers in simple hydrocarbon liquids (e.g. alkanes), small, transient, and weakly illuminating volumes make it difficult to obtain a sufficient amount of light without compromising a certain level of details (e.g. temporal resolution). Spectral acquisitions possibly accumulate light from consecutive processes induced by collisional energy transfer to polyatomic molecules (dissociation, formation of excited fragments and recombination), but there may also be a considerable portion of secondary, non-radiative deactivation processes. In combination with ill-defined gas-phase compositions, the complexity of interpreting the spectra increases.

For voltages below the breakdown level, faster, more filamentary and generally more luminous streamers emerge from liquids with halogenated molecules such as tetrachloromethane.[5,6] The mechanisms behind the acceleration of streamers in halogenated liquids is not fully understood, but may be related to a more concentrated space charge analogously to the mechanism for corona-streamers in electronegative gases. In this article we present spectroscopic investigations of the light emitted from filamentary positive and negative streamers for a fixed voltage level in liquid 1,2-dichloroethane ($C_2H_4Cl_2$), dichloromethane (CH_2Cl_2), trichloroethene (C_2HCl_3), tetrachloroethene (C_2Cl_4), and tetrachloromethane (CCl_4). The chlorination degree of the liquids range from 0.25 to 0.80, and interactions with electrons are well documented in the gaseous phase.[7-9] We present for the same liquids measurements of conventional streamer properties: streamer current, charge, propagation length and velocity.

2. Theoretical recalls

Broadening and shift of atomic lines in streamer-plasmas are mainly caused by pressure interactions, whereby the presence of others atoms and charged species perturbs the energy levels of the emitting atoms. Stark-effects occur from interactions between the emitting atom and charged particles (electrons and ions),[10,11] Van der Waals effects from interactions between the emitting atom and polarizable neutral particles,[12] and resonance broadening from interactions between identical atoms when the upper or lower state at the emitted line is a resonance state.[13] Consequently, plasma parameters can be derived from assessing atomic line profiles, but being a theoretically complicated task, one often considers borderline conditions of either very "low" or "high" densities where respectively the *impact* or the *quasi-static* approximation applies.[3,14] The approximate equations for the line broadening at the full width at half maximum, $\Delta\lambda$, for the respective interactions: Stark,[10] Van der Waals with impact approximation (VdW imp.),[12] Van der Waals with quasi-static approximation (VdW q.stat.),[14] and resonance (res),[13] are

$$\Delta\lambda_{\text{Stark}} = 2\left[1 + 1{,}75\alpha(1 - 0.75\,R_{\text{D}})\right]\omega$$
$$(\omega \sim N_{\text{e}})$$

(1)

$$\Delta\lambda_{VdW}^{imp} = 8.1\frac{\lambda^2}{2\pi c}C_6^{2/5}w^{3/5}N_g \tag{2}$$

$$\left(N_g << \left(\frac{3\pi C_6}{8w}\right)^{-0.6}\right)$$

$$\Delta\lambda_{VdW}^{q.stat} = 0.411\pi^2\frac{\lambda^2}{c}C_6 N_g^2 \tag{3}$$

$$\Delta\lambda_{res,I} = 4\left(\frac{g_0}{g_1}\right)^{1/2}C_3 N_I \lambda^2 \tag{4}$$

$$\left(C_3 = \frac{e^2 f_0 \lambda_0}{16\pi^2 \varepsilon_0 m_e c^2}\right)$$

Here, N_e, N_g and N_I are the densities of electrons, neutral atoms, and identical atoms, ω and α are tabulated Stark broadening parameters (of electrons and singly ionized ions respectively)[10], R_D is the Debye shielding parameter, C_6 the Van der Waals interaction constant, λ the wavelength of the emitted line, f_0 and λ_0 are the oscillator strength and the wavelength of the resonant transition respectively, g_0 and g_1 are the statistical weights of atomic ground-state and of the upper level of the ground-state transition, c is the vacuum light speed, ε_0, e, m_e and w is the vacuum permittivity, electron charge, electron mass and the mean relative velocity of atoms. The Van der Waals constant can be calculated for each line from,[12]

$$C_6 = \frac{1}{2h\varepsilon_0}e^2\gamma\left|\langle r_u^2\rangle - \langle r_l^2\rangle\right| \tag{5}$$

where γ is the mean polarizability of perturbers, h the Planck constant and $\langle r^2\rangle$ the mean square radius for respective upper and lower atomic level. The latter calculates approximately from,

$$\langle r^2\rangle = a_0^2\frac{n^{*2}}{2}\left\langle 5n^{*2} + 1 - 3l(l+1)\right\rangle \tag{6}$$

$$n^* = \left(\frac{I_H}{I_X - E_X}\right)^{1/2}$$

where a_0 is the Bohr radius, l, n^* and E_X the angular quantum number, effective quantum number and excitation energy of the atomic level, while I_H and I_X are ionization energies of a hydrogen atom and the radiating atom, respectively.

3. Experiment

Streamers have been induced in a 5±0.3 mm point-to-plane gap by applying 0.1/50 µs high-voltage impulses with a fixed voltage level of -30 kV, applied either to the point or to the plane electrode. Point electrodes were made by electrochemically etching a 100 µm wolfram wire into near-hyperbolical shaped points with radii in the range 1.1–1.3 µm. Alternatively, we used triangular-shaped Ogura™ needles with about the same tip radii. The shape of the points was verified with a microscope. The approximation to a hyperboloid is typically only valid the first 40–50 µm of the point-length. The plane electrode was insulated with a Teflon cap in order to prevent electric breakdown resulting from streamers traversing the electrode gap. We used a 10 ml Teflon test cell with two optically aligned fused-silica windows, see figure 1. The liquids had a declared purity better than 99%, and were not further purified before introduced into the test cell.

Experiments were performed in two parts: one for the measurement of individual streamer lengths, illuminations times, streamer charge and current, and one for the spectroscopic investigations, where the light emitted from a series of streamers was accumulated.

In the first part, we used a gated image intensifier camera in order to picture the different light-emitting regions of the streamer, a synchronously pulsed high-intensity light-emitting diode for shadowgraphic imaging, alternatively a photo-multiplier tube for studying the temporal streamer emission. Both the time of image and exposure could be varied and were controlled with a TTL gate/delay signal generator (exposure > 100 ns), allowing images to be taken during different stages of propagation. The current and charge induced to the external circuit were measured respectively on a resistor and a capacitor placed alternately in series with the point electrode on the low-voltage side, see figure 1. The point electrode was insulated from ground and shielded up to about one millimeter from the tip in order to reduce capacitance to the plane. This electrode arrangement was designed for the Ogura™ needles only. The measurements of current and charge of negative streamers required the alternative setup of

3
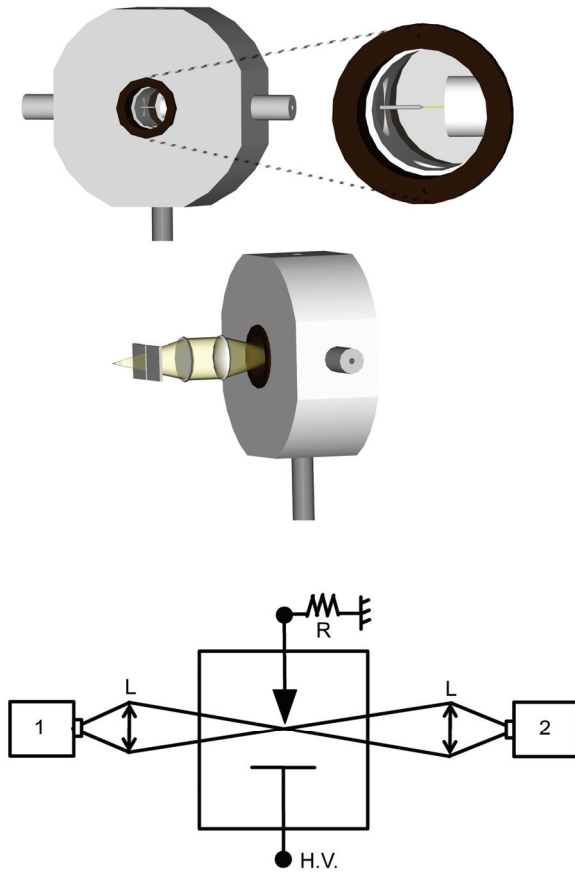
Figure 1. Upper: illustration of test cell with 5 mm point-to-plane gap, ~12 mm diameter plane, and ~18 mm diameter fused silica windows, and the condenser and secondary focusing lens system. Lower: general experimental outline, (1) gated image intensifier camera / monochromator, (2) photomultiplier tube / high-intensity light-emitting diode. The current and charge induced to the external circuit is measured on a resistor / capacitor placed in series with the effectively grounded point electrode.

a *positive* high-voltage impulse to the plane electrode. Due to pulse-source limitations, we here only managed a pulse risetime of 500 ns. Mean values and standard deviations for the individual measurements will be presented.

In the second part, series of high-voltage impulses were applied at 1 Hz repetition rate, and controlled by the TTL-signal gate/delay generator. Optical emission from the 10–15 μm region at the apex of the point electrode was collected with a condenser and secondary focusing lens system (fused silica lenses), see figure 1. In this setup, the image of the point is focused directly onto the 10 μm wide entrance slit of the monochromator, located perpendicular to the point-to-plane axis. The small distance (25 mm) from the point electrode to the condenser lens facilitates the amount of light to the spectrograph. The spectrograph (SpectraPro-300i,

focal length f = 300 mm, f/4 aperture), is equipped with three blazed (reflection) diffraction gratings with different resolutions, one with 150 grooves per millimetre and two with 1200 grooves per millimetre, blazed at 750 nm and 300 nm. A continuously open charge-coupled device (CCD) is located directly on the exit plane of the spectrograph, and cooled to a temperature of 153 K in order to reduce the dark current. Since the detector collects only a small amount of light from each streamer, it was necessary to integrate the light emitted during a series of 1500 – 2000 streamers in order to obtain useful data. Only (un-guarded) wolfram needles were used for this part, as these were more reliable at producing streamers for each applied impulse during long series of impulses. The total number of impulses applied determined the number of streamers recorded, and single acquisitions were performed with exposure durations up to one or two hours. The spectral range of the system in wavelengths is from 300 to 1000 nm, and the instrumental broadening $\Delta\lambda_{ins}$, measured by recording profiles of argon and neon lines from low-pressure discharge lamps, is 0.11 nm for the 1200 grooves per millimetre grating, and 2.8 nm for the 150 grooves per millimetre grating. Radiant energies have been quantified for wavelengths up to 900 nm by measuring the response of the spectrograph arrangement to a broadband light source with known spectral irradiance.

4. Results

4.1. Streamer visualization and electrical characteristics

A 30 kV impulse voltage initiates fast, filamentary and light-emitting streamers in all liquids for both point polarities, see examples in figure 2. General remarks can be made for the majority of streamers observed, whilst more specific details for each case can be found in table 1. Light, even visible to the eye is generated after some arbitrary delay, usually within one microsecond after the voltage reaches its maximum value. During such times, shadowgraphic images display faint shadows of 5–20 μm thick filaments, one or two being orders of magnitudes more luminous than the rest (figure 2e). Due to the relatively long exposures used, only rough estimations of the initial filament diameter can be made. In the microseconds following the initial illumination, the weakly illuminated

Table 1. Peak current I_{P1}, charge Q_{P1}, propagation velocity v_{P1}, and propagation length L_{P1} during the initial illumination. I_{P2} is the peak current of the first re-illumination, $\Delta t_{\text{lag-1}}$ the time from the moment of maximum voltage until streamer initiation, $\Delta t_{\text{lag-2}}$ the subsequent time lag until the first re-illumination, and Δt_{illum} is the total illumination time. Approximate or empty values reflect a limited number of observations (see text).

| Liquid	p	I_{P1} (mA)	I_{P2} (mA)	v_{P1} (km s^{-1})	Q_{P1} (nC)	L_{P1} (mm)	$\Delta t_{\text{lag-1}}$ (ns)	$\Delta t_{\text{lag-2}}$ (µs)	Δt_{illum} (ns)
CH_2Cl_2	+	34±4	148±45	14±1.6	1.6±0.4	1.6±0.5	-14±17	0.9±0.1	158±50
	-	13±1	~30	~14	1.3±0.8	1.1±0.4	~0	0.6±0.3	~74
$C_2H_4Cl_2$	+	31±6	96±34	23±4	0.9±0.3	1.2±0.4	45±80	0.5±0.3	116±58
	-				0.7±1.2	1.2±0.5			~80
CCl_4	+	180±10	-	21±3	30±7	~5	1500±780	-	291±43
	-	25±14	-	12±2	13±3	1.8±1.4	219±225	-	122±85
C_2Cl_4	+	103±10	-	22±2	21±1	~5	712±880	-	259±35
	-	30±15	-	10±4	5±3	1.6±1.5	447±358	-	163±80
C_2HCl_3	+	160±10	-	29±5	9.8±0.5	~5	156±146	-	185±45
	-	15		~13	2±1	1.0±0.4			~50

filaments rapidly disappear while the more luminous filament continues to expand laterally, see figure 2e,f and figure 3. In all cases, the duration of the initial emission is proportional to the length of the luminous filament on synchronized images by a factor equal to the average velocity of streamer propagation (table 1). In tetrachloromethane, tetrachloroethene, and trichloroethene, nearly all positive streamers and a few negative streamers reach the adjacent electrode during the initial illumination. Re-illuminations, of intensity and duration comparable to the initial, are, for both point polarities, only observed with dichloromethane and 1,2-dichloroethane. Normally, two or three re-illuminations occur with microsecond intervals, and synchronized images suggest a more pronounced stepped propagation in these liquids.

As shown in figure 4, oscillograms of streamer current and luminous intensity closely resemble each other. The current magnitude is several times lower during the initial illumination in dichloromethane and 1,2-dichloroethane compared to the other liquids. The slower impulse rise-time during electrical measurements with a point cathode often induced slow and weakly illuminating streamers, limiting the amount of relevant data obtained.

4.2. Spectroscopic results

Figure 5 shows the spectra obtained with a 150 grooves per millimetre grating for positive and negative streamers. Superimposed on a broad continuum, we can identify the rovibrational C_2 Swan bands $(d^3\Pi g \rightarrow a^3\Pi u, \Delta \upsilon = -2,...,2)$ between wavelengths 420 to 700 nm, the Balmer H_α emission line at 656 nm, and from wavelengths 720 to 960 nm numerous emission lines from atomic chlorine. The latter are characterized by 4s–4p optical transitions[15] and have previously been observed in different plasmas of chlorinated compounds.[16-18] We did not succeed to identify the strongest lines from atomic Wolfram, thus the degree of erosion on the point-electrode from each streamer is too small to produce a sufficient concentration in the plasma. As shown for 1,2-dichloroethane in figure 5, the H_α line in dichloromethane and 1,2-dichloroethane appears to consist of two components, one narrow and one very wide (25-35 nm), similar to that observed for streamers in transformer oil under DC-voltage conditions.[4] Atomic lines of sufficient intensity could be resolved on a 1200 grooves per millimetre grating by accumulating light from a few thousand streamers. Of the chlorine lines generally obeying this prerequisite are the ^4P–$^4S^0$ multiplets (7256.62 Å and 7547.07 Å) and three of the ^4P–$^4D^0$ multiplets (8333.31 Å, 8375.94 Å and 8428.25 Å). The lines are of particular interest as they can be obtained and compared for all experiments. Similarly, the Balmer-alpha line was obtained for the partly chlorinated liquids. With the exception of dichloromethane, we identified the 9094.83 Å line from atomic carbon, characterized by a 3s–3p transition.[15] The line can be resolved in 1,2-dichloroethane using a 1200 grooves per
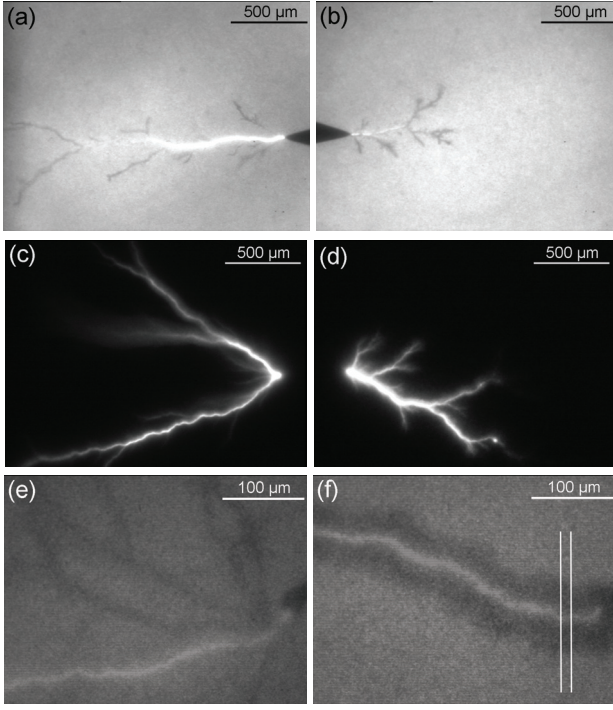
Figure 2. Light-intensified (incl. shadowgraphic) streamer images at 30 kV, (a,c) p+ [point anode] in $C_2H_4Cl_2$ during first 2 µs, (b,d) p- [point cathode] in $C_2H_4Cl_2$ during first 2 µs, (e) p+ in CCl_4 during first 0.5 µs, (f) p+ in CCl_4 during first 6 µs, vertical lines indicate the slit field-of-view.
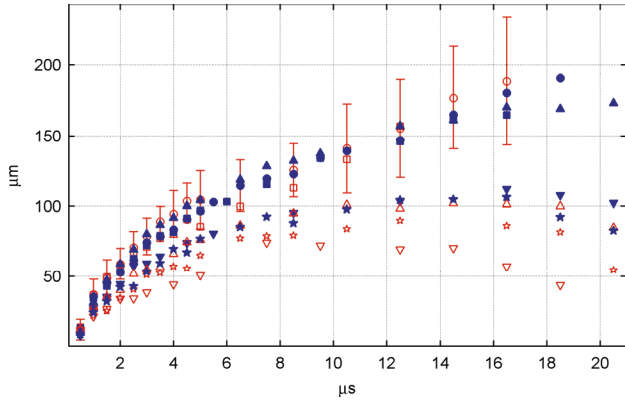
Figure 3. Expansion of the filament diameter from individual captures at fixed times after voltage application, (●) CH_2Cl_2 p+ [410], (○) CH_2Cl_2 p- [410] incl. standard deviation, (■) $C_2H_4Cl_2$ p+ [290], (□) $C_2H_4Cl_2$ p- [290], (▼) CCl_4 p+ [206], (▽) CCl_4 p- [90], (★) C_2Cl_4 p+ [140], (☆) C_2Cl_4 p- [105], (▲) C_2HCl_3 p+ [305], (△) C_2HCl_3 p- [100]. Superscripts in parenthesis indicate filament pressure (in bars) after first 0.5 µs, deduced from adiabatic volume expansion.

millimetre grating, in tetrachloromethane, tetra-chloroethene, and trichloroethene it merges with neighbouring lines of atomic chlorine (not shown here). The characteristic broadening, shift and
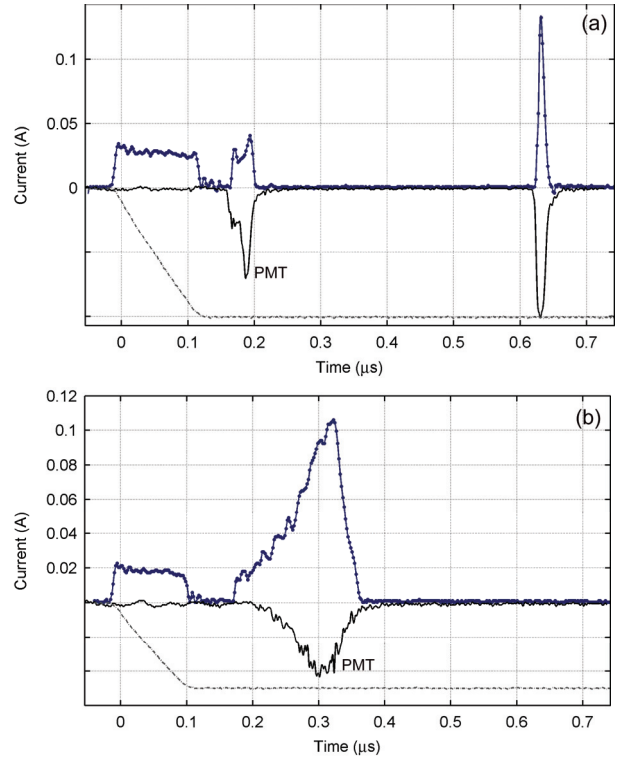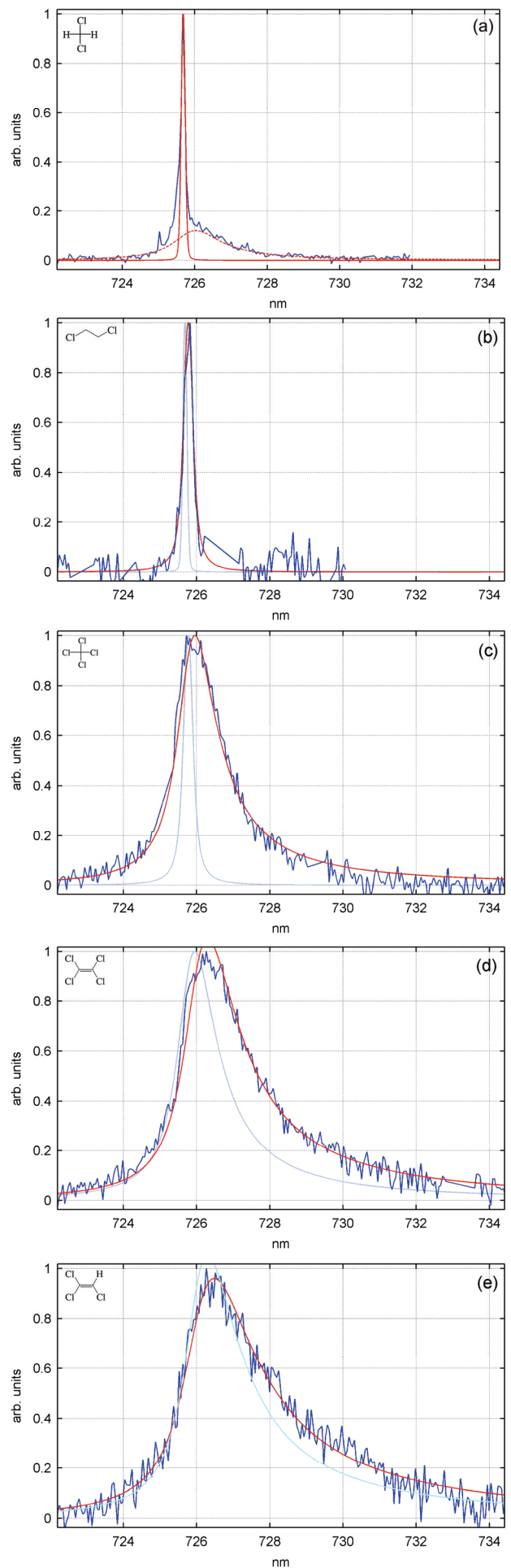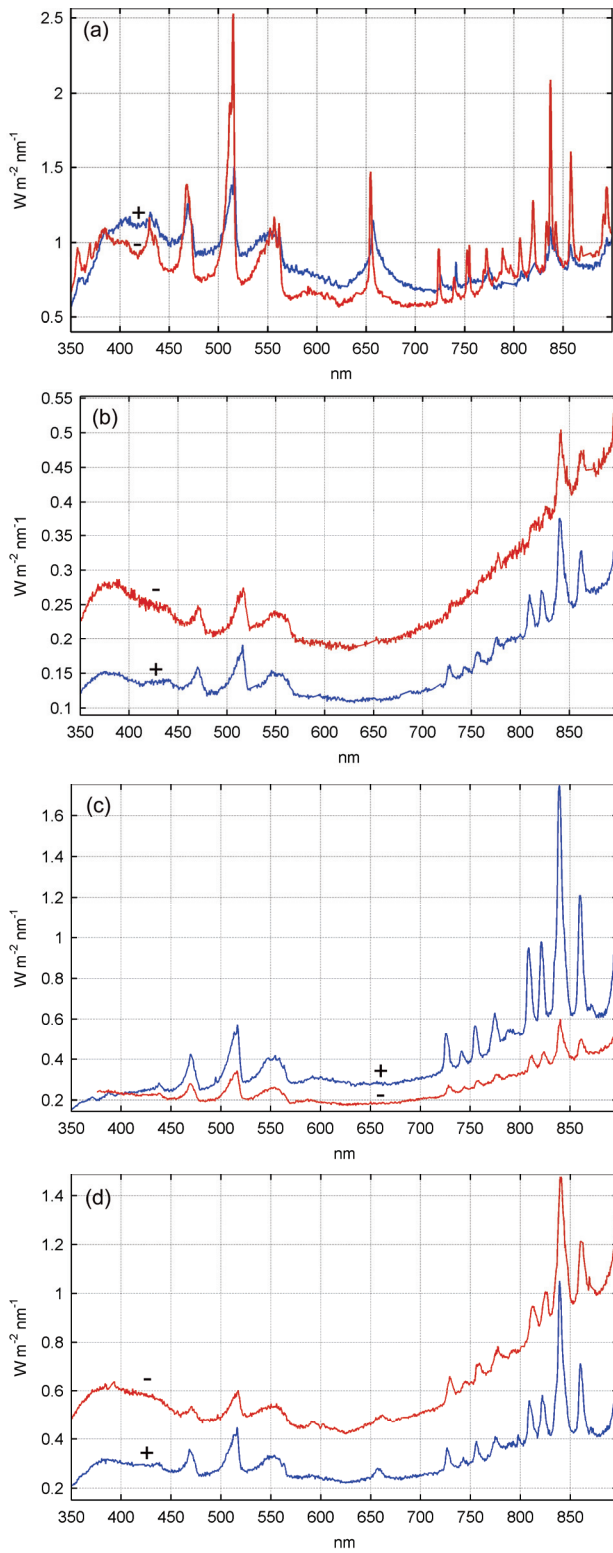

Figure 4. Oscillograms of streamer current (full dotted line), photomultiplier current (full line), and high-voltage impulse (dotted line), p+ (a) $C_2H_4Cl_2$, (b) CCl_4, sampled with a bandwidth of 300 MHz. A systematic 43 ns delay in the photomultiplier signal is not shown. The displacement current during the rise of the applied voltage appears separate from the streamer current.

asymmetry of all emitted lines varied significantly with the type of liquid studied, see figure 6, whereas differences between the two streamer polarities were comparatively small. The most broadened lines have a pronounced red-wing asymmetry and a shift towards higher wavelengths. In dichloromethane, superposed wide components could be discerned from the otherwise optically thin lines even with a high-resolution grating, and is indicated for one line in figure 6a.

When evaluating the red-winged atomic lines emitted from positive and negative streamers in tetrachloromethane, trichloroethene and tetra-chloroethene, we consider the quasi-static Van der Waals effect (3), for which case the wing profile follows a Holtsmark distribution function,[12]

$$P_{Holts}(\lambda > \lambda_{ul}) = \frac{1}{2}\left[\frac{\Delta\lambda}{(\lambda - \lambda_{ul})^3}\right]^{\frac{1}{2}} \exp\left(-\frac{\pi}{4}\frac{\Delta\lambda}{\lambda - \lambda_{ul}}\right) \quad (7)$$

$$P_{Holts}(\lambda \leq \lambda_{ul}) = 0$$

Figure 5. (Above) Calibrated emission spectra for positive (+) and negative streamers (−), (a) $C_2H_4Cl_2$, (b) CCl_4, (c) C_2Cl_4, (d) C_2HCl_3, with the average spectral intensity of one streamer. The instrumental broadening $\Delta\lambda_{instr}$ is 2.8 nm.

Figure 6. (Rigth) Measured (noisy) and simulated (smooth) profiles for the 725.6 nm chlorine line from positive streamers, (a) CH_2Cl_2, (b) $C_2H_4Cl_2$, (c) CCl_4, (d) C_2Cl_4, (e) C_2HCl_3. Each figure indicates the profile of the previous line. The instrumental broadening $\Delta\lambda_{instr}$ is 0.11 nm.

7
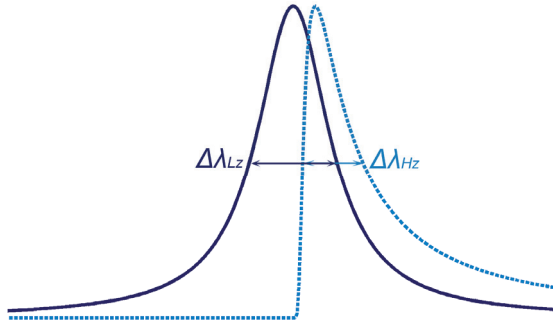
Figure 7. A Lorentzian (—) and a Holtsmark profile (---) with the same principal wavelength. The convolution of the two profiles gives a red-winged profile whose asymmetry depends on the line broadenings $\Delta\lambda_{Lz}$ and $\Delta\lambda_{Hz}$.

where λ_{ul} is the characteristic wavelength of the atomic transition, and $\Delta\lambda$ the broadening of the line. For the thinner and symmetrical lines obtained with dichloromethane and 1,2-dichloroethane, a Lorentzian profile can be adapted to the full profile, implying interactions within the impact approximation (2). The Lorentzian profile follows,

$$P_{Lorz}(\lambda) = \frac{2}{\pi}\frac{\Delta\lambda}{\Delta\lambda^2 + 4(\lambda - \lambda_{ul})^2} \qquad (8)$$

Since the Lorentzian profile can be adapted to the blue-wings of all observed lines, Stark or resonance interactions should always be considered.[3] Both line profiles are shown in figure 7, and their convolution resembles the experimental lines. Possibly, some experimental profiles can be found on the borderline between the two above approximations. Resonance effects have been considered since the lower atomic levels of all observed chlorine lines are dipole-coupled with the ground state.[15] By fitting the simulated and experimental profiles, and by combining the approximations for atomic broadening (1)-(4) with the instrumental transfer function in a numerical convolution, we have deduced a unique solution for the number density of the respective species in the plasma. We considered complete molecular dissociation and a perturber polarizability averaged over the ground state polarizabilities of the individual atoms. For the partly chlorinated liquids, the electron density has initially been evaluated from broadening of the Balmer-alpha line by a method of interpolating tabulated data.[10] This allows a rough identification of the contribution from Stark effects for the thin and symmetrical chorine lines. For chlorine, there is generally an insignificant

Table 2. Broadenings $\Delta\lambda$ of the 725.6 nm line for positive streamers, obtained from fitting experimental and simulated profiles. S_{Strk} and S_{VdW} would be the corresponding Stark and Van-der-Waals red-shifts, whereas S_{exp} is the value obtained experimentally (total shift).

Liquid	$\Delta\lambda_{Stark}$ (Å)	$\Delta\lambda_{vdw}$ (Å)	S_{Strk} (Å)	S_{VdW} (Å)	S_{exp} (Å)
CH_2Cl_2	.14/(13[a])	.4[b] /(1.0[a,c])			
$C_2H_4Cl_2$	.49	1.7[b]			
CCl_4	9.4	1.4[c]	5.4	0.5	3.2
C_2Cl_4	11	3.9[c]	5.9	1.4	6.4
C_2HCl_3	14	6.2[c]	7.4	2.2	8.4

[a]Alternative value deduced from a superimposed wide component. [b]Convolution of a Lorentzian and a Gaussian profile. [c]Convolution of a Lorentzian and a Holtsmark profile.

Table 3. Electron density N_e, gas density N_g, and degree of ionization N_e/N_g calculated from broadening parameters in table 2. In parenthesis; alternative values deduced from superimposed wide components. N_g/N_c is the ratio of the gas density to the critical density of the liquid,[d] and γ is the mean atomic polarizability in (5). Streamer polarity is given by p.

Liquid	p	N_e (10^{23} m^{-3})	N_g (10^{26} m^{-3})	N_e/N_g (10^{-3})	N_g/N_c (10^{-2})	γ (10^{-30} m^3)
CH_2Cl_2	+	0.1/(9)	<.02[a]/(2[b])	5/(4.5)		1.49
	-	0.1	<.02[a]			1.49
$C_2H_4Cl_2$	+	0.4 /(12[c])	0.1[a]	4.0	0.4	1.32
	-	0.3 /(13[c])	0.1[a]	3.0	0.4	1.32
CCl_4	+	8.0	2.0[b]	4.0	9.2	2.10
	-	4.0	3.0[b]	1.3	13.8	2.10
C_2Cl_4	+	8.0	3.3[b]	2.4		2.04
	-	6.0	4.6[b]	1.3		2.04
C_2HCl_3	+	10	4.5[b]	2.2		1.79
	-	10	7.3[b]	1.4		1.79

[a]Impact approximation. [b]Quasi-static approximation. [c]Based on the Balmer-alpha line with a low-resolution grating.
[d]Lide D R 2004 *Handbook of Chemistry and Physics* 84th ed. (Boca Raton: CRC) p 6.49.

contribution from the resonance broadenings due to weak oscillator strengths for the ground state transitions,[15] while significant contributions from Stark and Van der Waal interactions, see table 2 presenting results for the 725.6 nm line. The red shifts of the principal wavelengths agree reasonably with these interactions (calculated by similar methods[10,12]). Results from the evaluation of several atomic lines are presented in table 3, while simulated profiles have been included in figure 6. Obtained gas densities are high, except

for the re-illuminating streamers in dichloromethane and 1,2-dichloroethane, which can be understood as a pressure relaxation due to the relatively long delay between the first discharge and the re-illumination (see table 1). The gas densities span more than two orders of magnitudes, ranging roughly from 10% of the critical of the liquid, down to atmospheric densities for a superheated gas ($> 10^3$ K). The degree of ionization is comparatively high in all cases. Negative streamers are usually slightly denser, and slightly less ionized. The optically thin profiles for dichloromethane and 1,2-dichloroethane (figures 6a, 6b) are described by a Voigt function (the convolution of the Lorentzian profile with the Gaussian instrumental function), while profiles for tetrachloromethane, trichloroethene and tetra-chloroethene (figures 6c, 6d, 6e) are described by a convolution of a Lorentzian with a Holtsmark distribution function. According to tabulated Stark-broadening data for atomic chlorine, the electron temperature has only a weak effect on the line-specific Stark parameter ω.[10] The influence on electron density is always less than a factor of two when varying the electron temperature from 5×10^3 to 80×10^3 K.

Electronic excitation temperatures of the chlorine atoms cannot be determined from Boltzmann plots because the upper energy levels for the transitions identified are too closely positioned, spanning no more than 0.4 eV (3.5%).[15] However, radiant energies for properly resolved emission lines have been quantified by numerically integrating the average spectral energy distributions for one streamer, $P_{abs}(\lambda)$. Combined with the streamer illumination durations of table 1, and the initial filament diameters in Figure 3, we obtained mean value estimates for the corresponding radiant emittance, and for the net emission factor in the plasma, ε_λ. Atomic excitation temperatures T_{ex} could then be calculated from the relation[19]

$$\varepsilon_\lambda = \frac{E_u - E_l}{4\pi} A_{u,l} P_e(\lambda) \frac{N_g \, n_{Cl}}{Z(T_{ex})} \, g_u \, e^{\frac{-E_u}{kT_{ex}}}$$

$$\left(\int P_e(\lambda) \, d\lambda = 1 \right)$$

(9)

Here, A_{ul}, E_u and E_l are the Einstein coefficient and upper and lower atomic levels of the spontaneous emission respectively, g_u the degeneracy of populated states at the excited level, n_{Cl} the molecular degree of chlorination, and Z the electronic partition function of

Table 4. Excitation temperatures deduced from the emissivity of the 725.6 nm line, assuming a constant 15 μm streamer diameter, (p+) point anode, (p-) point cathode.

Liquid	T_{ex}^{p+} (10^3 K)	T_{ex}^{p-} (10^3 K)
$C_2H_4Cl_2$	6.8	7.5
CCl_4	6.7	5.8
C_2Cl_4	6.6	6.1
C_2HCl_3	6.6	6.4

the atom (or ion).[15,20,21] We neglect possible absorption losses, but correct for the fact that the streamer partly illuminates the active parts of the CCD detector. Comparable excitation temperatures in the range $6 \times 10^3 – 7 \times 10^3$ K have been deduced for the initial illumination where N_g is known, see table 4. The assumptions regarding streamer dimensions, validity of intensity calibration and level of absorption may be erroneous to an uncertain degree. Still, if the spectral intensity is varied by a factor of five, only a 10% change to the excitation temperatures results. For a general atomic excitation temperature of 7×10^3 K, the relative peak intensities of neighbouring lines in the range 900–920 nm for 1,2-dichloroethane imply a ratio of 1:20 between the number of radiating carbon and chlorine atoms, respectively.

4.3. Swan bands

The Swan bands are of the strongest rovibrational bands of the C_2 radical and most likely formed by collisions between free carbon atoms in the plasmas. Vibrational band heads for the Swan band sequences $\Delta v = -1$, $\Delta v = 0$ and $\Delta v = 1$ could be resolved with a 1200 grooves per millimetre grating, see figure 8. In some cases we could also determine peak positions of rotational lines within the $\Delta v = 0$ sequence. The relative intensity of the band heads is related to the vibrational temperature, T_v, whereas the rotational structure of a given vibrational band is related to the rotational temperature T_r. Thus, apparent vibrational and rotational mean temperatures can be derived from reproducing the experimental bands in a computer simulation, assuming vibrationally and rotationally excited states with a Boltzmann distribution.[22] We simulated the triplet band system from standard expressions of the vibrational and rotational term energies for a diatomic molecule, including Budo's
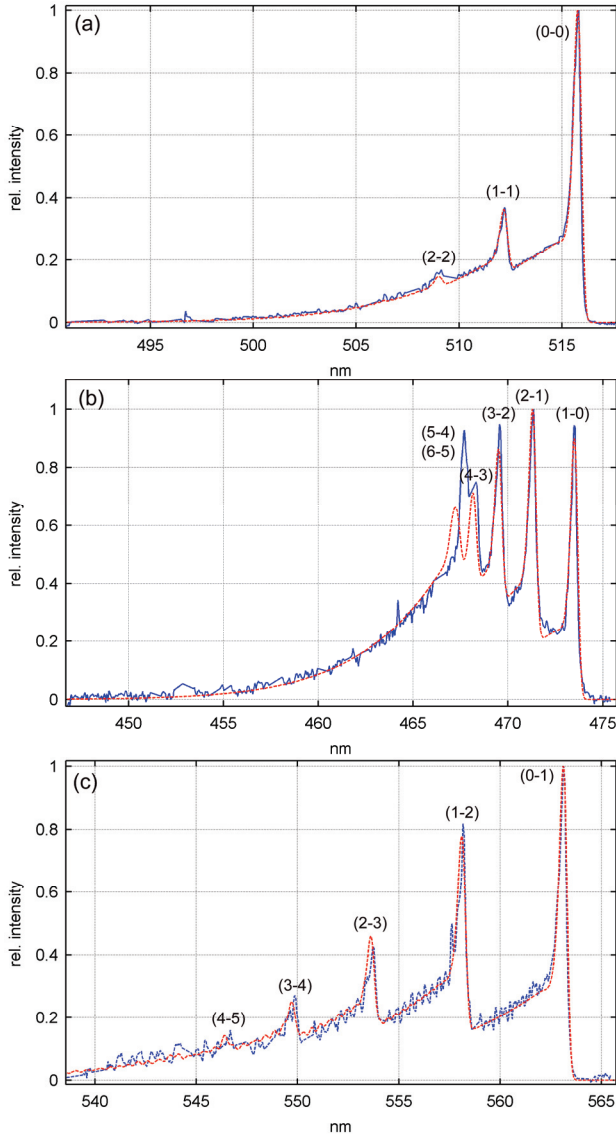
Figure 8. Measured (─) and simulated (---) Swan bands in C$_2$H$_4$Cl$_2$ p-, (a) $\Delta v = 0$, (b) $\Delta v = -1$, (c) $\Delta v = 1$.

rotational term formulae for the $^3\Pi$ state and neglecting interactions with the rotation of the nuclei.[22] We used tabulated values for the electronic term energy, for the vibrational and rotational equilibrium constants,[22] and for the vibrational transition probabilities.[23] Unresolved rovibrational band-shapes have been obtained by convoluting calculated lines with the instrumental transfer function before superimposing their relative contributions. The procedure of correctly adapting the profile of the band heads required the lines to be additionally broadened by 2–3 Å, indicative of a physical broadening mechanism. The derived temperatures are presented in table 5, whereas simulated bands have been included in figure 8. The vibrational and rotational modes are never in equilibrium, vibrational temperatures are maximum twice as large as the rotational (the $\Delta v = -1$ sequence

Table 5. Rotational and vibrational temperatures of the C$_2$ radicals. Values in parenthesis have a low accuracy.

Liquid	p	$Tr_{\Delta v0}$ (kK)	$Tv_{\Delta v0}$ (kK)	$Tr_{\Delta v-1}$ (kK)	$Tv_{\Delta v-1}$ (kK)	$Tr_{\Delta v1}$ (kK)	$Tv_{\Delta v1}$ (kK)
CH$_2$Cl$_2$	+	3.9	(4.2)	4.0	5.2		
	-	3.3	(3.3)	3.5	5.2	2.5	2.5
C$_2$H$_4$Cl$_2$	+	2.8	(3.7)	3.5	5.0	1.8	3.4
	-	2.2	(3.2)	2.9	5.0	2.2	3.5
CCl$_4$	+	5.8	(5.8)	5.5	9.5	5.8	5.8
	-	5.5	(5.5)	5.5	10.3		
C$_2$Cl$_4$	+	4.1	(4.3)	4.1	8.0	3.0	3.5
	-	4.0	(4.0)	4.0	8.0	3.0	3.5
C$_2$HCl$_3$	+	4.0	(4.0)	4.0	8.0	3.0	3.5
	-	4.0	(4.0)	4.0	9.0	3.0	3.0

for tetrachloromethane, trichloroethene and tetrachloroethene). There is generally an agreement within 20% between rotational temperatures obtained for the three sequences, while vibrational temperatures vary more. The accuracy of the rotational temperatures can be found by evaluating the difference between experimental and computed spectra from the ratio $\Delta S/S$, ΔS being the surface trapped between the experimental and simulated spectra, and S the total surface delimited by the spectral band within the chosen window.[24] Thus, considering the $\Delta v = 0$ sequence, a 10% change in derived temperature for the range $2 \times 10^3 – 6 \times 10^3$ K corresponds roughly to a $|\Delta S/S|$ of respectively 7 to 10%. A larger uncertainty is expected for derived vibrational temperatures, as we did not always manage to reproduce the relative intensities of all band heads, thus, there may be more than one solution. Moreover, we did not arrive at the correct wavelength for the $n_{v'v'}$(6-5) transition, which should lie about 10 Å at higher wavelengths than simulated,[25] see figure 8b. Derived rotational temperatures may reflect the gas kinetic temperature of the plasma if the C$_2$ radicals are excited directly from the ground state.

4.4. Light emitted during breakdown

We have made a limited survey of single breakdown-streamers from a point anode in tetrachloromethane. The breakdown initiates directly subsequent to the initial current pulse, and emits an intense light during about 300 ns. By comparing the emission spectra from the breakdown arc with those of the prebreakdown
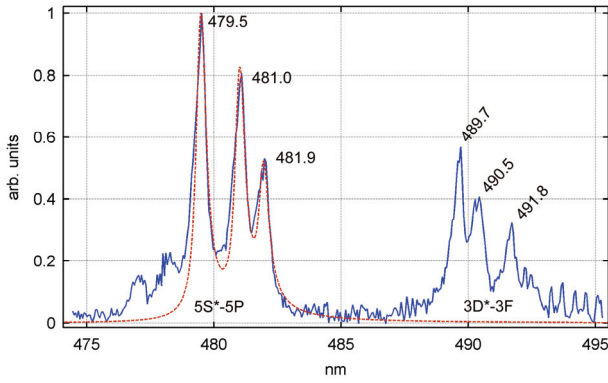
Figure 9. Measured (—) and simulated (---) line spectre from singly ionized chlorine in the breakdown plasma of positive streamers in CCl_4.

streamers, we find that electronically excited chlorine atoms and rovibrationally excited C_2 radicals emit more light by a ratio of 4 x 10^4 and 4 x 10^3, respectively. For an electron temperature of 5 x 10^3 K, the density of electrons and neutrals deduced from the atomic ^4P–$^4S^0$ multiplets were 4 x 10^{23} m^{-3} and 1.5 x 10^{26} – 2.5 x 10^{26} m^{-3}, respectively. Compared to the prebreakdown streamers, the gas is equally dense but 50% less ionized. Solving (9) with the obtained spectral emission and gas density, we deduce atomic excitation temperatures of about 1.2 x 10^4 K. Rotational and vibrational temperatures deduced from the shape of C_2 Swan bands were much lower: 2.2 x 10^3 – 2.7 x 10^3 K and 3.3 x 10^3 – 4.4 x 10^3 K respectively. As shown in figure 9, the spectra moreover contain six lines from two multiplets of singly ionized chlorine, $^5S^*$–^5P (13.4–15.9 eV) and $^3D^*$–^3F (15.7–18.2 eV).[15] Stark-broadening data exist only for the former,[10] whose profiles have been reproduced with plasma parameters comparable to those deduced from the atomic lines (N_e = 5.5 x 10^{23} m^{-3}, N_g = 2.5 x 10^{26} m^{-3}), see figure 9. The lower electronic levels of the ionic transitions are metastables, thus only Stark and quasi-static Van der Waals effects have been considered. The respective line broadenings are 3.8 Å and 0.06 Å, hence the more symmetrical profiles. Solving (9) for these lines, assuming only singly ionized cathions, we obtain an ionic excitation temperature of 2.1 x 10^4 K.

4.5. Post-experimental examination of liquids

To various degrees, the liquids gradually darkened and got a pale yellow colour during experimentation, but without altering the reproducibility of spectroscopic results. We found that black particles had aggregated in the liquids, most prominent for

dichloromethane. After particle filtering, the liquids were subjected to both UV-VIS absorption and FT-IR spectrometry, which did not detect a significant change from the original liquids. We did not attempt to collect and analyse the gas accumulating inside the test-cell.

5. Discussion

A fast propagating streamer almost "instantly" brings the liquid to a local supercritical thermodynamic state that develops into a high-density, superheated and illuminated gas. The gaseous filament in the trail of the propagation expands laterally the following microseconds due to pressure relaxation. Initial pressures deduced from the volumic expansions lie in the same range as those implied from the spectroscopically obtained densities using ideal gas law (~100 – 400 bar), but are too approximate partly due to a large scatter of measured filament diameters (figure 3). The transient nature of the streamers normally results in non-equilibrium plasmas in which the different species do not have sufficient time to thermalize. These plasmas are regularly characterized by different "temperatures": $T_e > T_{ex} \geq T_g$ and $T_v > T_r \geq T_g$. The results of our spectral analysis may, however, be interpreted to suggest streamer plasmas in a state not far from partial local thermodynamic equilibrium. First, in view of the relative small energy gap between the observed excited 4p and first ionized state of chlorine (~11 vs. 13 eV), we can consider a closer inequality between electron temperatures and excitation temperatures, $T_e \geq T_{ex} \approx 7$ x 10^3 K.[26] Second, gas kinetic temperatures deduced from the rotational temperatures of the excited C_2 radical are relatively close below excitations energies, and the rotational temperatures again not very far below the vibrational ones. We have not obtained a good indication of the electron temperature. Certainly, electron temperatures must be several times higher than 7 x 10^3 K during impact ionization, supposedly in a ionizing stage prior to the most intense light emission.

On a molecular level, inelastic electron-molecule interactions and vibrational-translational relaxations can both lead to the dissociation of the chlorocarbons, the former most directly from dissociative attachment processes with epithermal electrons.[7-9] Here, the excess reaction energy (<1.5 eV) distributes internally in the dissociation

fragments via vibrational and rotational excitations, whereas e.g. an immediate 4p excitation or ionization of atomic chlorine would require a consecutive collision with a more energetic electron (>10 eV).[27] Collisional and radiative processes consequently determine population of atomic and molecular levels, in which case apparent rotational temperatures do not directly reflect the gas kinetic temperature. For a dense "vapour" with components closer to local thermal equilibrium, dissociation of the chlorinated molecules and excitation and ionization of atomic species may occur because of the elevated temperature, thus indirectly from inelastic electron-molecule interactions, e.g. dissociative and auto-ionizing attachment processes. The dense conditions imply an increased coupling between the different particles, tending to equilibrate their respective temperatures more rapidly. Vibrational-translational relaxation times at conditions close to critical densities can be extrapolated from an inverse linear pressure dependence for collision-induced energy conversion in gases of vibrationally excited chlorocarbons,[28] and are accordingly on the order of nanoseconds. Comparable relaxation times have been experimentally reported for vibrationally excited liquid chlorocarbons.[29] For an equilibrated system, the temperature and the chemical composition completely determine population of excited atomic states and the ionization degree.[30] Consequently, for chlorocarbons dissociated in thermal equilibrium, a temperature of above 10^4 K would be required to ionize to the level here reported.

We have assessed the energy and the chemical composition of the illuminated phase from isobaric and isothermal calculations on an equivalent system in complete thermodynamic equilibrium, using a commercialized computational method of Gibbs energy-minimization.[31] Here, the dependence on temperature and pressure for the thermal dissociation into atomic species (C, H and Cl), which is normally positive with temperature and negative with pressure, depends on the original chemical composition of the system. For tetrachloromethane, tetrachloroethene, and trichloroethene at their respective temperatures (table 5), atomic chlorine exists also at very high pressures (>50% dissociation at 400 bar), while at pressures above ~50 bar, most of the hydrogen in trichloroethene constitute hydrochloric acid. Similarly, with dichloromethane and 1,2-dichloro-ethane, an increased stability with pressure for hydrochloric acid means that a lower pressure is required to obtain the same degree of dissociation

Table 6. Energy densities in the illuminated phase of non re-illuminating streamers. $U_\emptyset$ is an experimental value deduced from injected energy and calculated for filament diameters 15 and 25 μm. $U_{\rho,T}$ is a theoretical value for an equivalent thermodynamic equilibrium state.

Liquid	p	$U_{\emptyset\text{-}15\mu m}$ (MJ/L)	$U_{\emptyset\text{-}25\mu m}$ (MJ/L)	$U_{\rho,T}$ (MJ/L)
CCl_4	+	1.02	0.37	0.28
	-	1.22	0.44	0.40
C_2Cl_4	+	0.71	0.26	0.38
	-	0.53	0.19	0.53
C_2HCl_3	+	0.33	0.12	0.58
	-	0.34	0.12	1.01

into atomic chlorine and hydrogen, implying for the high-density conditions a weakened atomic radiation. Common for all liquids is that graphite would take up most of the carbon below temperatures $4.5 \times 10^3 – 5 \times 10^3$ K, in line with the observations of black particles and a relative weak emission from atomic carbon. We have evaluated the increase in volume energy density for each equivalent equilibrium state against the typical energy density deposited in a non-re-illuminating streamer filament, see table 6. The latter was estimated from the product of the charge of the initial current pulse and the applied voltage, divided by the streamer volume. Main uncertainties arise from rough estimates of initial filament diameters (figure 3). The estimates in table 6 are given for two filament diameters within the range of measured values, and show a stronger dependence on the type of liquid than on the polarity of the streamer. The values moreover resemble energy densities calculated for the equivalent equilibrium states. A more detailed comparison between experimental and theoretical estimates requires a higher precision for the initial filament diameters.

The results of the present study can be compared to results previously obtained in various liquids under similar voltage conditions. In liquid nitrogen with dissolved hydrogen, vibrational temperatures and densities of neutral and charged species are comparable to those obtained in this study ($T_v = 3.8 \times 10^3$ K, $N_g = 3 \times 10^{26}$ m^{-3}, $N_e = 10^{23} – 10^{24}$ m^{-3}), whereas rotational temperatures deduced from excited N_2 molecules were much lower ($T_r = 350 – 500$ K).[3,32] In water, comparable rotational temperatures have been reported for

excited hydroxyl radicals ($\sim 4 \times 10^3$ K), and comparably higher electron densities from the Balmer-alpha emission ($N_e = 5 \times 10^{24} - 8 \times 10^{24}$ m^{-3}).[33] Electron densities reported for filamentary positive streamers in n-pentane and cyclohexane are comparable to those here obtained for the least chlorinated liquids: dichloromethane and 1,2-dichloroethane ($N_e = 4 \times 10^{22} - 7 \times 10^{22}$ m^{-3}).[2]

6. Conclusion

The broadening of atomic lines indicates a high gas density ($\sim 10\%$ of critical) and a relatively high degree of ionization (~ 1‰) in the immediate trail of fast propagating positive and negative streamers in the chlorinated liquids. Intense re-illuminations occur during the pressure relaxation in dichloromethane and 1,2-dichloroethane, and effectively reduce the time-averaged broadening of their emitted lines. Averaged C$_2$ Swan bands suggest gas temperatures differing in the range $2 \times 10^3 - 6 \times 10^3$ K, whereas the absolute intensity of atomic radiation suggests excitation temperatures of $6 \times 10^3 - 7 \times 10^3$ K. The spectroscopic data can be interpreted to suggest a partial local thermodynamic equilibrium in the plasma of the streamers. It is believed that the high pressure and the high electron density help equilibrate the temperatures of the various particles. The energy-consumption and qualitative chemical composition of the illuminated phase are similar to that of an equivalent system in complete thermodynamic equilibrium. On the other hand, thermal effects may not alone account for the high degree of ionization. The streamer phenomenon is transient in both temperature and pressure, thus making it more difficult to interpret the spectra of the time-averaged emission. Time-resolved spectroscopy would be a suitable method to separate between different stages of streamer illumination and propagation.

Acknowledgement

References

[1] Bonifaci N and Denat A 1991 *IEEE Trans. Dielectr. Electr. Insul.* **26** 610-4

[2] Denat A, Bonifaci N and Nur M 1998 *IEEE Trans. Dielectr. Electr. Insul.* **5** 382-7

[3] Bonifaci N, Denat A and Frayssines P E 2006 *J. Electrostat.* **64** 445-9

[4] Bårmann P, Kröll S and Sunesson A 1997 *J. Phys. D : Appl. Phys.* **30** 856-63

[5] Beroual A, Zahn M, Badent A, Kist K, Schwabe A J, Yamashita H, Yamazawa K, Danikas M, Chadband W G and Torshin Y 1998 *IEEE Electr. Insul. Mag.* **14** 6-17

[6] Sakamoto S and Yamada H 1979 *IEEE Trans. Dielectr. Electr. Insul.* **15** 171-81

[7] Aflatooni K and Burrow P D 2000 *J. Chem. Phys.* **113** 1455-64

[8] Johnson J R, Christophorou L G and Carter J G 1977 *J. Chem. Phys.* **67** 2196-215

[9] Oster T, Kuhn A and Illenberger E 1989 *Int. J. Mass Spectrometry and Ion Processes* **89** 1-72

[10] Griem H R 1974 *Spectral Line Broadening by Plasmas* (New York: Academic)

[11] Bastien F and Marode E 1977 *J. Quant. Spectrosc. Radiat. Transfer* **17** 453-69

[12] Lochte-Holtgreven W 1968 *Plasma diagnostics* (Amsterdam: North-Holland Publ. Company)

[13] Griem H R 1997 *Principles of Plasma Spectroscopy* (Cambridge: Cambridge University Press)

[14] Margenau H 1935 *Physical Review* **48** 755-65

[15] Ralchenko Yu, Jou F-C, Kelleher D E, Kramida A E, Musgrove A, Reader J, Wiese W L and Olsen K 2007 NIST Atomic Spectra Database (ver. 3.1.3), http://physics.nist.gov/asd3 (Gaithersburg: National Institute of Standards and Technology)

[16] Konjevic N and Wiese W L 1976 *J. Phys. Chem. Ref. Data* **5** 259-308

[17] Konjevic N and Wiese W L 1990 *J. Phys. Chem. Ref. Data* **19** 1307-85

[18] Konjevic N, Lesage A, Fuhr J R and Wiese W L 2002 *J. Phys. Chem. Ref. Data* **31** 819-927

[19] Sobel'man I I, Vainshtein L A and Yukov E A 1995 *Excitation of Atoms and Broadening of Spectral Lines*, 2nd ed. (Heidelberg: Springer)

[20] Tamaki S and Kuroda T 1987 *Spectrochimica Acta, Part B (Atomic Spectroscopy)* **42B** 1105-11

[21] Galan L, Smith R and Winefordner J D 1968 *Spectrochimica Acta, Part B (Atomic Spectroscopy)* **23B** 521-5

[22] Herzberg G 1950 *Molecular Spectra and Molecular Structure, Volume 1: Spectra of Diatomic Molecules* (New York: Van Nostrand Reinhold)

[23] Danylewych L L and Nicholls R W 1974 *Proc. R. Soc. Lond. A.* **339** 213-22

[24] Chelouah A, Marode E, Hartmann G and Achat S 1994 *J. Phys. D : Appl. Phys.* **27** 940-5

[25] Pearse R W B and Gaydon A G 1976 *The identification of molecular spectra* 4th ed. (London: Chapman and Hall)

[26] Karabourniotis D 2003 *Appl. Phys. Lett.* **83** 5395-7

[27] Ganas P S 1988 *J. Appl. Phys.* **63** 277-9

[28] Kondrat`ev V N 1964 *Chemical Kinetics of Gas Reactions (ADIWES International Series in the Physical Sciences)* (Oxford: Pergamon Press)

[29] Takagi K, Choi P K and Negishi K 1981 *J. Chem. Phys.* **74** 1424-7

[30] van der Mullen J A M 1990 *Physics Reports* **191** 109-220

[31] Cheynet B, Chevalier P-Y and Fischer W 2002 *Calphad* **26** 167-74

[32] Frayssines P E, Bonifaci N, Denat A and Lesaint O 2002 *J. Phys. D : Appl. Phys.* **35** 369-77

[33] Salazar J N, Bonifaci N, Denat A and Lesaint O 2005 *IEEE Proc. Int. Conf. Diel. Liquids (Coimbra)* 91-4

NTNU
Norwegian University of
Science and Technology